HIGH ENERGY COSMIC RAYS

Alexander Borisov

P.N. Lebedev Physical Institute, Moscow, Russia

10th Winter Workshop and School on Astroparticle physics,
17–29 December, Bose Institute, Mayapuri, Darjeeling

High energy CR phenomenon
or what are CRs of high energy? –

charged particles (protons & nuclei) travelling in outer space and sometimes arriving at the Earth

1) Experimental techniques for CR observations: direct (balloon-borne, satellite-based) & indirect or ground-base (EAS arrays, ČD, FD, Radio)
2) Energy spectra (both total and partial)
3) Mass composition (varies with energy)
4) Anisotropy
5) Hadronic Interactions (derived from comparison of experimental data with Monte Carlo simulations)
6) CR Origin: sources, acceleration, propagation (messengers of High Energy Universe)

High energy CR phenomenon

or what are CRs of high energy? –

charged particles (protons & nuclei) travelling in outer space and sometimes arriving at the Earth

1) Experimental techniques for CR observations: direct (balloon-borne, satellite-based) & indirect or ground-base (EAS arrays, ČD, FD, Radio)
2) Energy spectra (both total and partial)
3) Mass composition (varies with energy)
4) Anisotropy
5) Hadronic Interactions (derived from comparison of experimental data with Monte Carlo simulations)
6) CR Origin: sources, acceleration, propagation (messengers of High Energy Universe)

High energy CR phenomenon

or what are CRs of high energy? –

charged particles (protons & nuclei) travelling in outer space and sometimes arriving at the Earth

1) Experimental techniques for CR observations: direct (balloon-borne, satellite-based) & indirect or ground-base (EAS arrays, ČD, FD, Radio)
2) Energy spectra (both total and partial)
3) Mass composition (varies with energy)
4) Anisotropy
5) Hadronic Interactions (derived from comparison of experimental data with Monte Carlo simulations)
6) CR Origin: sources, acceleration, propagation (messengers of High Energy Universe)

Energy Spectrum of Primary Cosmic Rays

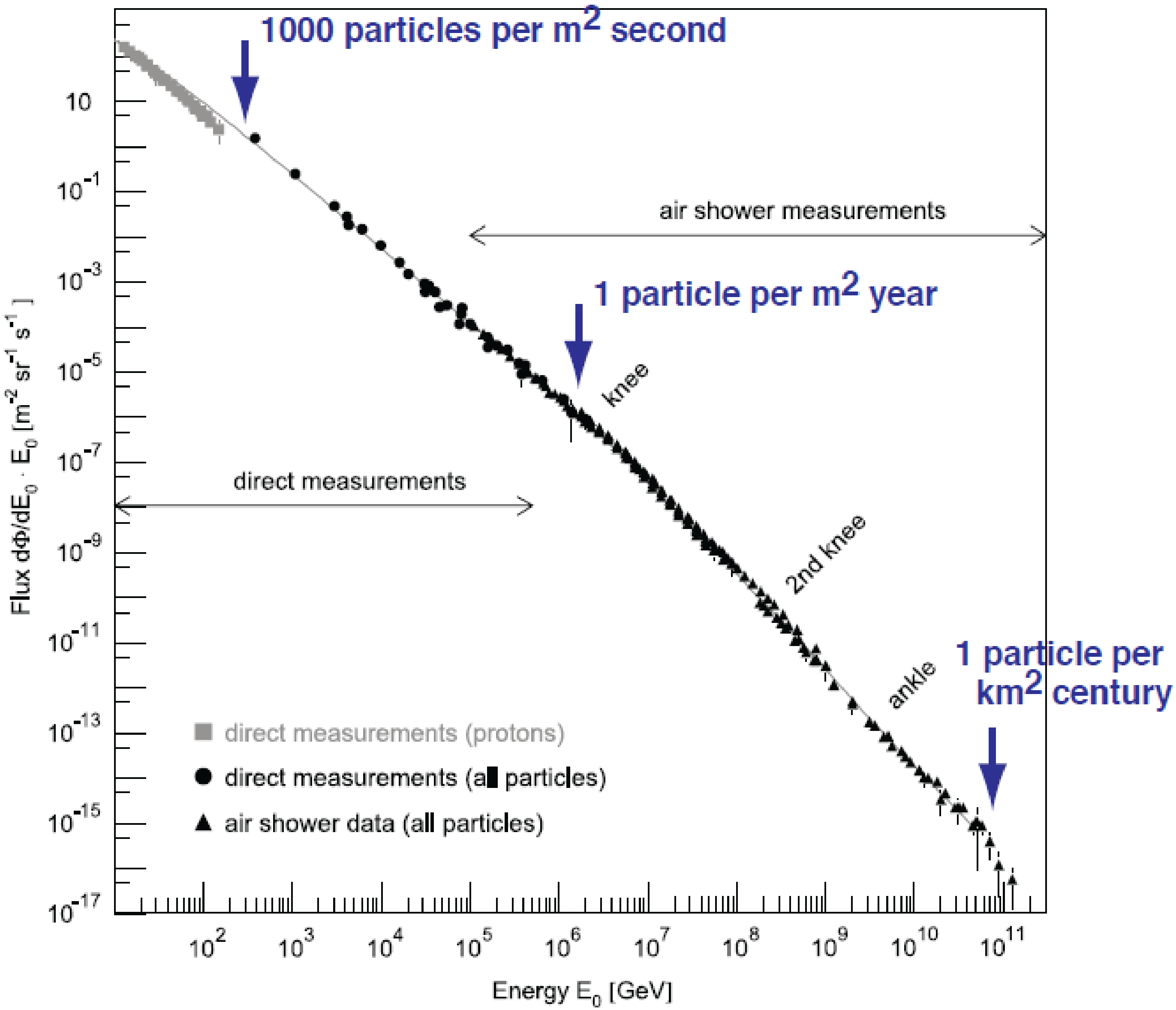

Fig. 1. All-particle energy spectrum of cosmic rays as measured directly with detectors above the atmosphere and with air shower detectors. At low energies, the flux of primary protons is shown.

Extensive air showers

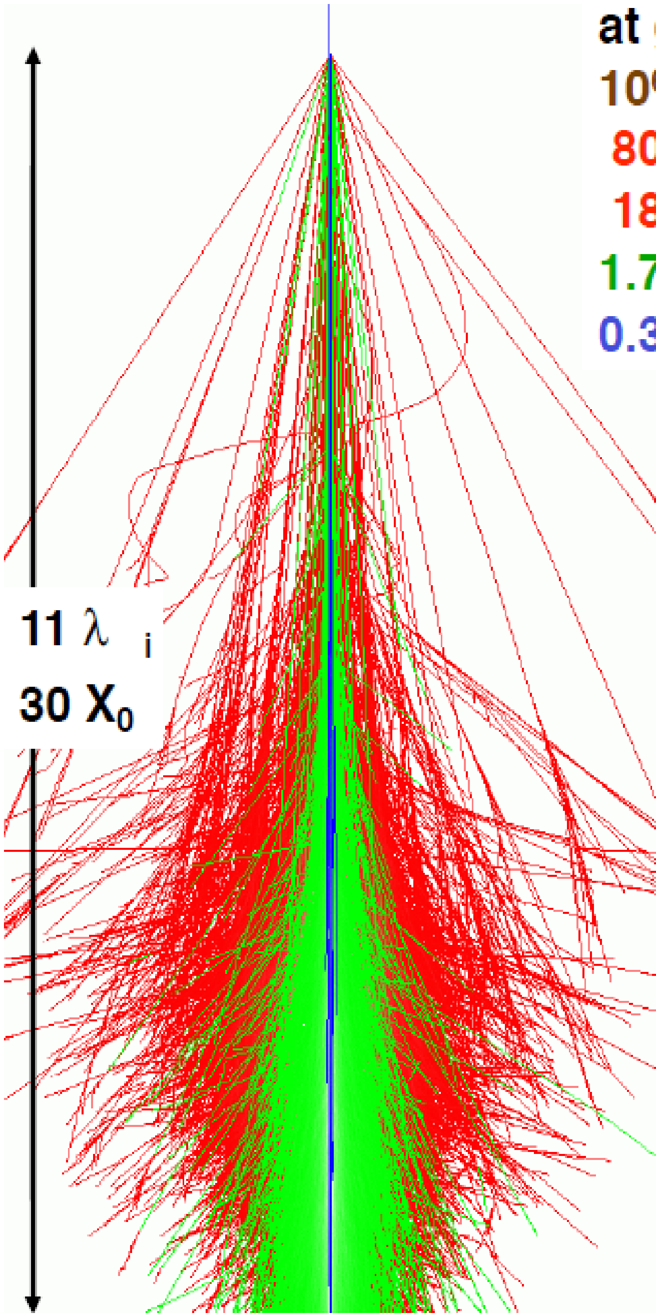

Proton 10^{15} eV:
at ground
10^6 particles
80% photons
18% elektr./positr.
1.7% muons
0.3% hadrons

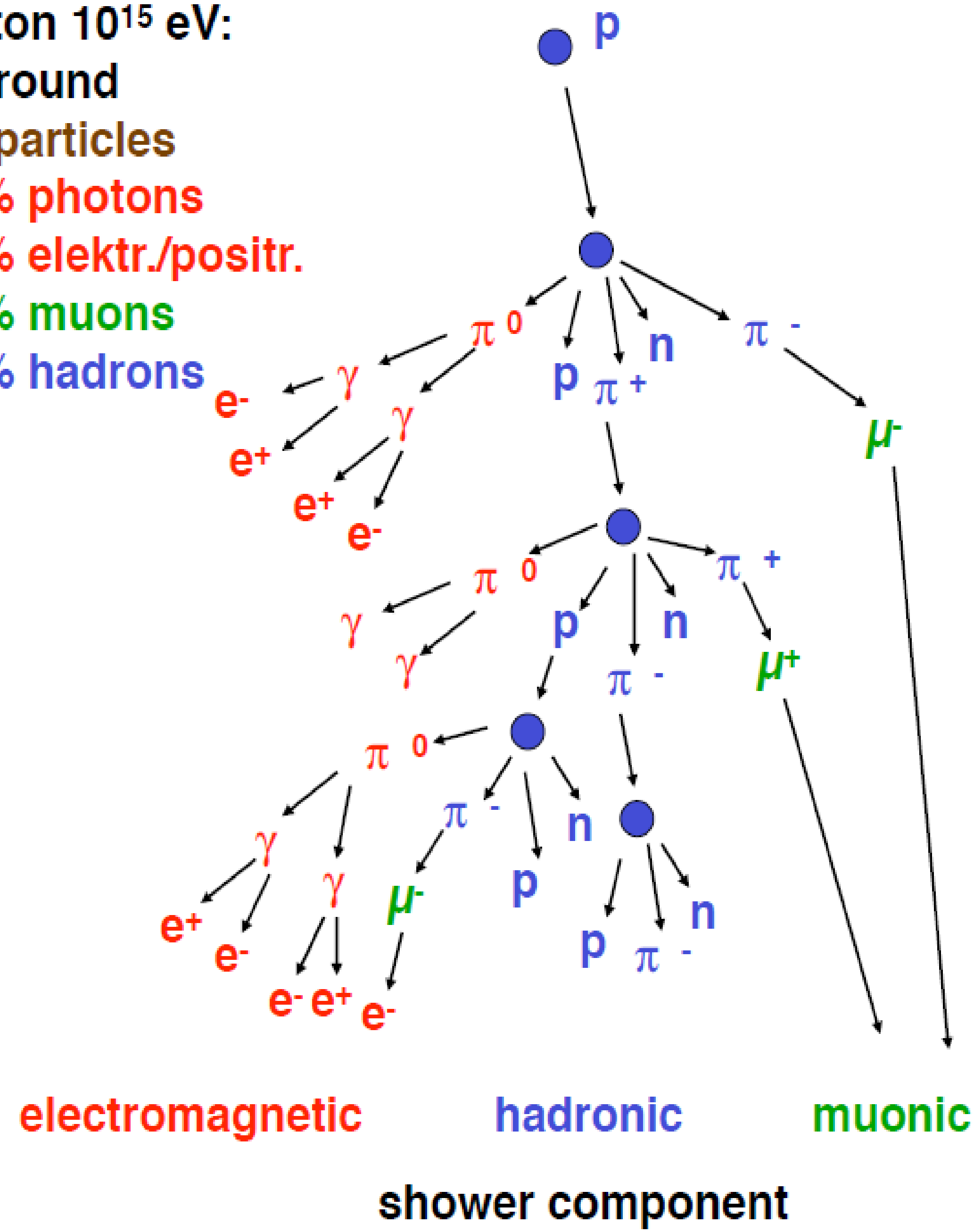

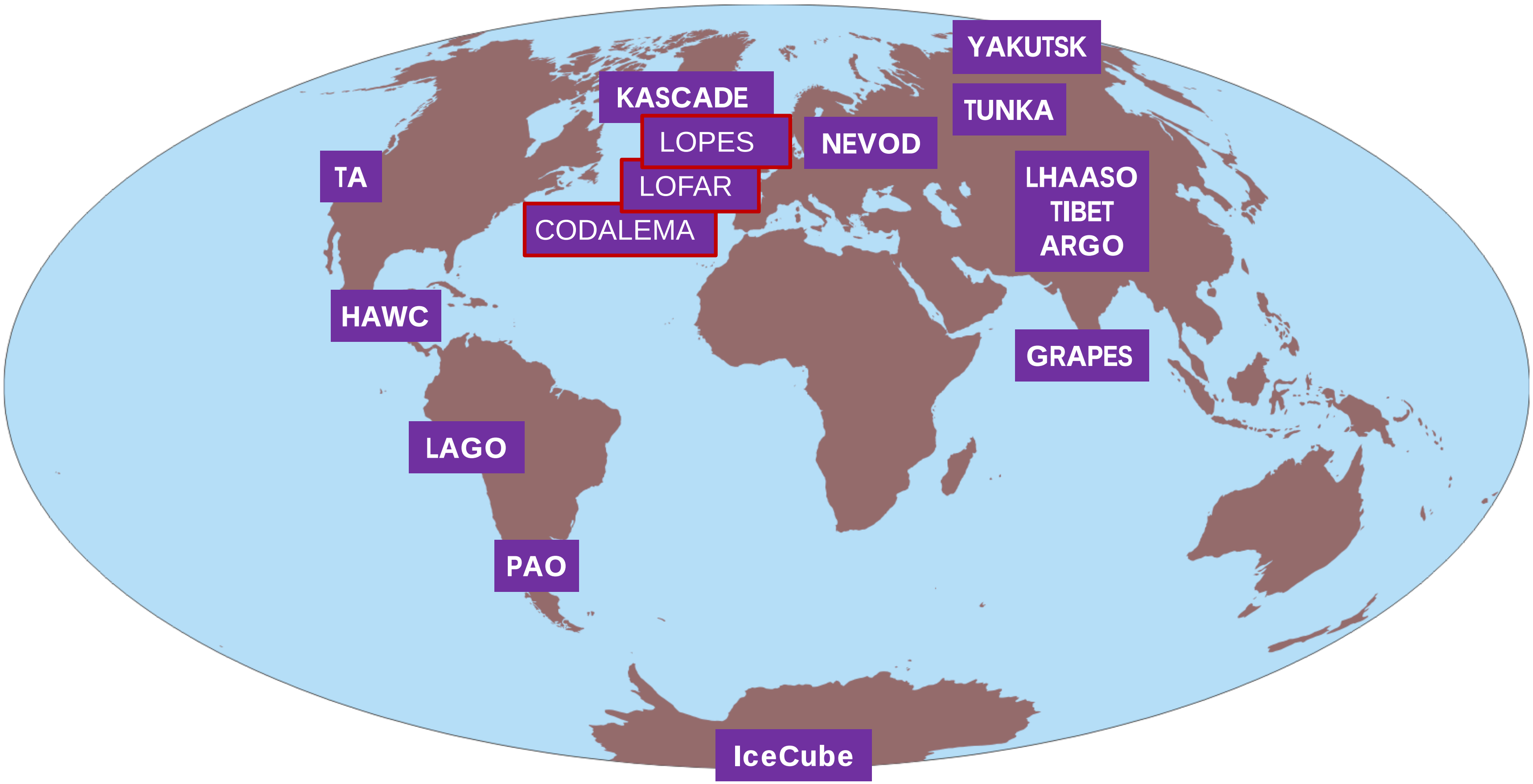
YAKUTSK
KASCADE
TUNKA
LOPES
NEVOD
TA
LOFAR
LHAASO
TIBET
ARGO
CODALEMA
HAWC
GRAPES
LAGO
PAO
IceCube

Energy Spectrum of Cosmic Rays

~1 particle/m²/second

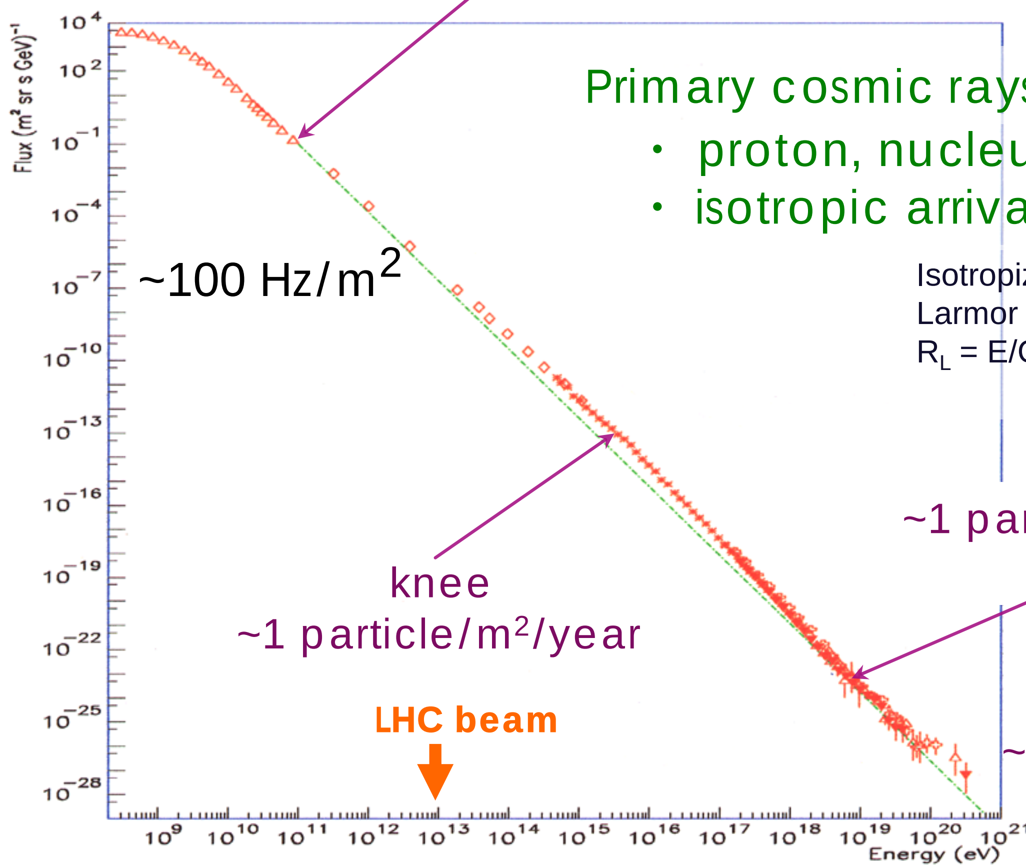

Primary cosmic rays:
- proton, nucleus
- isotropic arrival (~0.1%)

Isotropization during transport
Larmor radius
$R_L = E/QB \sim 0.4(A/Z)E(\text{PeV/nuc})/B(3\mu\text{G})$ pc
$\sim 100\ E(10^{20}\ \text{eV}) / ZxB(\text{nG})$ Mpc

~1 particle/m²/year
ankle

~1 / (100 km² Year)

10^{9} eV

ENERGY

10^{20} eV

Introduction to nuclear-electromagnetic cascade theory in application to the air absorber

Extensive air showers

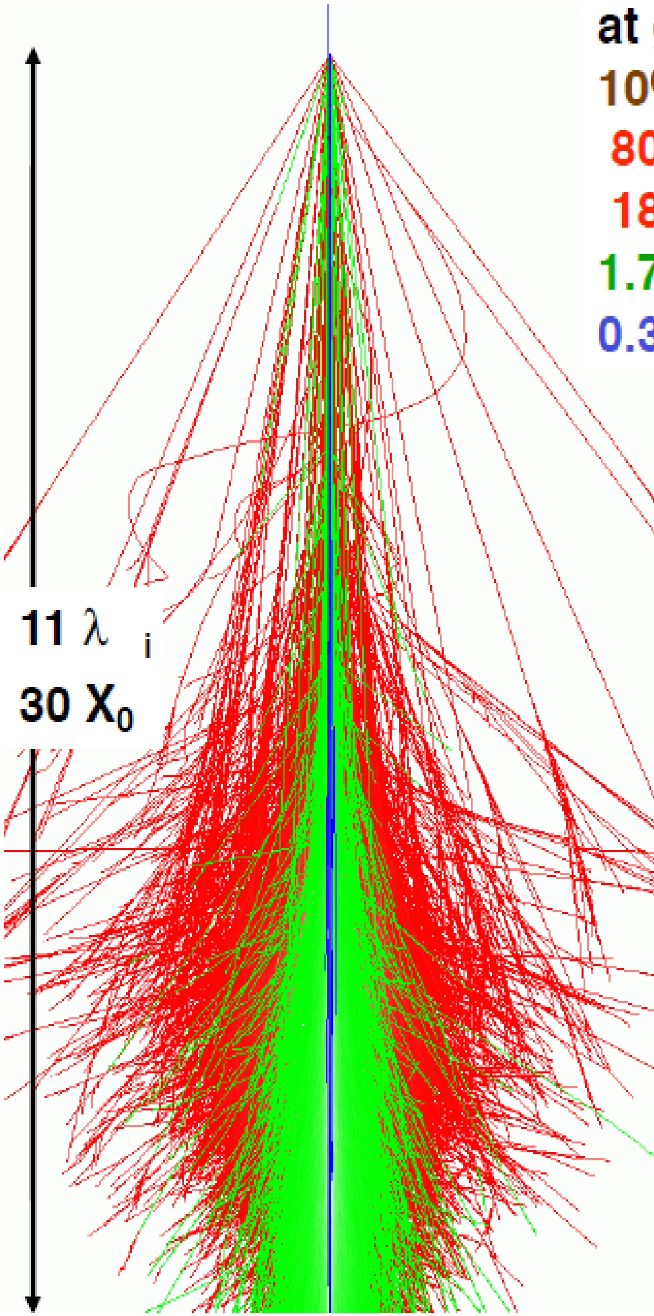

Proton 10^{15} eV:
at ground
10^6 particles
80% photons
18% elektr./positr.
1.7% muons
0.3% hadrons

$$\frac{dN}{dE} \sim E^{-\gamma},\ \gamma \sim 2.7$$

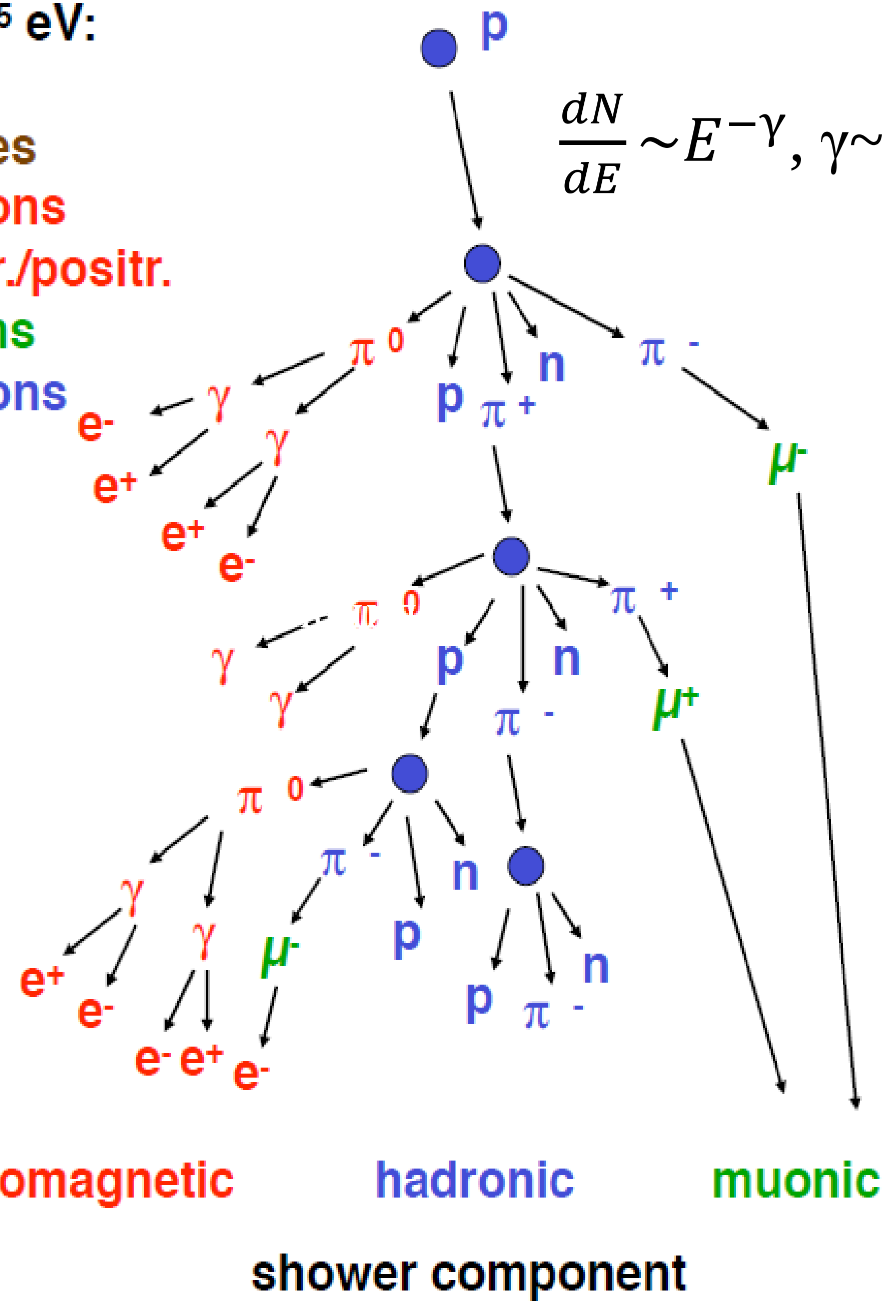

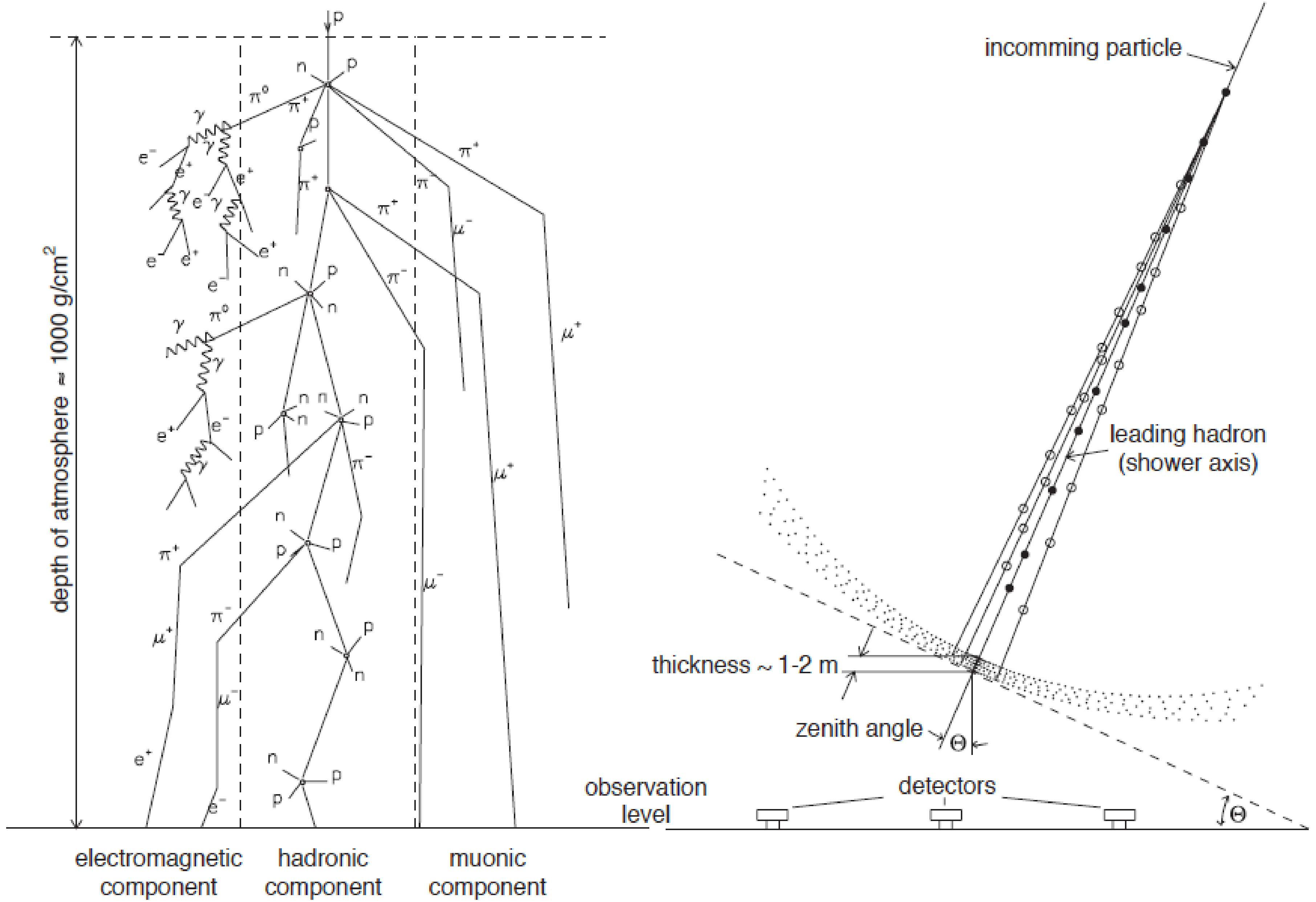

depth of atmosphere ≈ 1000 g/cm²
electromagnetic component
hadronic component
muonic component
incomming particle
leading hadron (shower axis)
thickness ~ 1-2 m
zenith angle
Θ
observation level
detectors

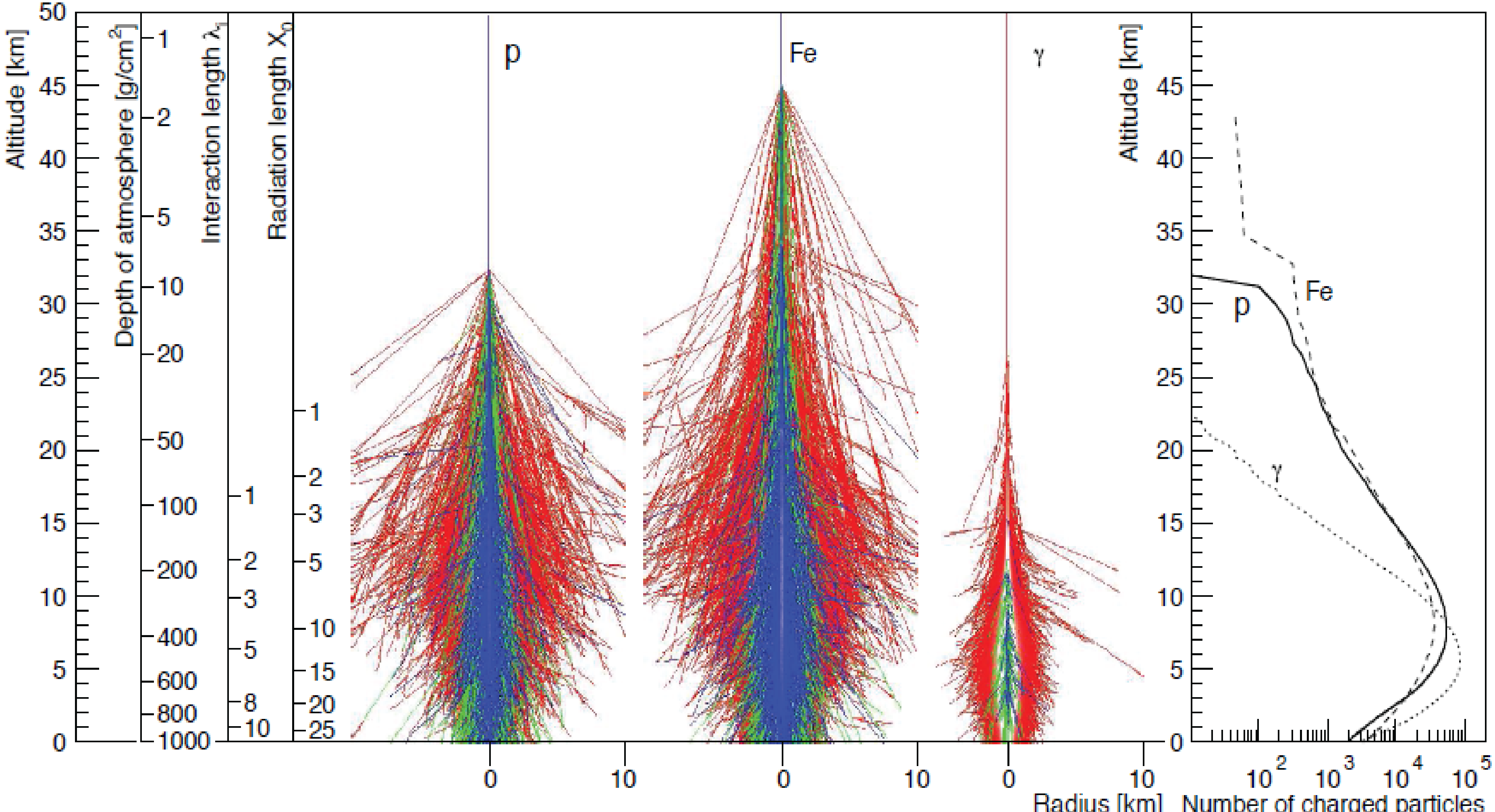

H = 1035 g/cm^2
~ 12 λ_{int}
~ 30 X_0

Typical size of an air shower:
at $E_0 \sim 10^{13}$ eV   R ~ 20 m
at $E_0 \sim 10^{20}$ eV   R ~ 7 km

A Heitler Model – Electromagnetic Cascades

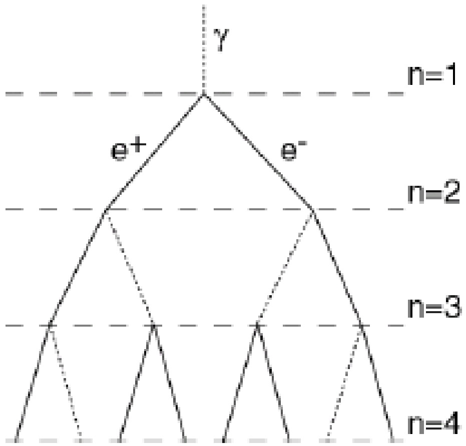

pair production $\gamma \rightarrow e^+ + e^-$

bremsstrahlung $e \rightarrow e + \gamma$

splitting length $d = X_0 \ln 2$

radiation length $X_0 = 36.7$ g/cm^2

after *n* splitting lengths: $x = nX_0 \ln 2$ **and** $N = 2^n = \exp\left(\frac{x}{X_0}\right)$

energy per particle $E = E_0/N$ **critical energy** $E_c^e = 85\ \mathrm{MeV}$

number of particles at shower maximum

$$N_{max} = 2^{n_c} = \frac{E_0}{E_c^e} \qquad n_c = \frac{\ln\left(\frac{E_0}{E_c^e}\right)}{\ln 2}$$

J. Matthews, Astrop. Phys. 22 (2005) 387

JRH, Mod. Phys. Lett. A 22 (2007) 1533

A Heitler Model – Electromagnetic Cascades

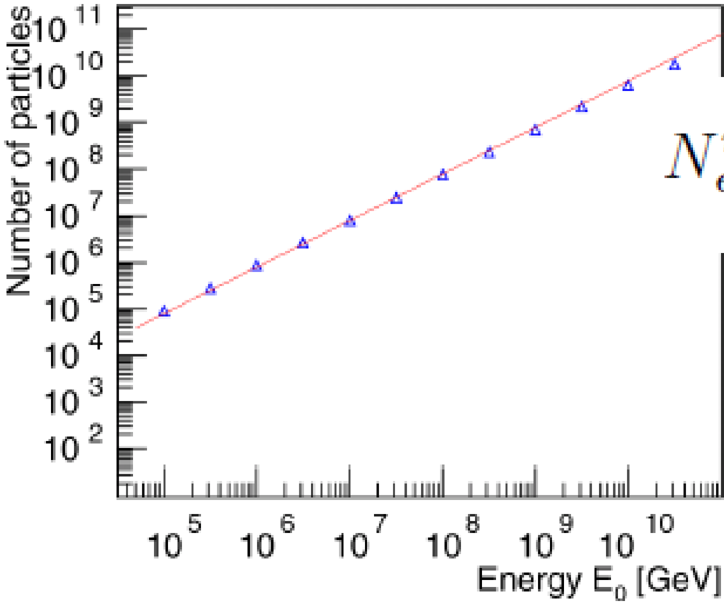

number of electrons at shower maximum

$$N_e^{max} = \frac{E_0}{gE_c^e} \approx 9.0 \cdot 10^5 \frac{E_0}{\mathrm{PeV}} \qquad g \approx 13$$

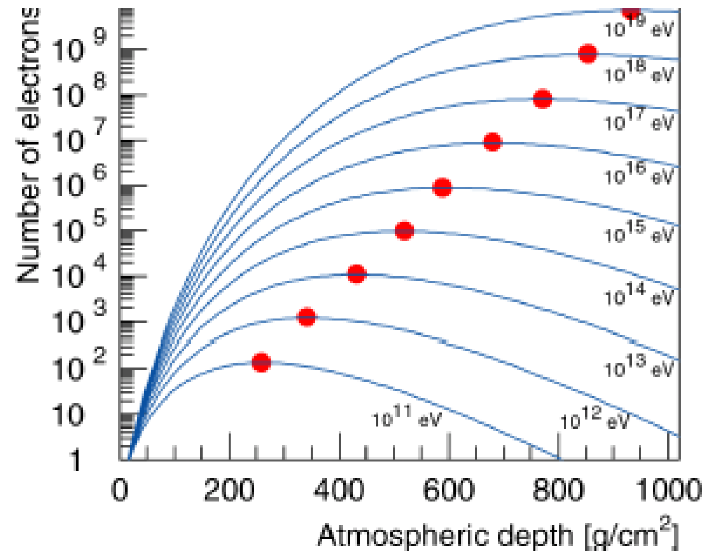

depth of shower maximum

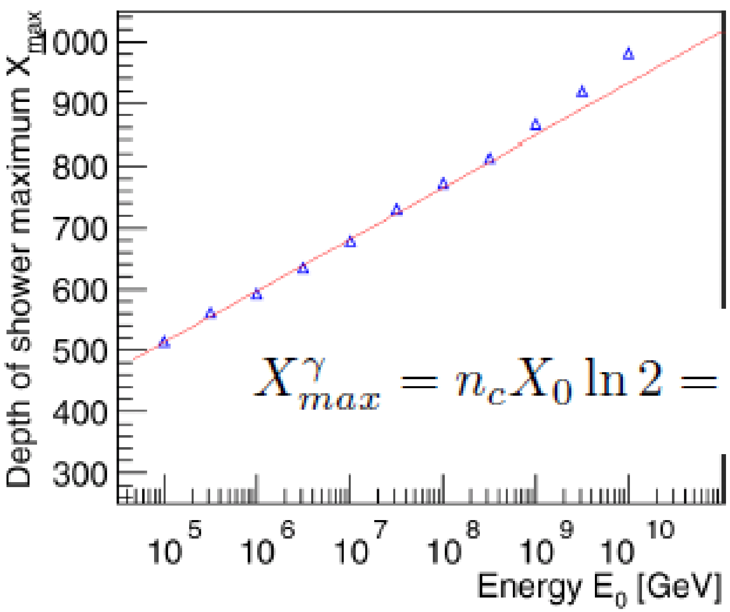

$$X_{max}^{\gamma} = n_c X_0 \ln 2 = X_0 \ln\left(\frac{E_0}{E_c^e}\right) \approx 597 \frac{\mathrm{g}}{\mathrm{cm}^2} + 84 \frac{\mathrm{g}}{\mathrm{cm}^2} \lg\left(\frac{E_0}{\mathrm{PeV}}\right)$$

JRH, Mod. Phys. Lett. A 22 (2007) 1533

A Heitler Model – Hadronic Cascades

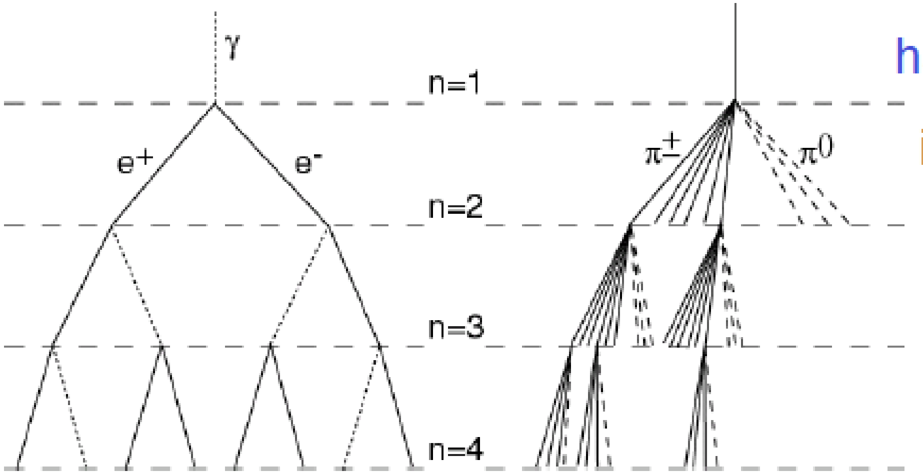

hadronic interaction $\pi + A \rightarrow \pi^0 + \pi^+ + \pi^-$

interaction length $\lambda_i^{\pi\text{-air}} \sim 120$ g/cm²

π → hadronic interaction
→ decay

„critical energy" $E_c^\pi \sim 20$ GeV

in each interaction $3/2 N_{ch}$ particles: N_{ch} π^{+-} and ½ N_{ch} π^0 $N_{ch} \sim 10$

after *n* interactions $N_\pi = (N_{ch})^n$ $E_\pi = \dfrac{E_0}{\left(\frac{3}{2}N_{ch}\right)^n}$

after n_c interactions $E_\pi = E_c^\pi$: $n_c = \dfrac{\ln E_0/E_c^\pi}{\ln \frac{3}{2}N_{ch}} = 0.85 \lg\left(\dfrac{E_0}{E_c^\pi}\right)$

superposition model

particle (E_0,A) → A proton showers with energy E_0/A

J. Matthews, Astrop. Phys. 22 (2005) 387

JRH, Mod. Phys. Lett. A 22 (2007) 1533

A Heitler Model – N_μ and N_e

Number of muons at shower maximum

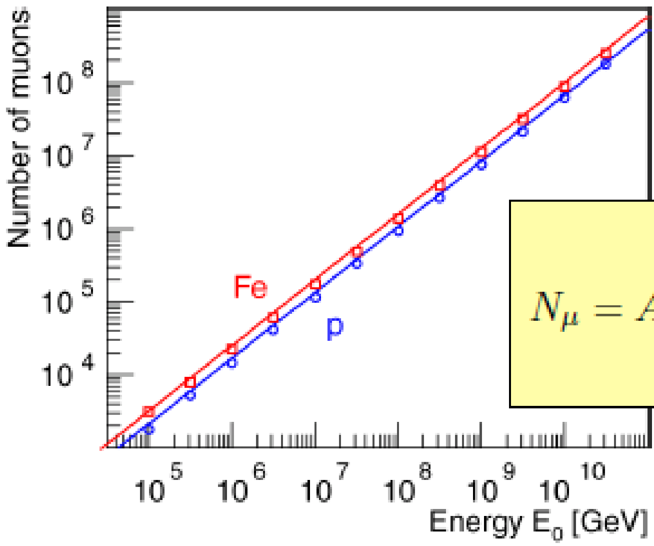

$$N_\mu = N_\pi = (N_{ch})^{n_c}$$

$$\ln N_\mu = n_c \ln N_{ch} = \beta \ln\left(\frac{E_0}{E_c^\pi}\right)$$

$$N_\mu = A\left(\frac{E_0}{AE_c^\pi}\right)^\beta = \left(\frac{E_0}{E_c^\pi}\right)^\beta A^{1-\beta} \approx 1.7\cdot 10^4 \cdot A^{0.10}\left(\frac{E_0}{1\ \mathrm{PeV}}\right)^{0.90}$$

Number of electrons at shower maximum

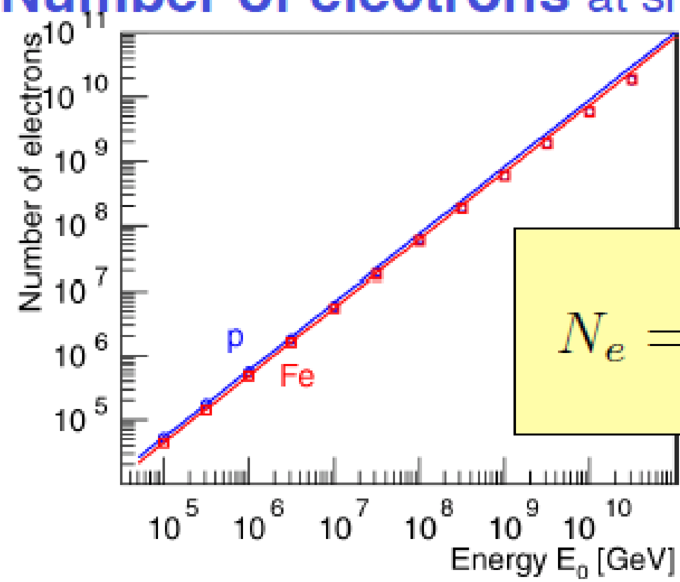

$$\frac{E_{em}}{E_0} = \frac{E_0 - N_\mu E_c^\pi}{E_0} = 1 - \left(\frac{E_0}{AE_c^\pi}\right)^{\beta-1}$$

$$N_e = \frac{E_{em}}{gE_c^e} \approx 6\cdot 10^5 \cdot A^{-0.046}\left(\frac{E_0}{1\ \mathrm{PeV}}\right)^{1.046}$$

JRH, Mod. Phys. Lett. A 22 (2007) 1533

A Heitler Model – N_μ vs. N_e

N_e-N_μ plane

$$N_\mu|_{A=const} \approx 0.18 A^{0.14} N_e^{0.86}$$

$$N_\mu|_{E_0=const} \approx 5.77 \cdot 10^{16} \left(\frac{E_0}{1\ \mathrm{PeV}}\right) N_e^{-2.17}$$

N_e-N_μ ratio

$$\frac{N_e}{N_\mu} \approx 35.1 \cdot \left(\frac{E_0}{A \cdot 1\ \mathrm{PeV}}\right)^{0.15}$$

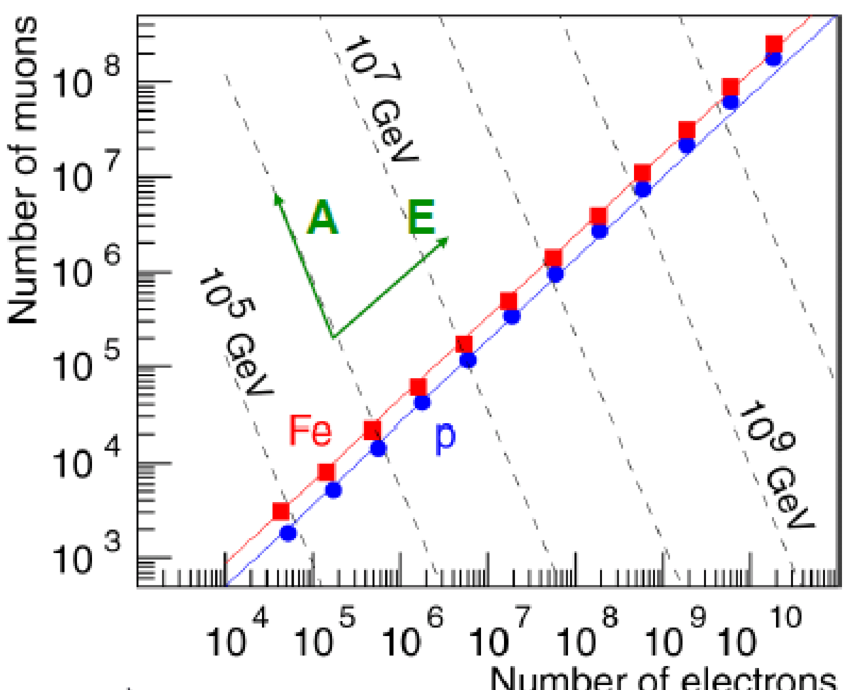

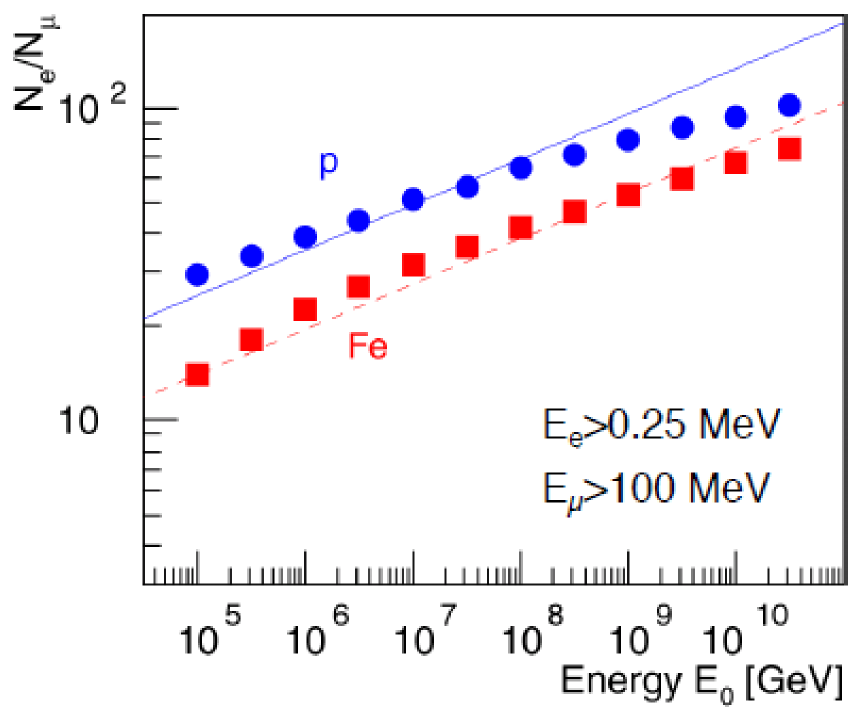

estimator for mass *A* of primary particle

JRH, Mod. Phys. Lett. A 22 (2007) 1533

A Heitler Model – X_{max}

$$X^p_{max} = \lambda_i^{p-air} \ln 2 + X_0 \ln\left(\frac{\kappa E_0}{3 N_{ch} E_c^e}\right)$$

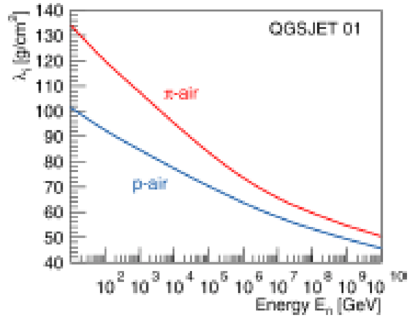

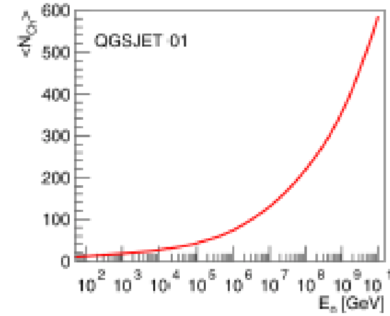

proton air interaction length $\lambda_i^{p-air} = \xi + \zeta \lg \frac{E_0}{\mathrm{PeV}}$

ζ=-4.88 g/cm²

multiplicity of charged particles produced in π-N interactions $N_{ch} = N_0 \left(\frac{E_0}{\mathrm{PeV}}\right)^\eta$ η=0.13

$$X^p_{max} = \xi \ln 2 - X_0 \left(\frac{3 N_0 E_c^e}{\kappa \cdot \mathrm{PeV}}\right) + \Lambda^p \lg\left(\frac{E_0}{\mathrm{PeV}}\right)$$

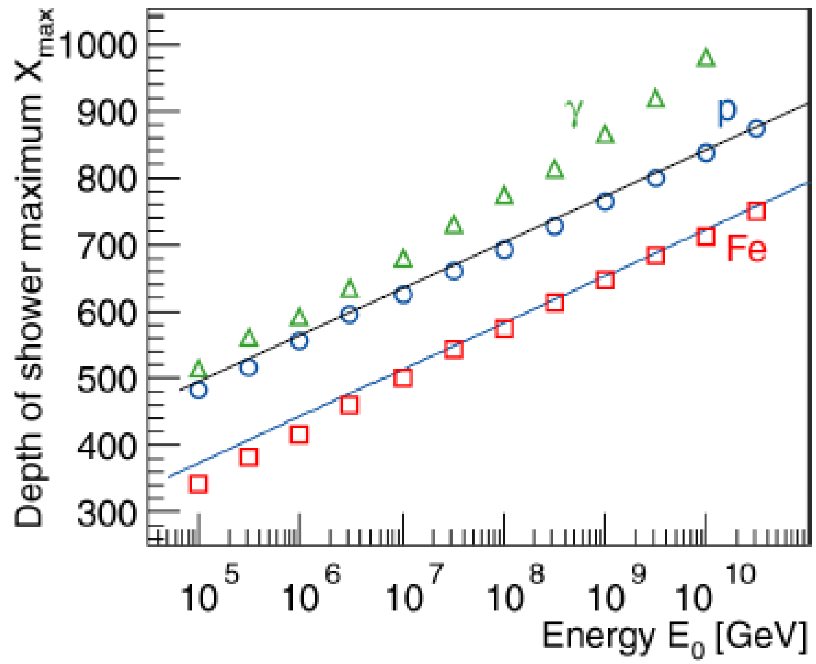

elongation rate

e/m shower $\Lambda^\gamma = X_0 \ln 10 \approx 84.4 \mathrm{g/cm}^2$

proton shower

$$\Lambda^p = X_0 \ln 10 - \eta X_0 \ln 10 + \zeta \ln 2 \approx 70 \mathrm{g/cm}^2$$

X_{max} for heavy nuclei

$$X^A_{max} = X^p_{max} - X_0 \ln A$$

➡ **estimator for mass *A* of primary particle**

JRH, Mod. Phys. Lett. A 22 (2007) 1533

J. Matthews, Astrop. Phys. 22 (2005) 387

KArlsruhe Shower Core and Array DEtector

Simultaneous measurement of
electromagnetic,
muonic,
hadronic
shower components

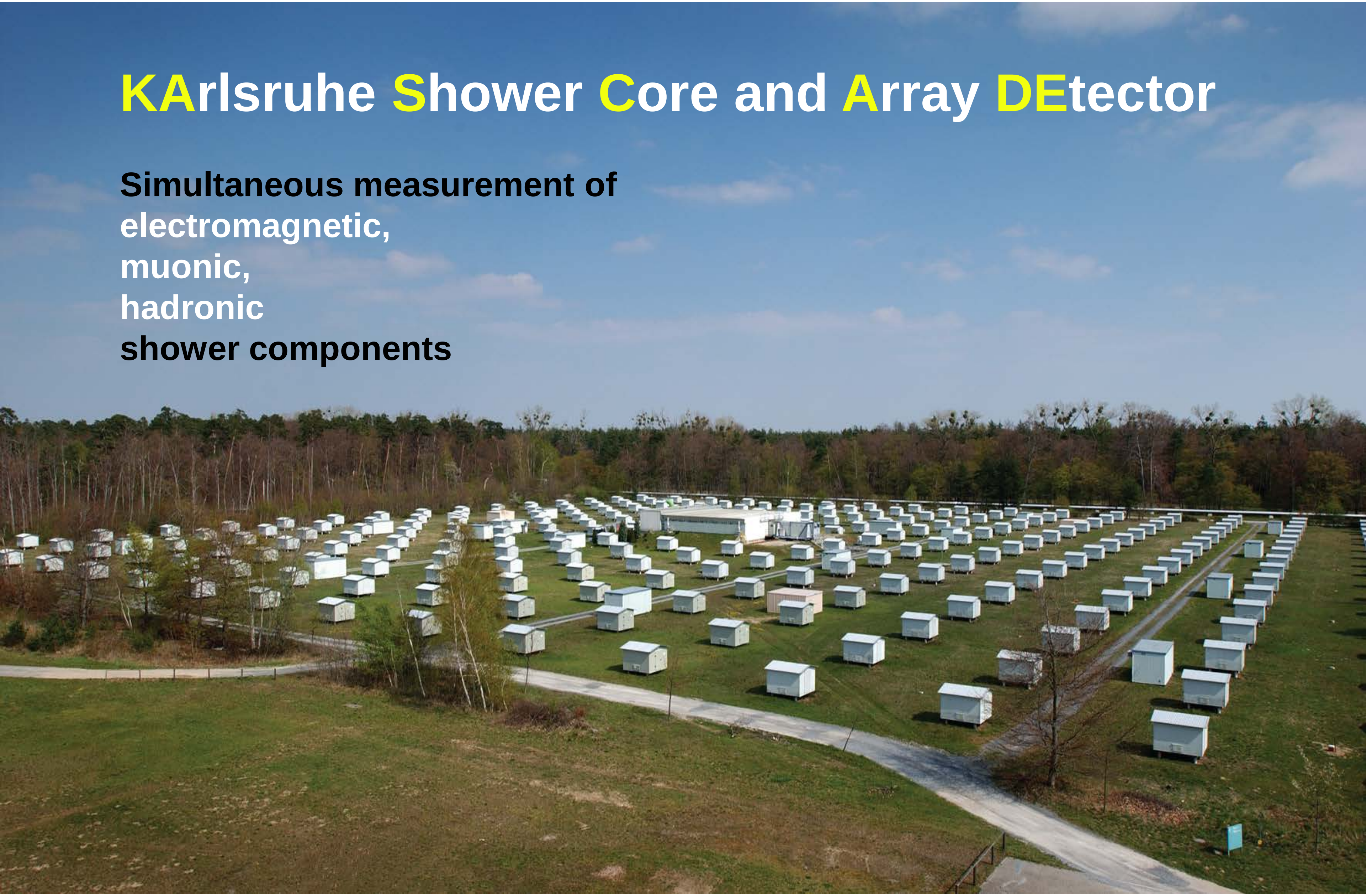

KArlsruhe Shower Core and Array DEtector

Simultaneous measurement of
electromagnetic,
muonic,
hadronic
shower components

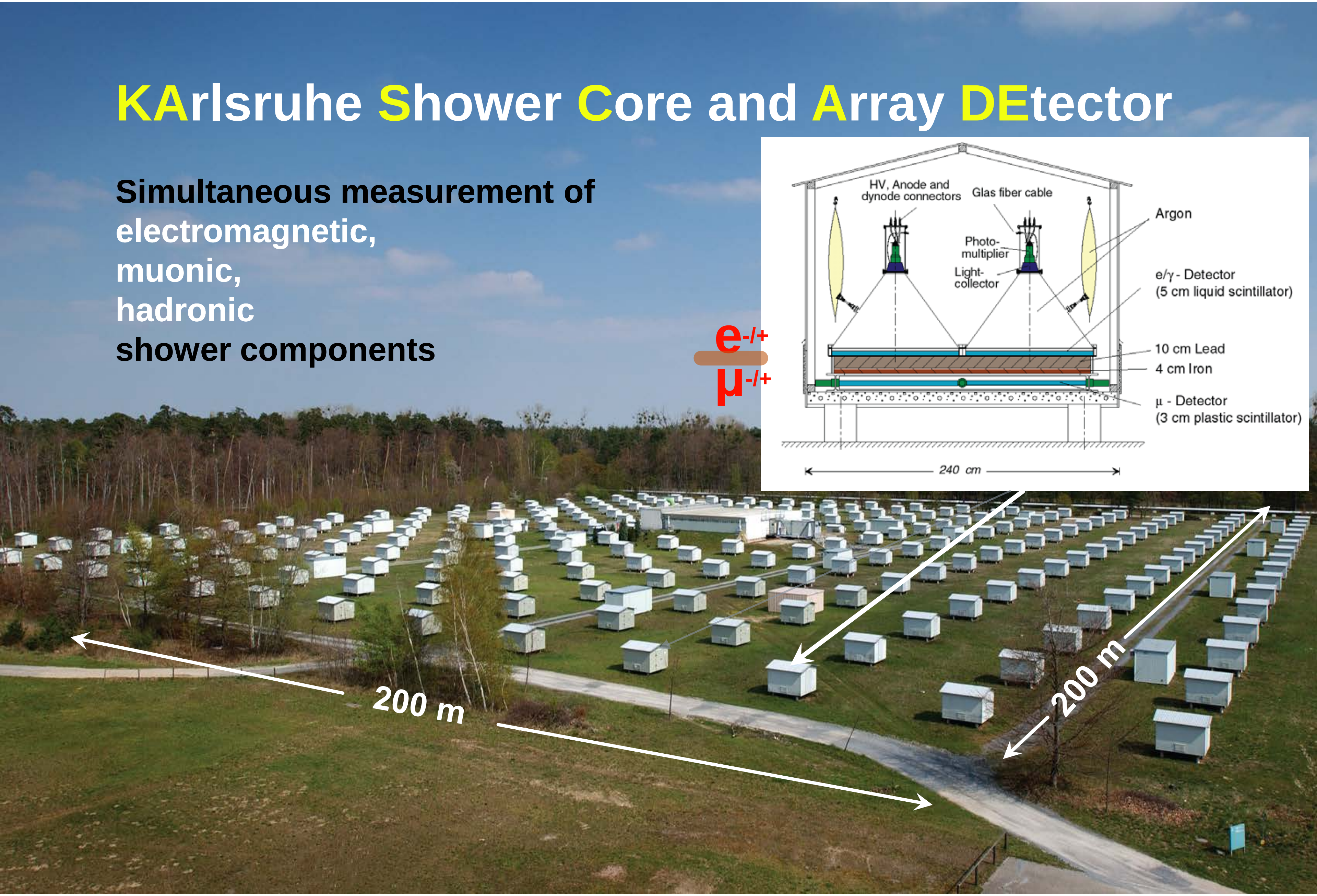

KASCADE Hadron Calorimeter

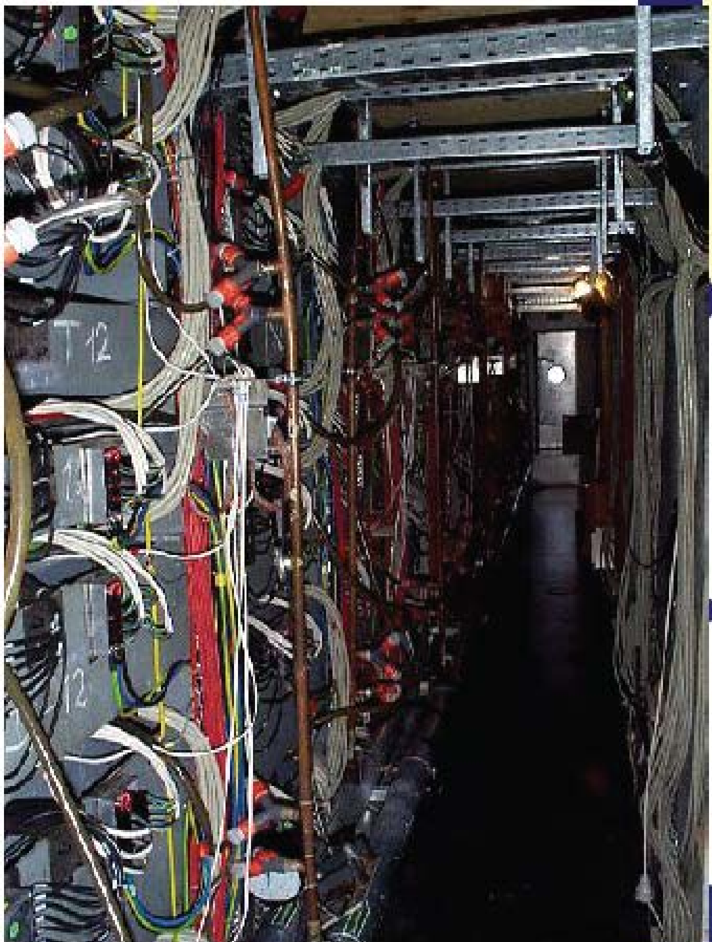

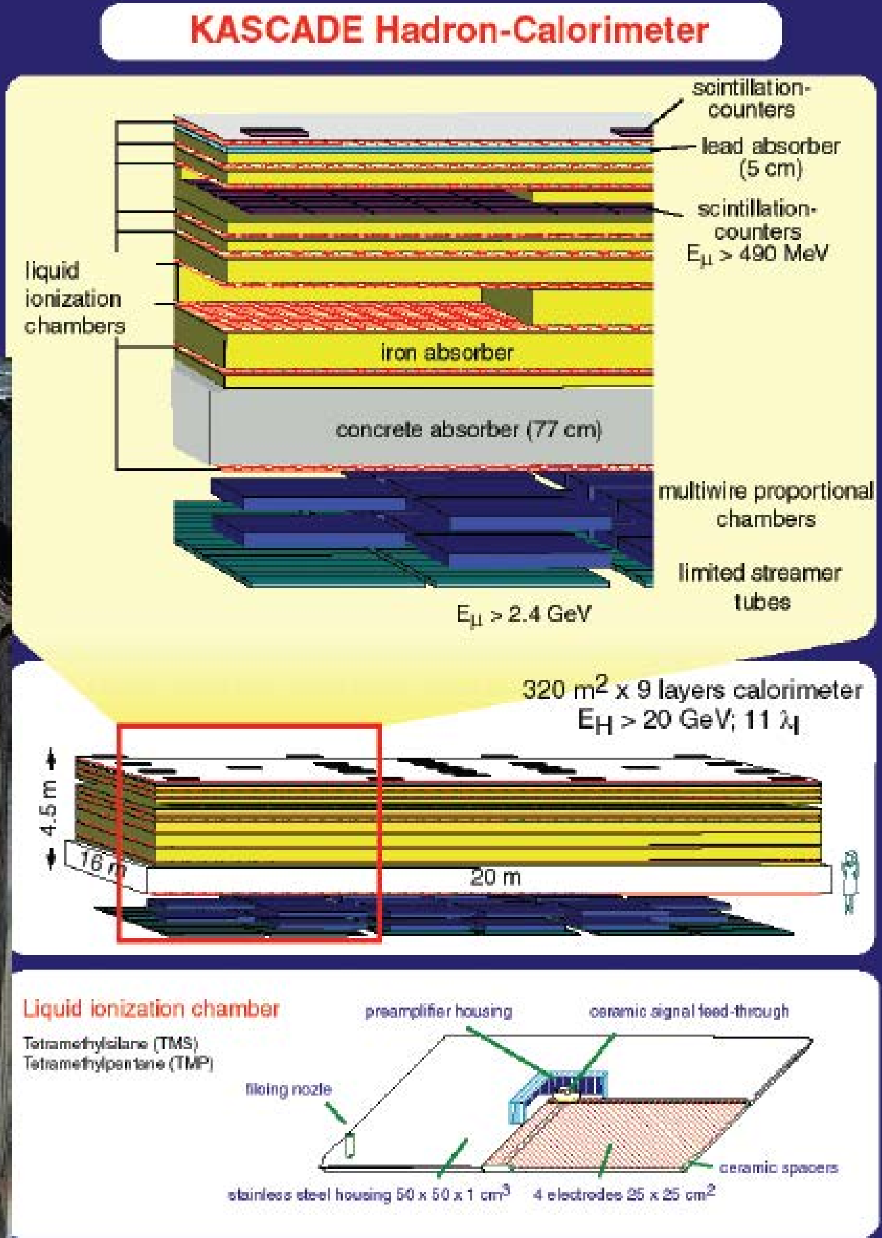

J. Engler et al., Nucl. Instr. Meth. A 427 (1999) 528

Reconstruction of hadrons

Unaccompanied hadron
E_H = 6.6 TeV

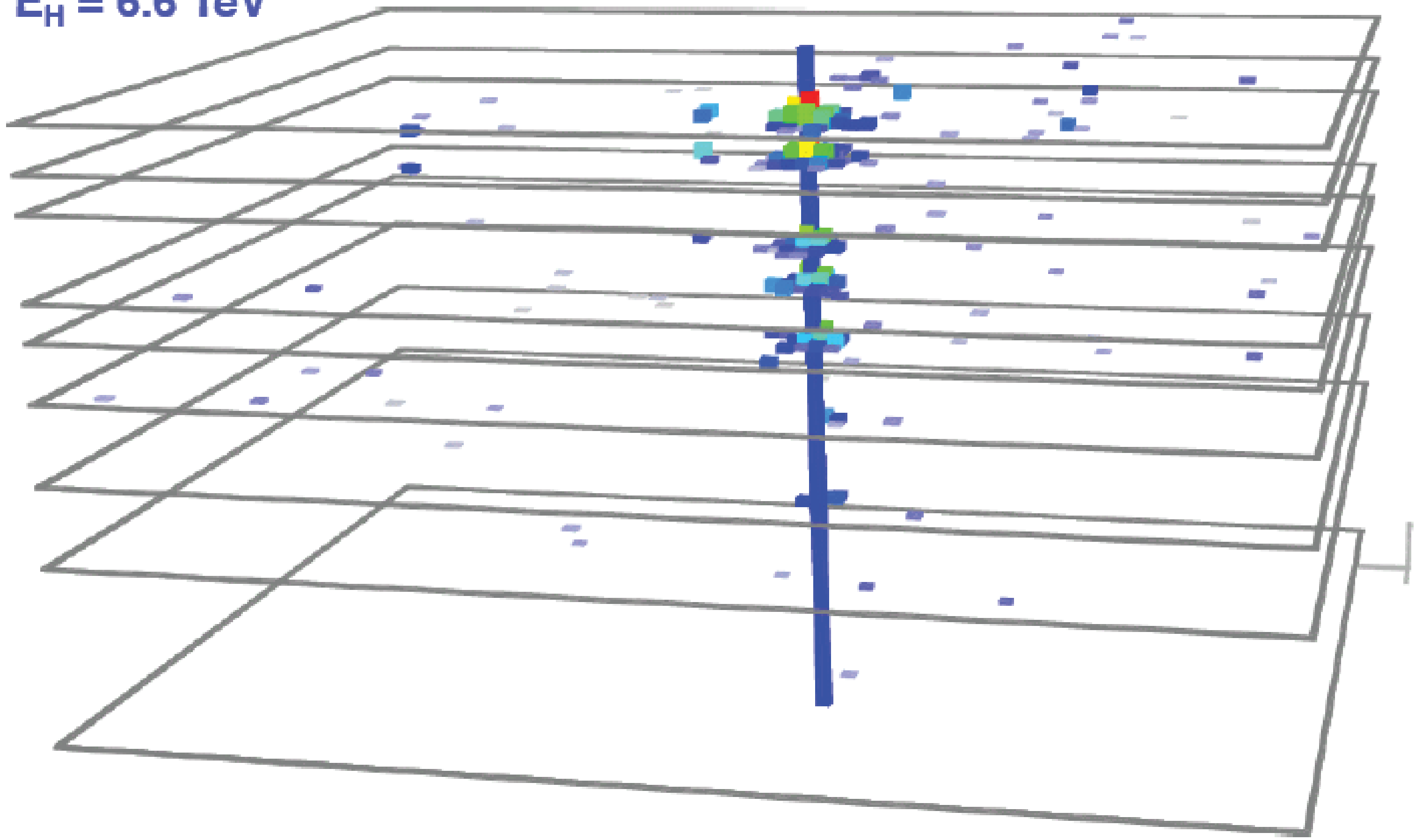

spatial resolution:

$\sigma_x \sim 10 - 12$ cm

angular resolution:

$\sigma_\theta \sim 1° - 3°$

energy resolution:

$$\frac{\sigma(E)}{E}[\%] \approx \frac{250}{\sqrt{E/\ \mathrm{GeV}}}$$

Hadronic shower core

$E_0 \sim 6$ PeV

Number of reconstructed hadrons $N_h = 143$

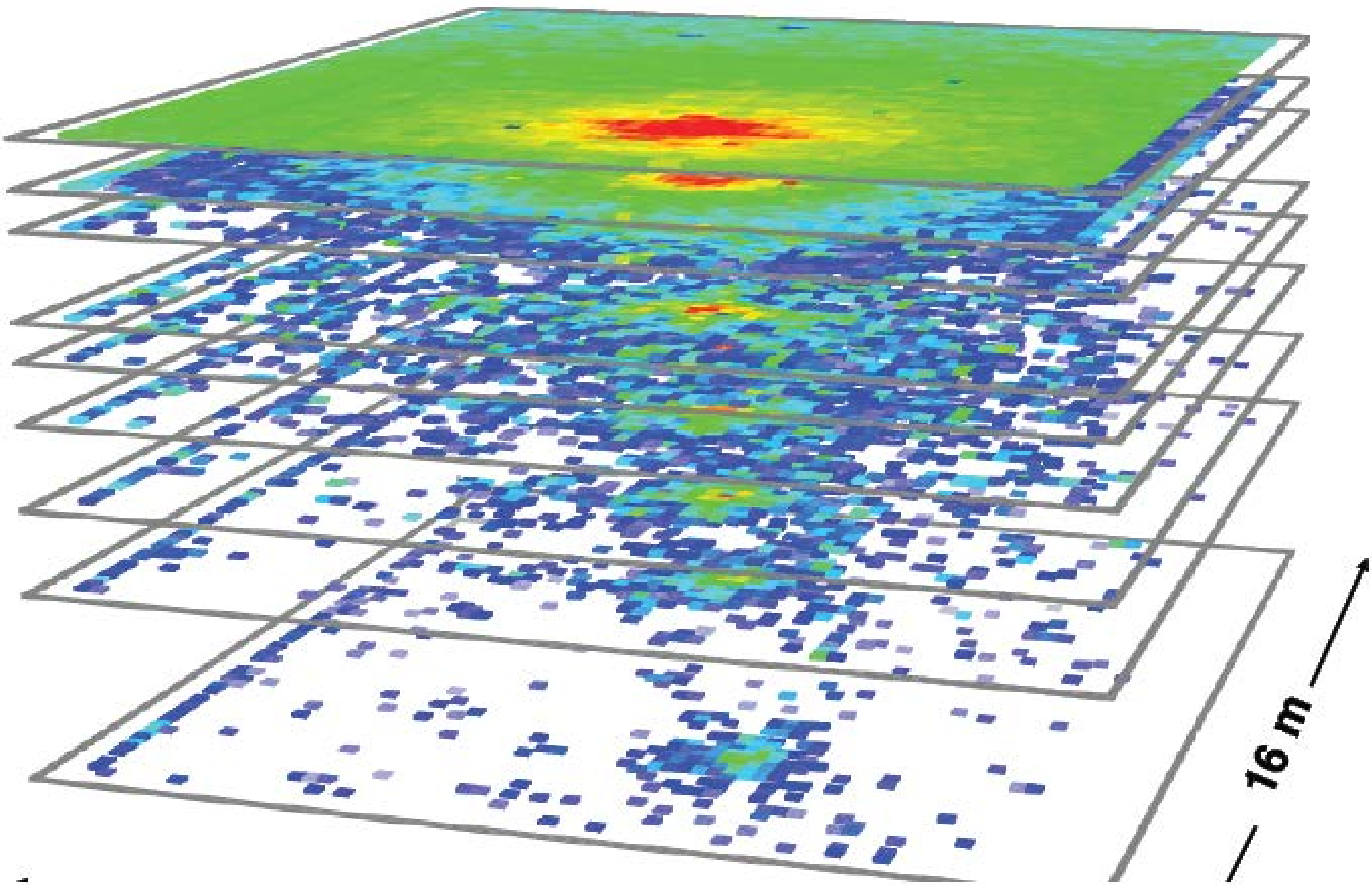

Hadronic shower core

$E_0 \sim 6$ PeV

Number of reconstructed hadrons $N_h = 143$

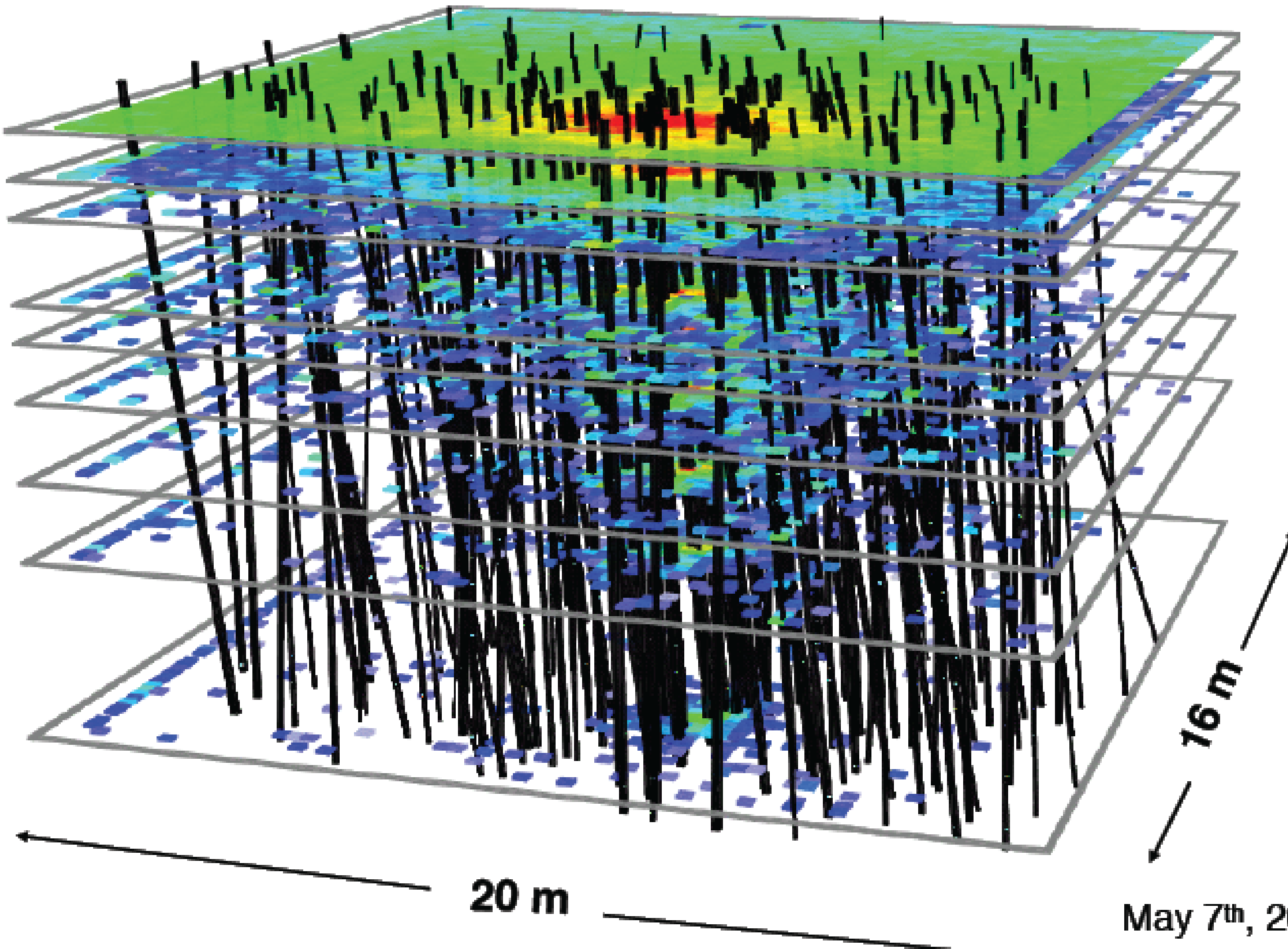

May 7th, 2002 9:45

Muon production height – KASCADE muon tracking detector

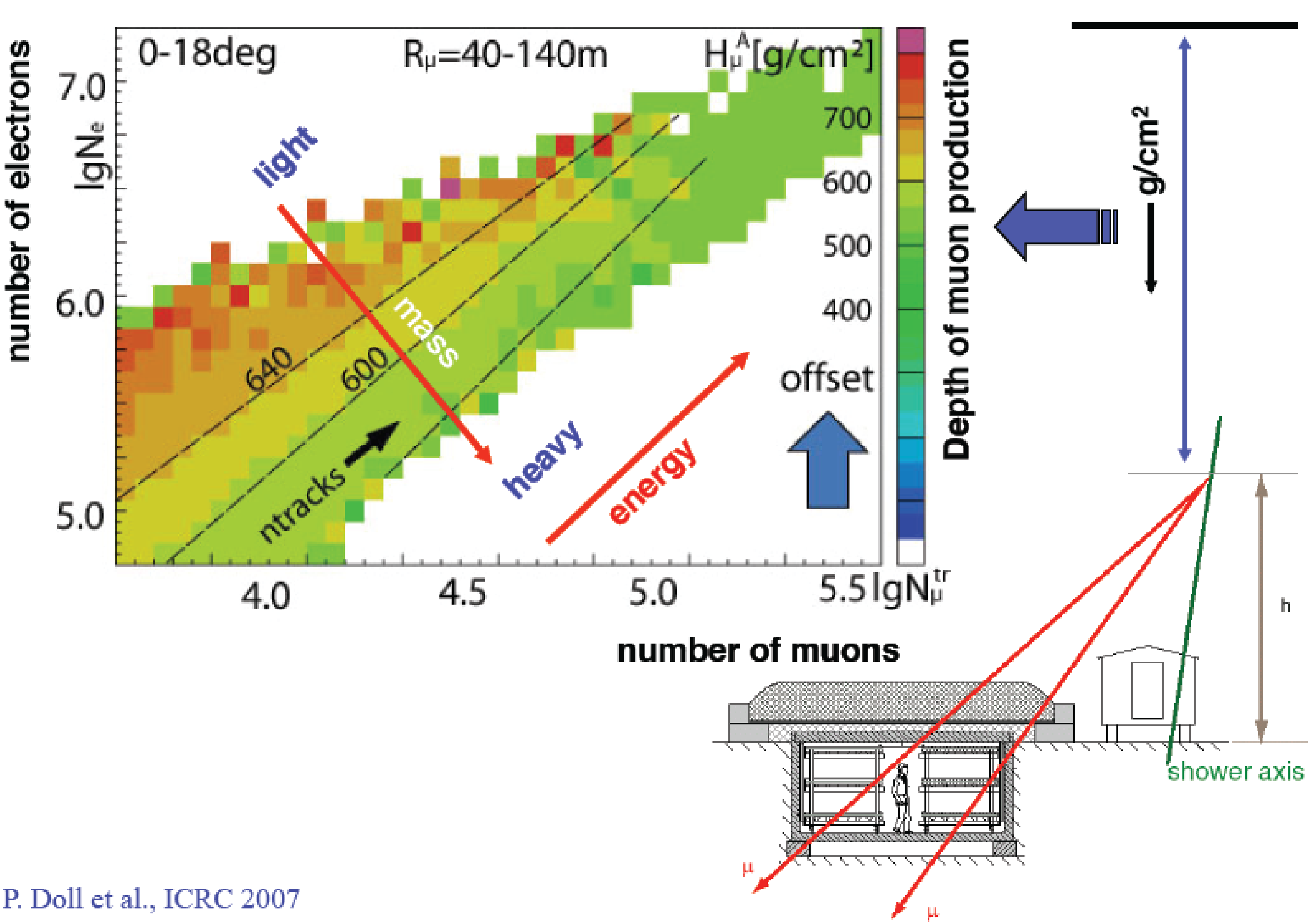

P. Doll et al., ICRC 2007

KASCADE observables – per single air-shower !

from detector array:

- shower direction Θ , ϕ
- shower core X_o , Y_o
- shower size N_e
- truncated (40m-200m) muon number N_μ^{tr}
- lateral particle distribution s, R_m

from calorimeter:

- number of reconstructed hadrons (E_h>100GeV) N_h^*
- sum of the reconstructed hadronic energy E_h^*
- energy of the leading hadron E_h^{max}
- parameters of the spatial hadron distributions λ,....

from central detector muon systems: (MWPC -LST- trigger plane)

- number of reconstructed muons (E_μ>2.4GeV) N_μ^* and local muon density ρ_μ^*
- number of reconstructed muons (E_μ>490MeV) N_μ^{tp} and ρ_μ^{tp}
- parameters of hit pattern: multifractal moments D_6 , D_{-6}
- arrival times of muons τ_μ

from Muon Tracking Detector:

- number of reconstructed muons (E_μ>800MeV) N_μ^{mtd} and ρ_μ^{mtd}
- angel of muons: tangential and radial angle: τ_μ , ρ_μ

Concept KASCADE-Grande

- Disententanglement of the threefold problem: E, A, interaction
- Measure shower parameters as much as possible
- Multi-detector system to get redundant information

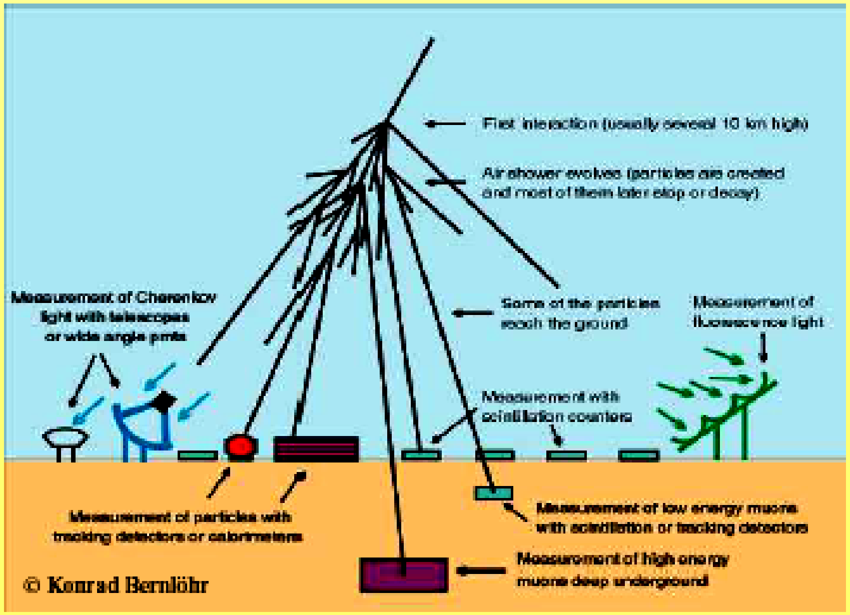

Experiment | **Simulation**

Primary Energy E
Primary Particle A

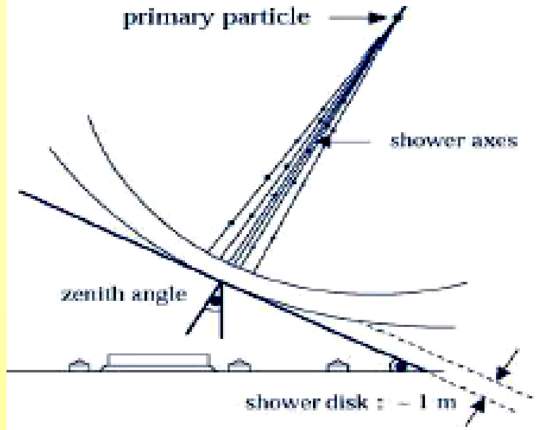

CORSIKA

DPMJET
QGSJET
SYBILL
VENUS
...

CRES

Detector-Response

Data Acquisition

KRETA

Reconstruction of EAS-Observables
e.g. N_e, N_h, N_μ , Lateral Distributions, ...

Comparisons
of the distributions
Neural Nets, Bayes Classifier

E_{est} A_{est}

Energy Spectra
Chemical Composition

Tests of
High-Energy
Interaction Models

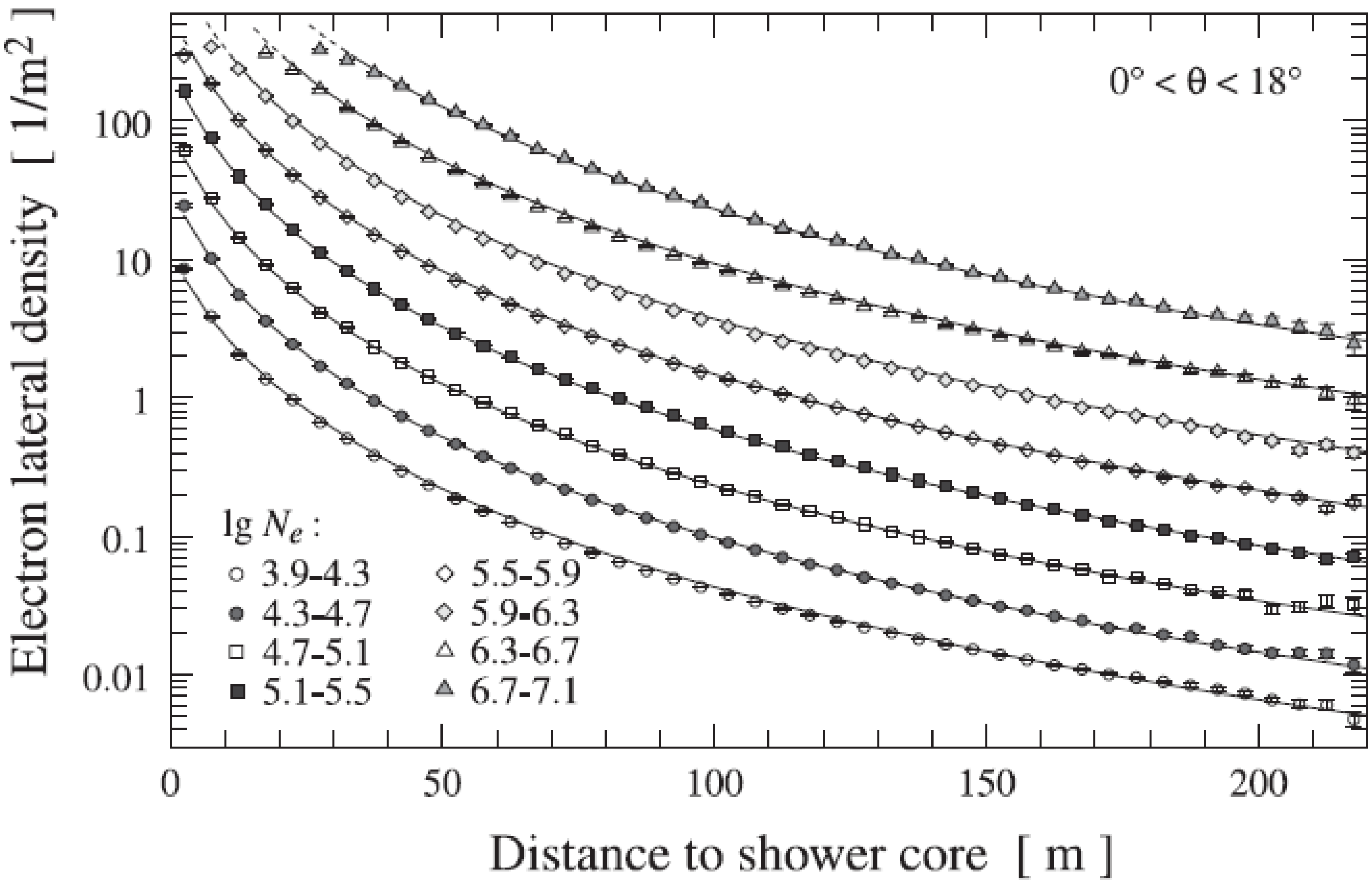

Fig. 2. Lateral distributions of electrons above a 5 MeV kinetic energy for zenith angles below 18°. The lines show NKG functions of fixed age parameter $s = 1.65$ but varying scale radius r_e (see the text).

KASCADE-Grande – Lateral distributions

NKG function

$$\rho(r,s,N_e) = \frac{N_e}{r_M^2}\frac{\Gamma(4.5-s)}{2\pi\Gamma(s)\Gamma(4.5-2s)}\left(\frac{r}{r_M}\right)^{s-2}\left(1+\frac{r}{r_M}\right)^{s-4.5}$$

Molier radius $r_M \approx 0.25\ X_0 \sim 80$ m for $e^{\pm}$

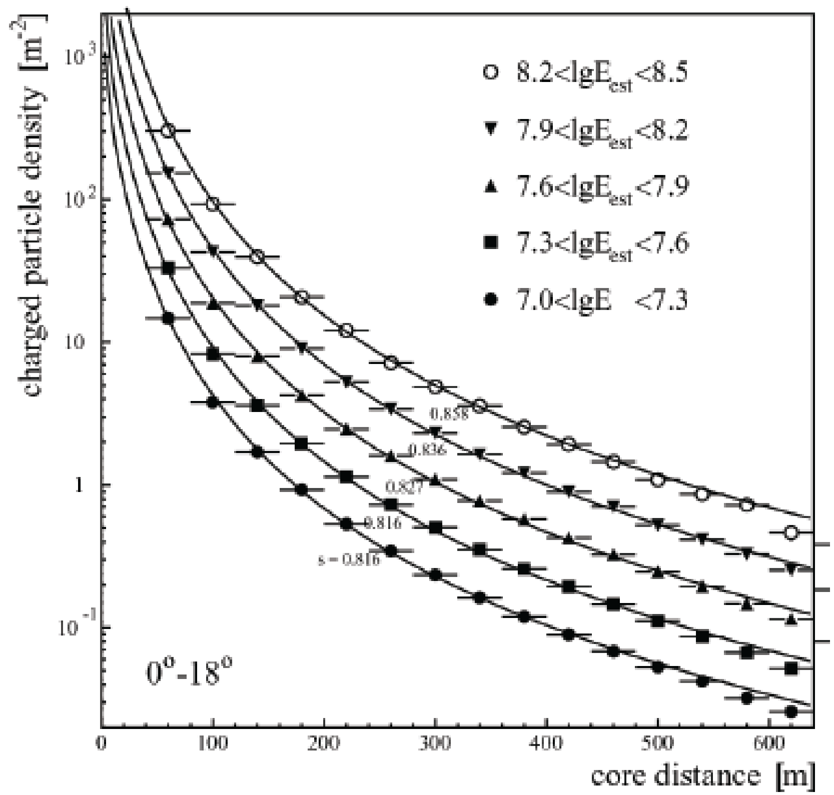

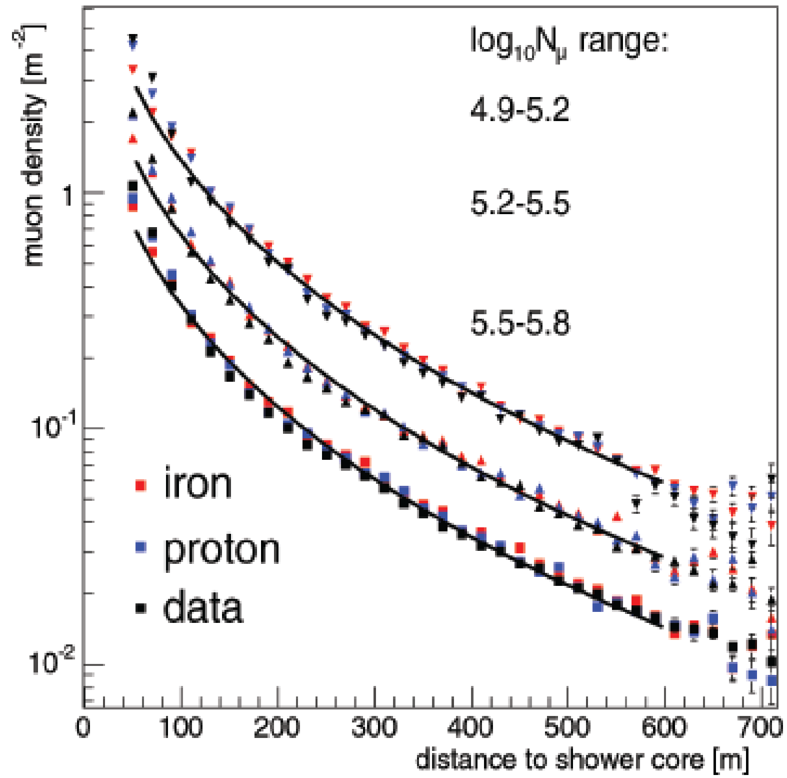

R. Glasstetter et al., Proc. 29th ICRC, Pune 6 (2005) 293

J. v. Buren et al., Proc. 29th ICRC, Pune 6 (2005) 301

KASCADE-Grande – Lateral distributions

NKG fu

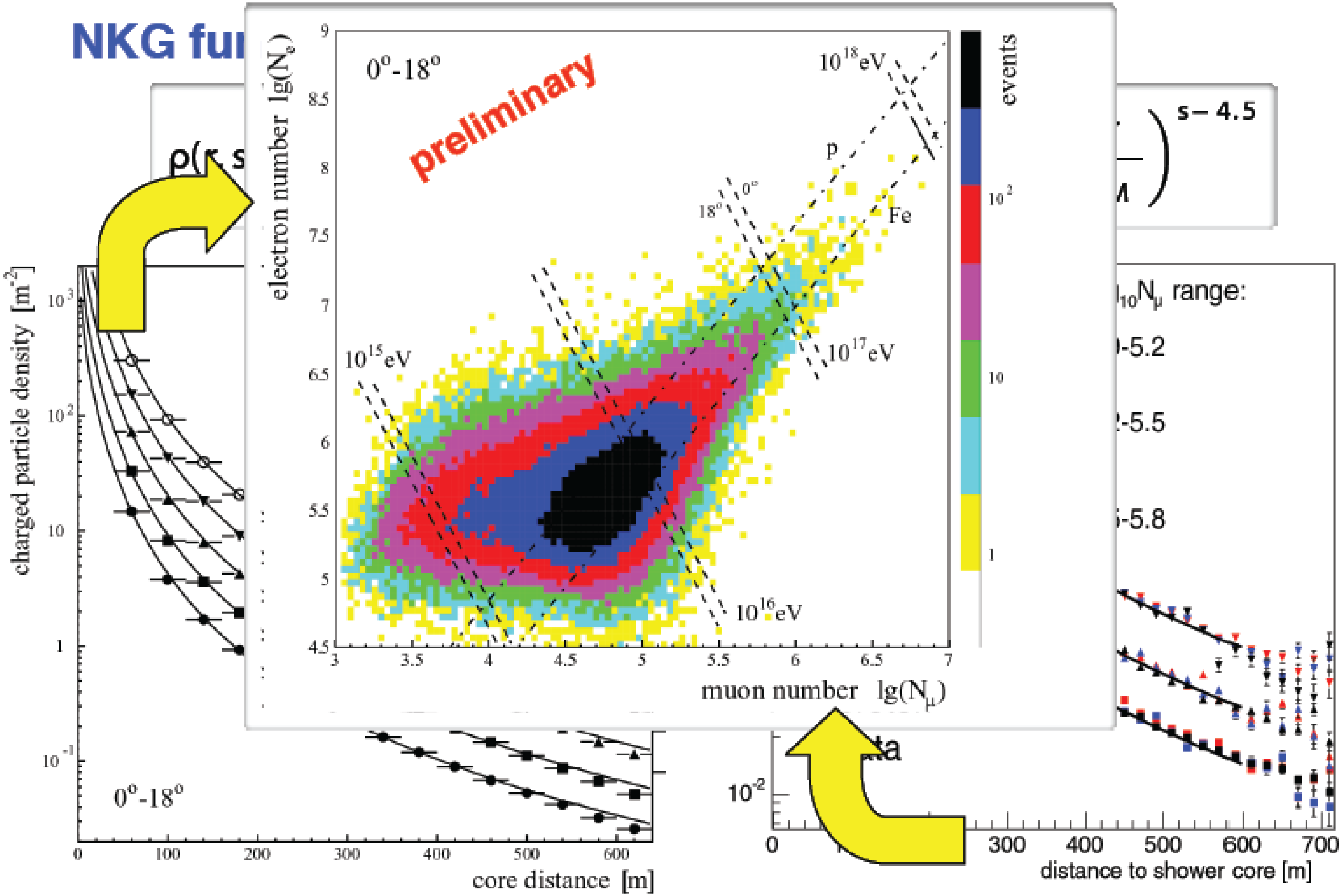

R. Glasstetter et al., Proc. 29th ICRC, Pune 6 (2005) 293

J. v. Buren et al., Proc. 29th ICRC, Pune 6 (2005) 301

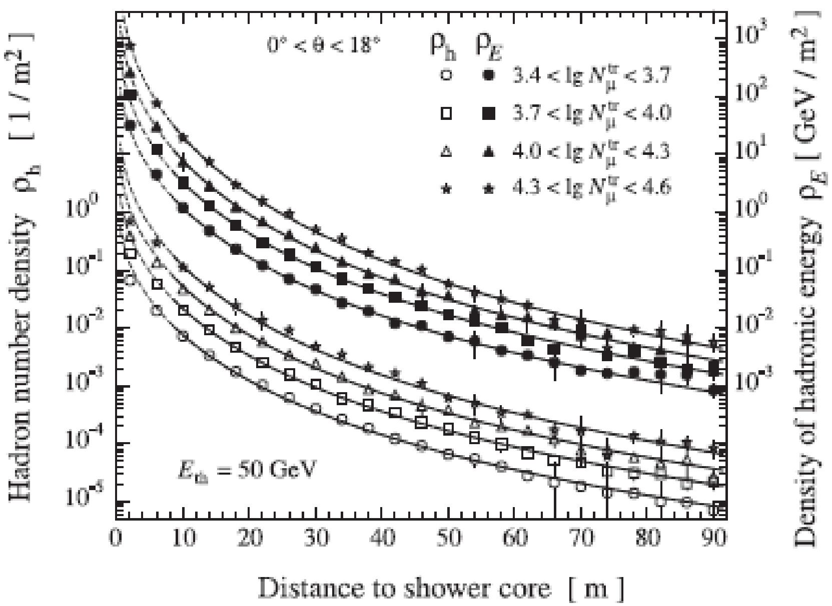

Fig. 12. Density of hadron number (left scale, open symbols) and of hadronic energy (right scale, filled symbols) versus the core distance for showers of truncated muon numbers as indicated. Threshold energy for hadrons is 50 GeV. The curves represent fits of the NKG formula to the data at $r \geqslant 8$ m with a radius fixed to $r_h = 10$ m.

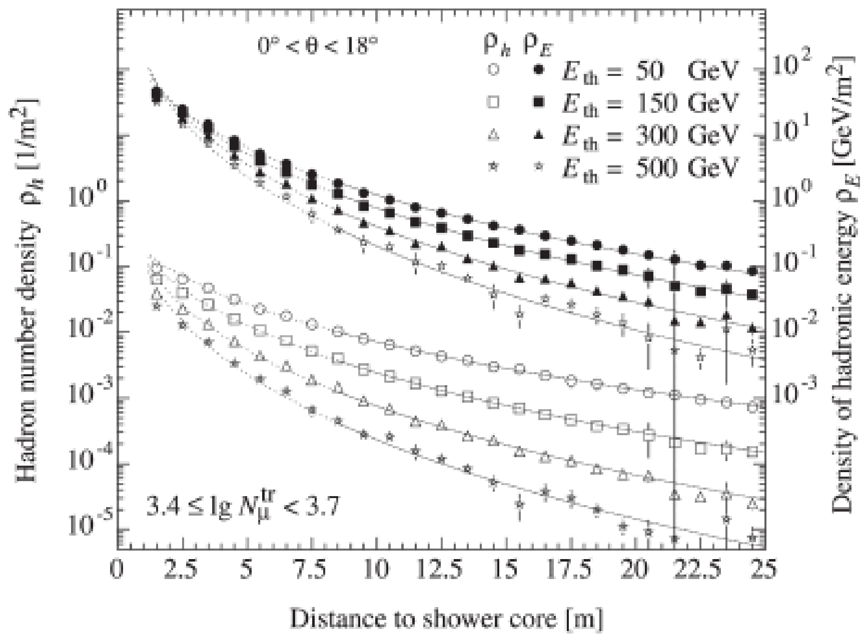

Fig. 14. Density of hadron number (left scale, open symbols) and of hadronic energy (right scale, filled symbols) versus shower core distance for various thresholds of hadron energy. The curves represent fits of the data to the NKG function as in Fig. 12.

YangBaJing Observatory and its Experiments

- Located at an elevation of 4300 m (Yangbajing , China)
- Atmospheric depth 606g/cm^2
- Wide field of view
- High duty cycle (>90%)

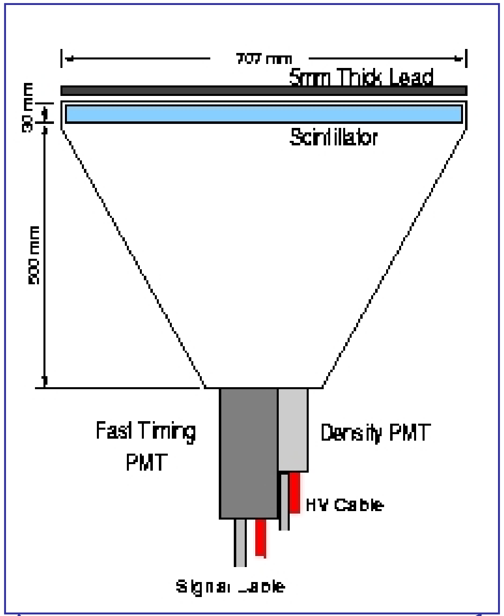

ASγ air shower array

ARGO Experimental Hall

Tibet Air Shower Array

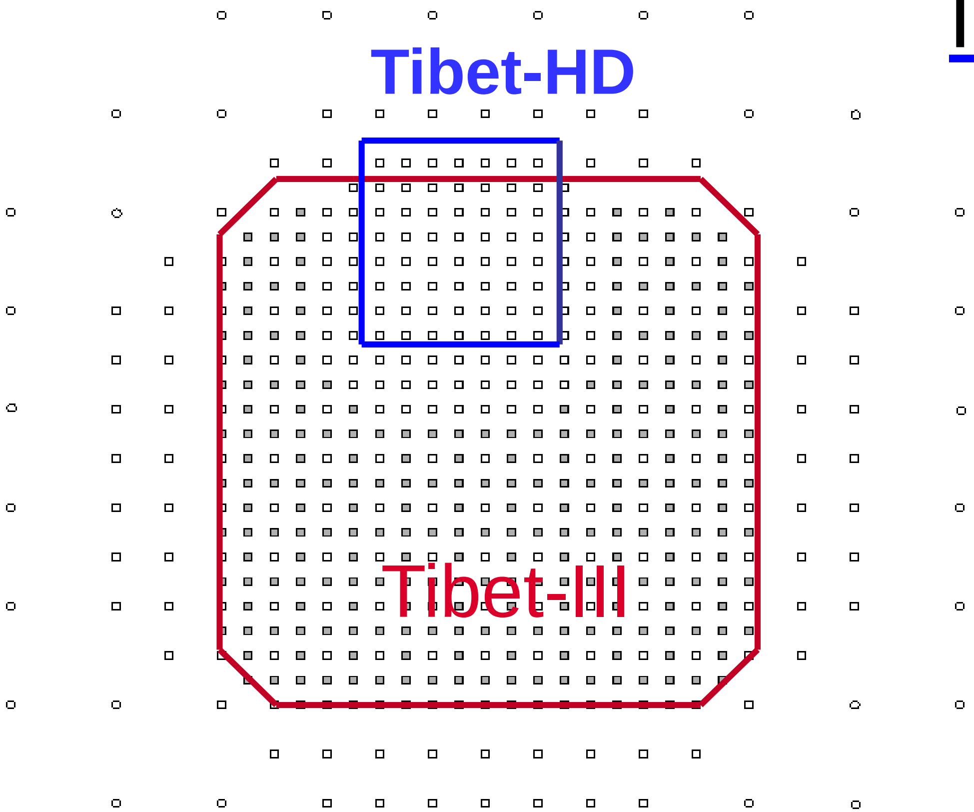

Tibet array: ~250 x 250 m^2

HD: 60 x 60m^2

Tibet-III: ~150x150 m^2

	Operation Time	Live Time	Selected Events	Mode Energy	Resolution (@3TeV)	Area
Tibet-HD	1997.2~1999.9	555.9 days	1.5×10^9	~3TeV	0.9^o	3600m^2
Tibet-III	1999.11~2001.5	456.8 days	5.5×10^9	~3TeV	0.9^o	22050m^2

Resistive Plate Chambers carpet

The ARGO-YBJ detector

Single layer of RPCs detectors

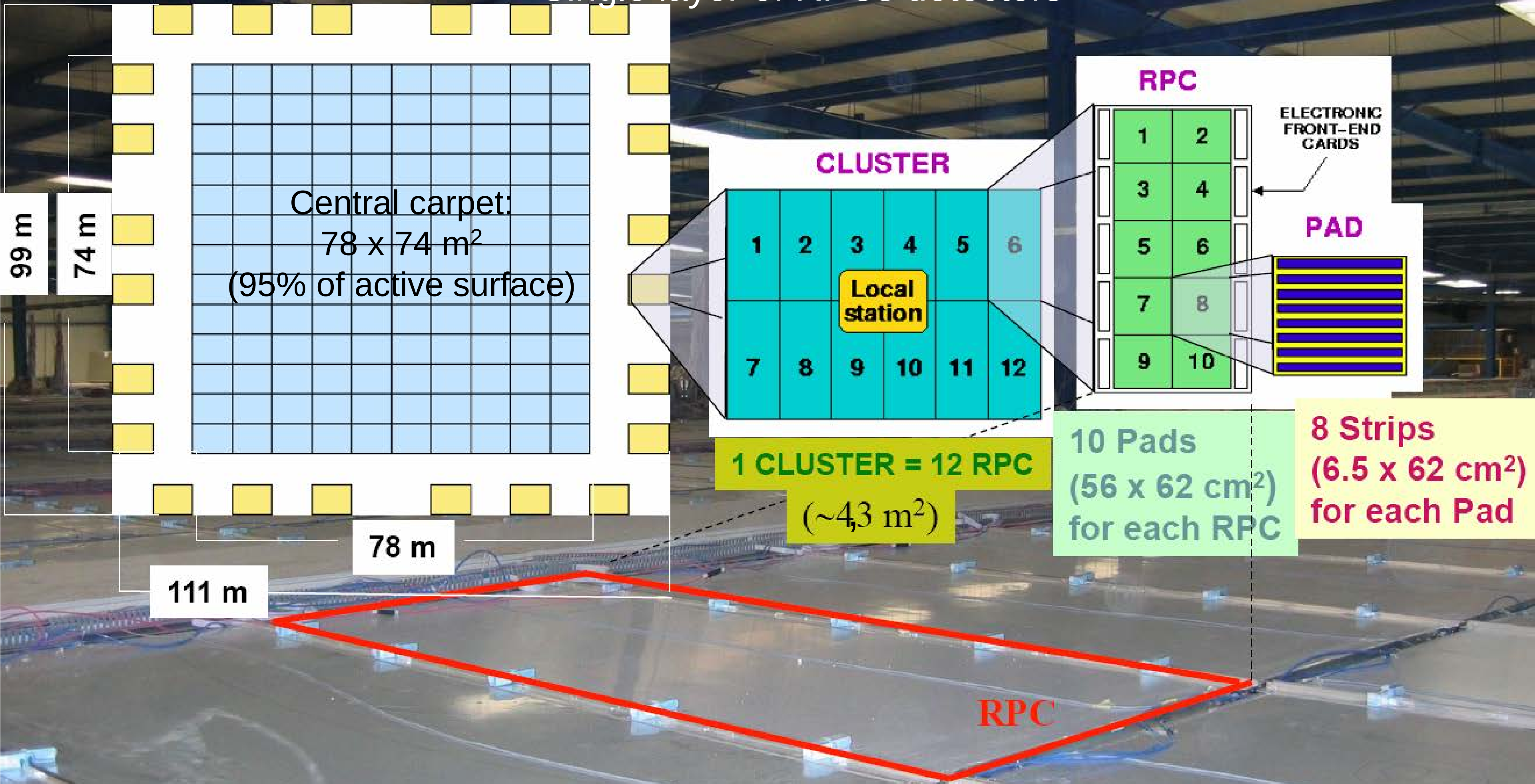

Strip counting

Pad = space-time pixel

Time resolution ~1.7 ns

Trigger requirement:
at least 20 particles on the carpet

+ Analog charge read-out on “Big Pads”

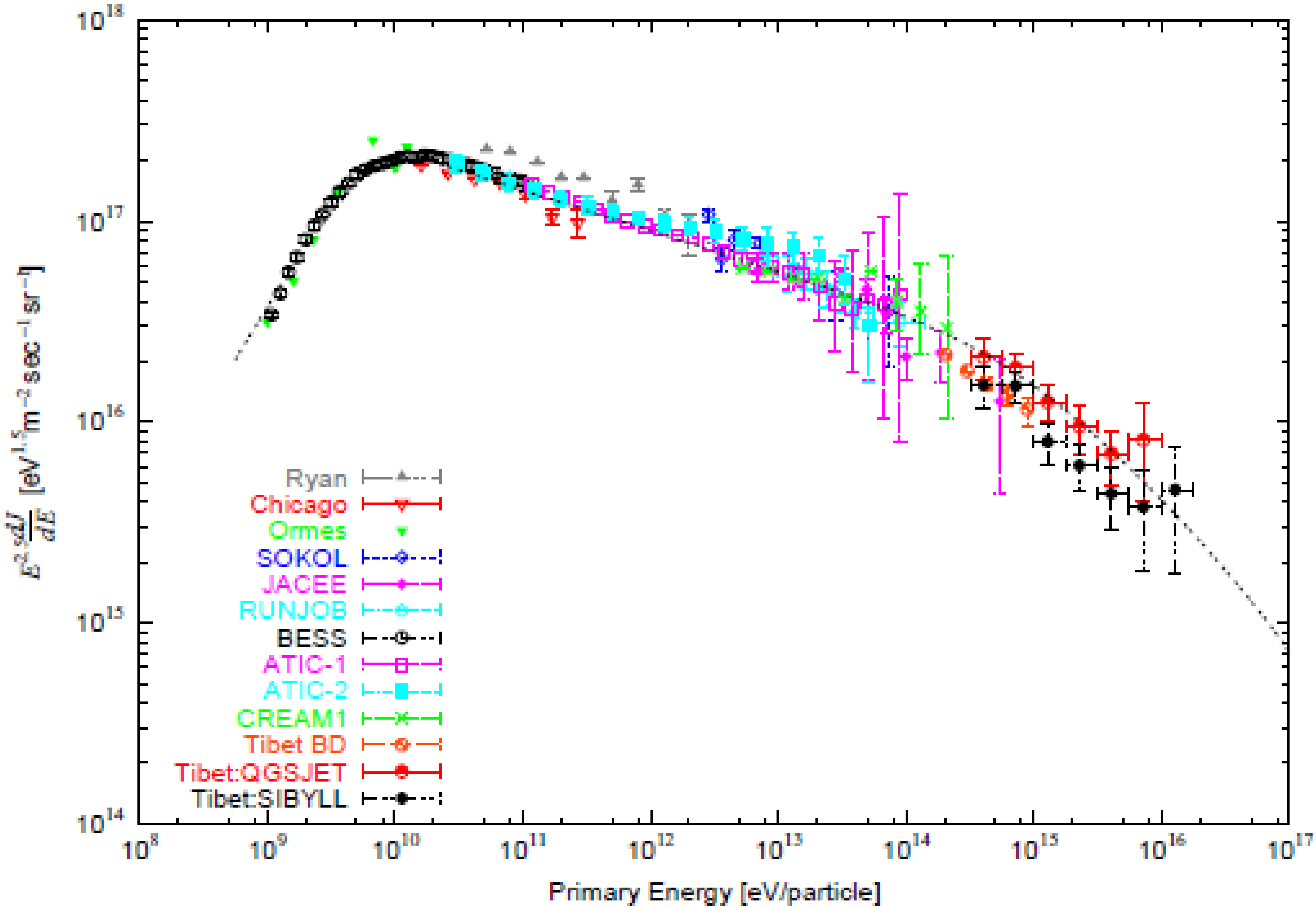

Fig. 1. Proton spectrum obtained by Tibet Hybrid Experiment and direct observations. Solid line is the broken power law spectrum with $\varepsilon_b = 7\times10^{14}$ eV and $\Delta\gamma = 0.4$.

Tunka Experiment

Lateral distribution of Cerenkov light

$$C(r) = \begin{cases} C_{120} \times \exp(s[120\,\mathrm{m} - r]) & 30\ \mathrm{m} < r < 120\ \mathrm{m} \\ C_{120} \times (r/120\,\mathrm{m})^{-a} & 120\ \mathrm{m} < r < 350\ \mathrm{m} \end{cases}$$

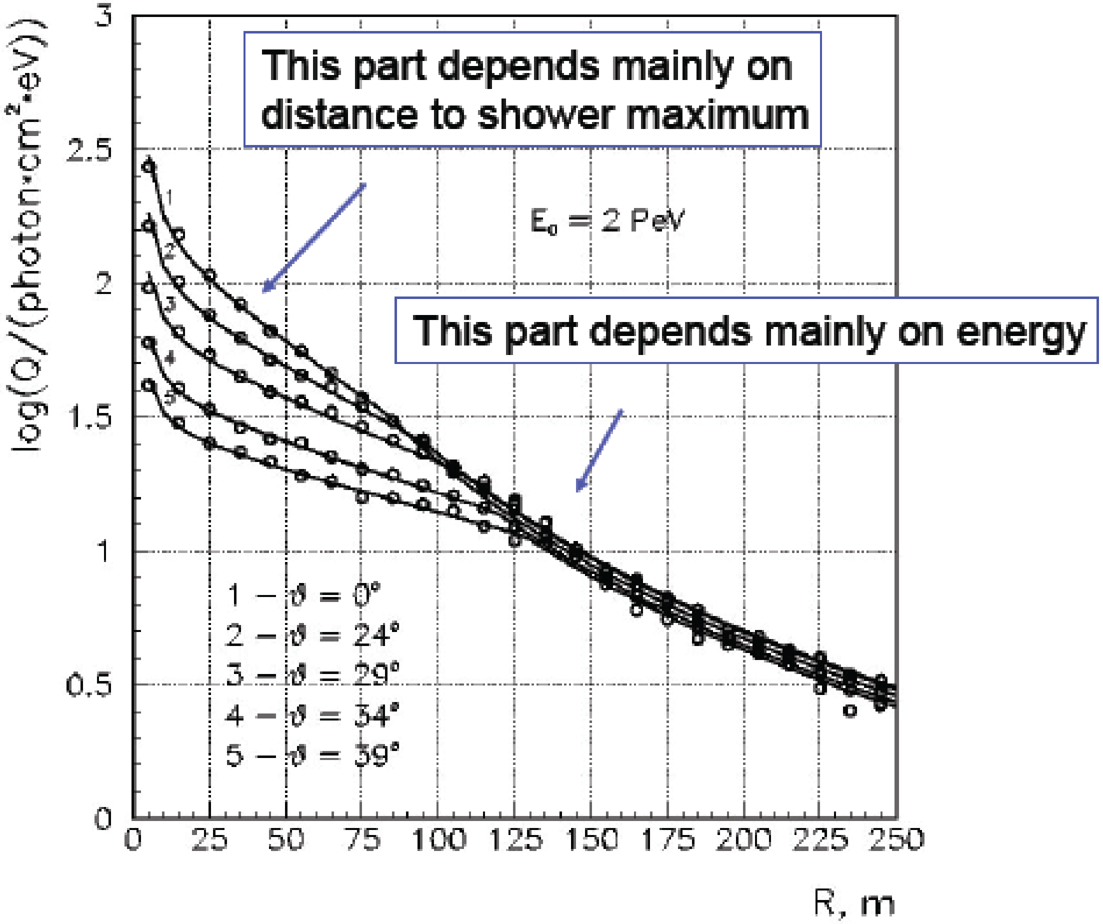

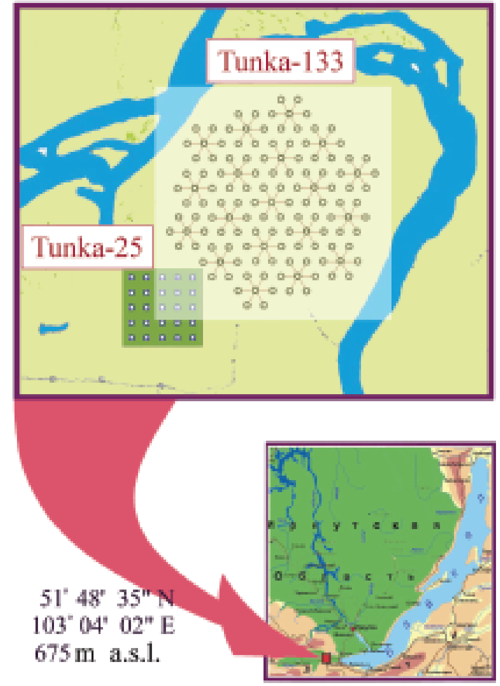

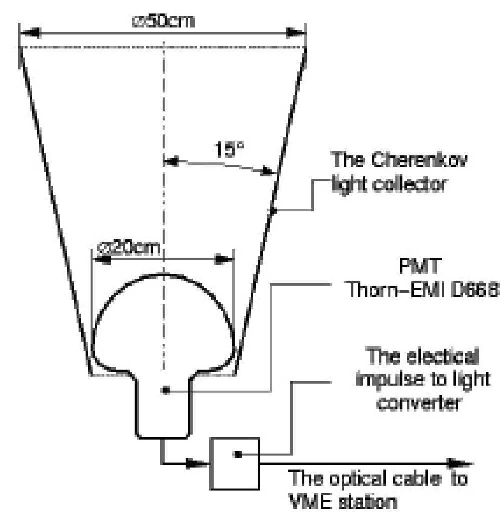

Cherenkov radiation

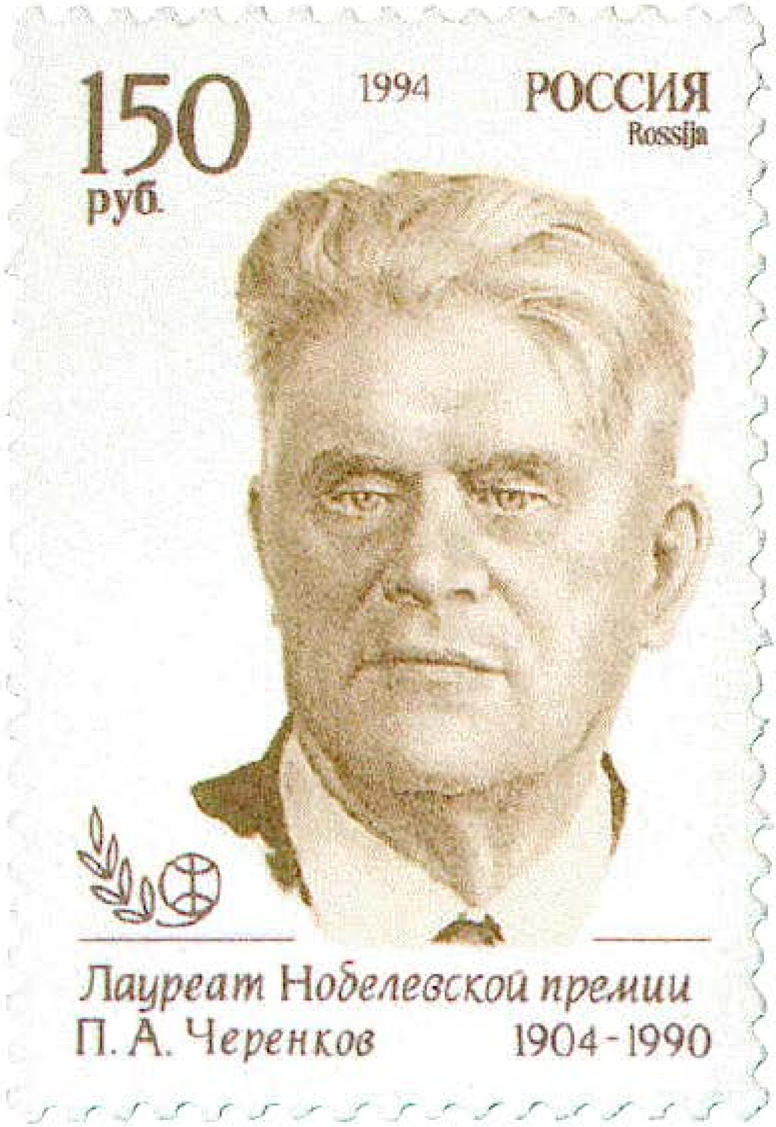

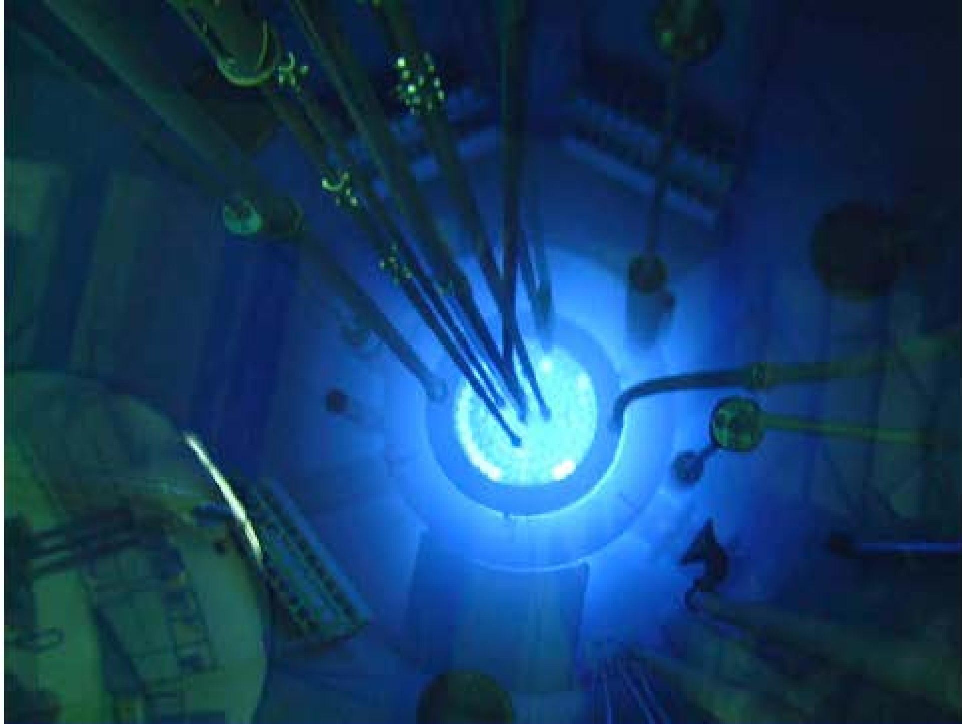

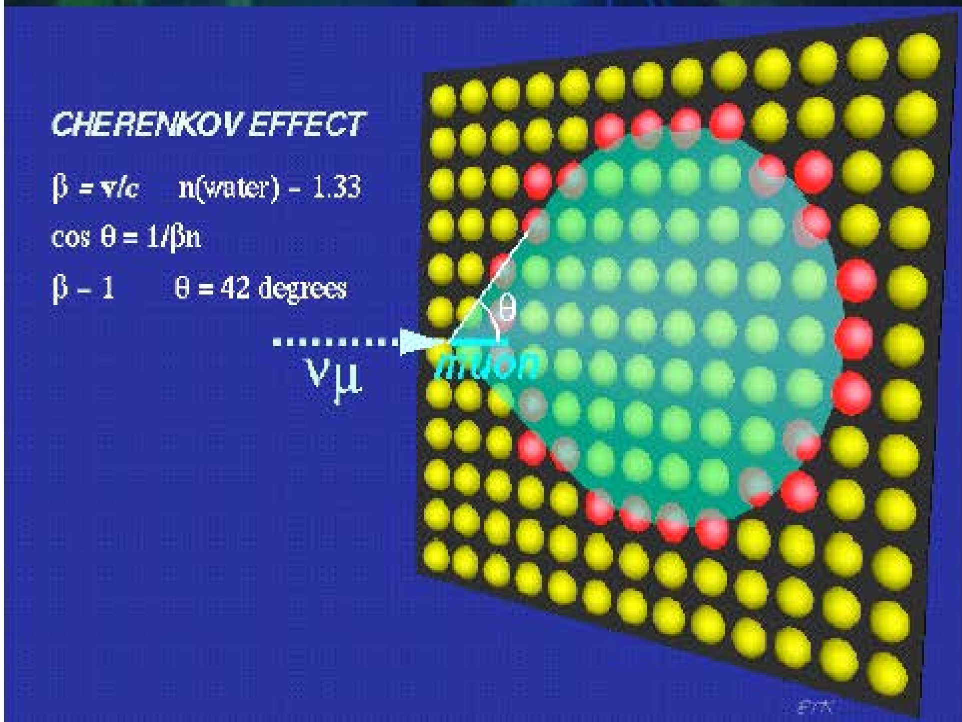

NOBEL PRIZE WINNERS OF LPI

The Pierre Auger Observatory

ΔE = 18% stat. 22% syst.

$\Delta\Theta < 1°$

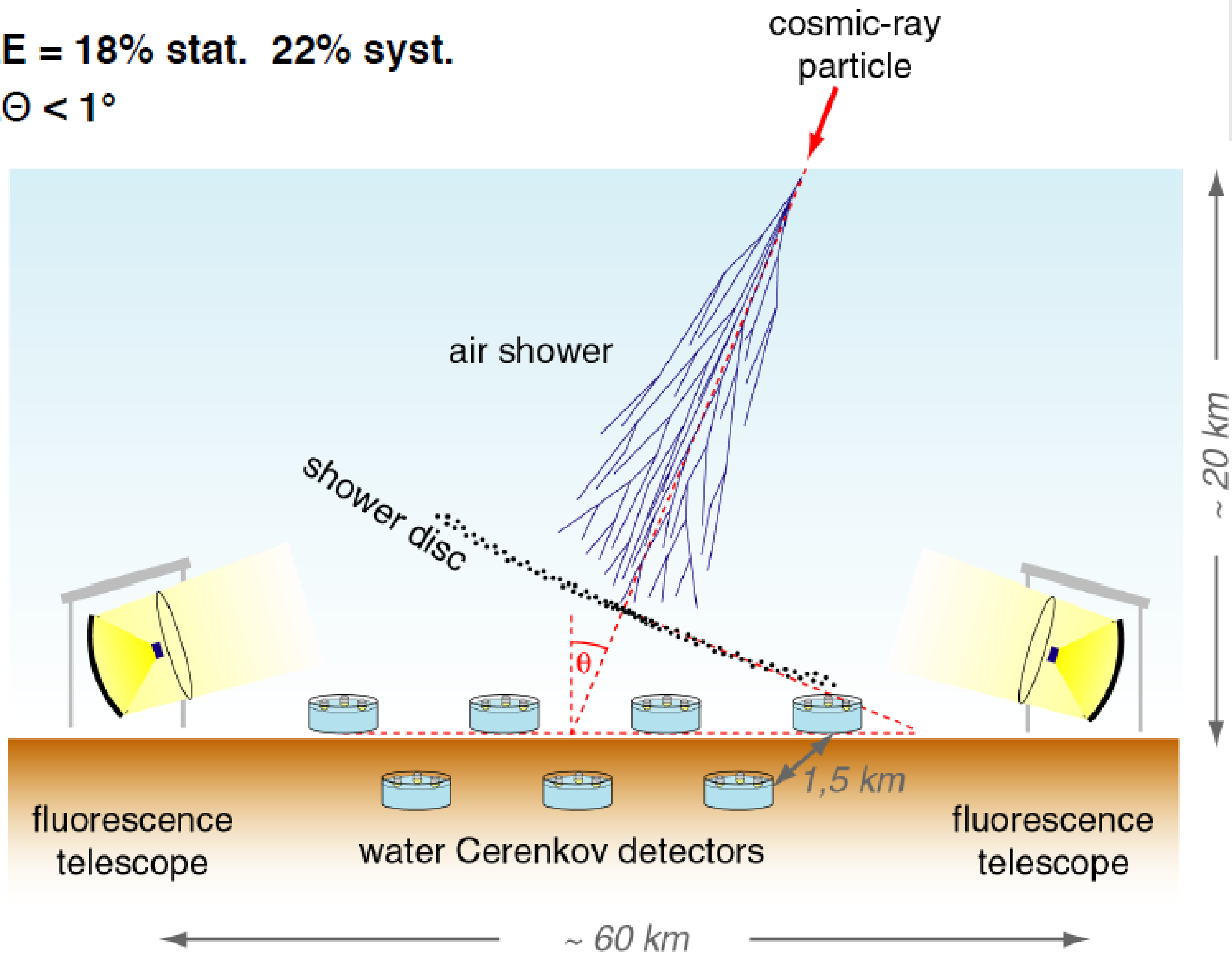

The detection principle

ΔE = 18% stat. 22% syst.

$\Delta\Theta < 1°$

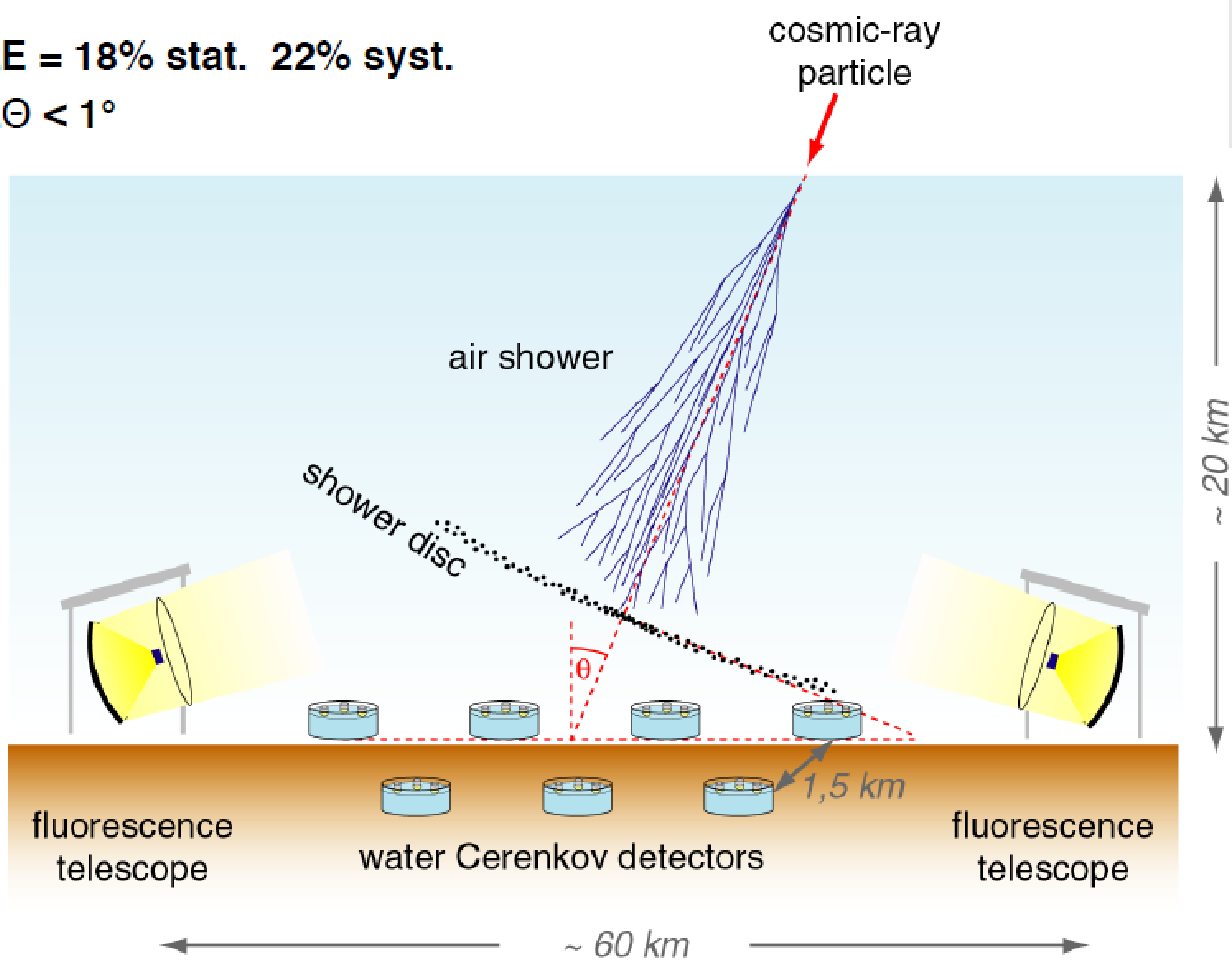

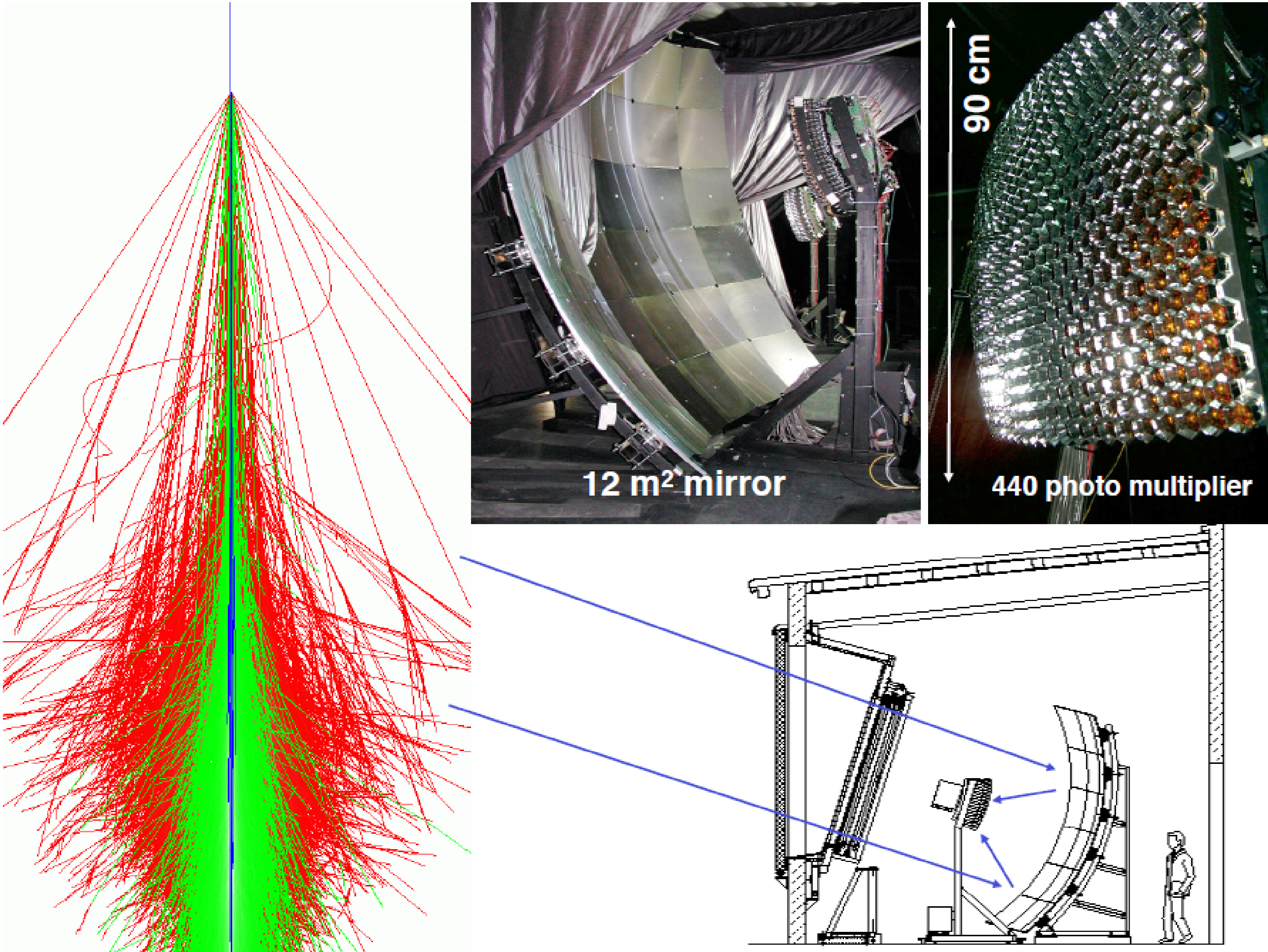
12 m² mirror
90 cm
440 photo multiplier

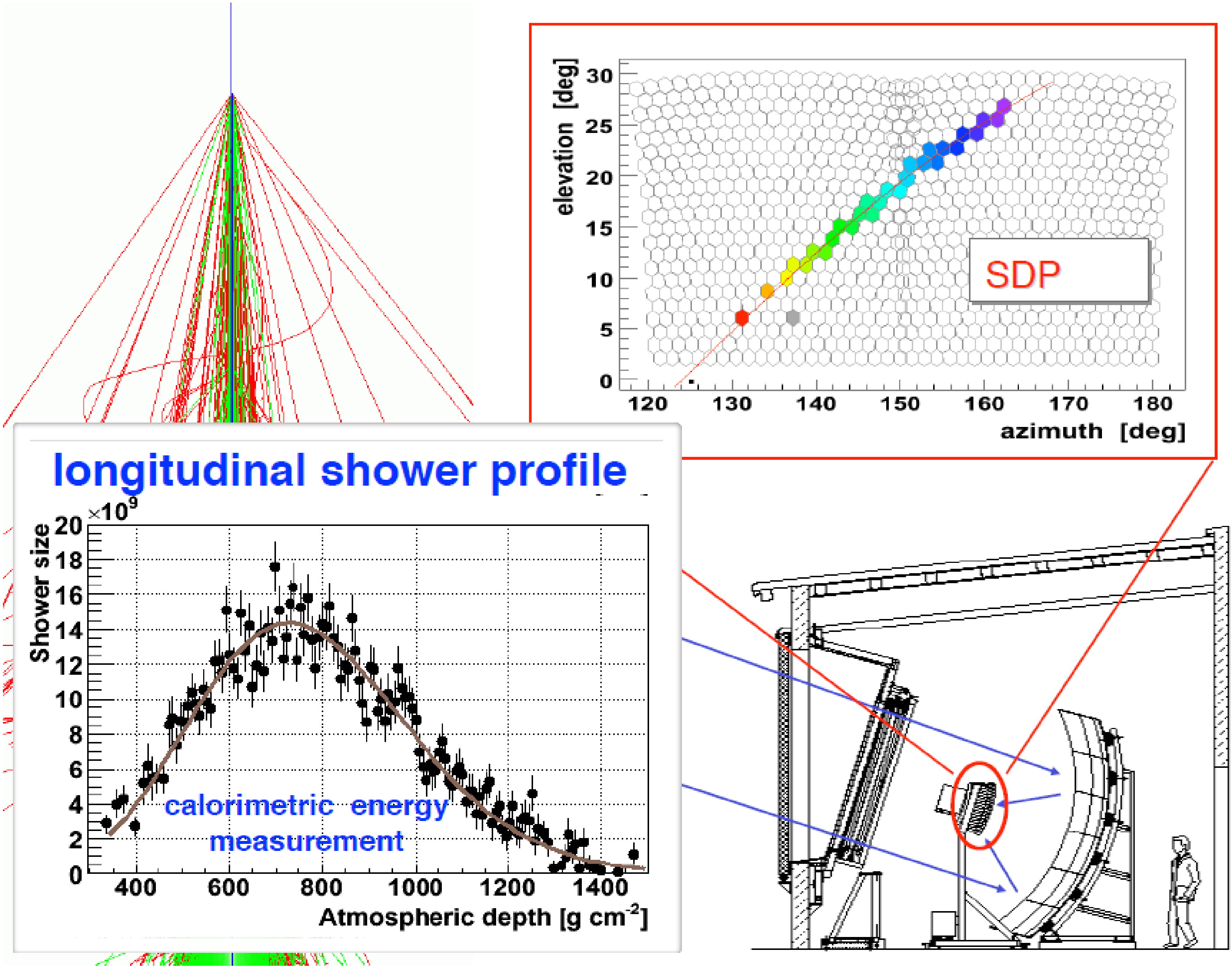

elevation [deg]
azimuth [deg]
SDP
longitudinal shower profile
×10^9
Shower size
Atmospheric depth [g cm^-2]
calorimetric energy
measurement

Measurement of Radio Emission in Extensive Air Showers

LOPES

Lofar Prototype Station

30 antennas operating at KASCADE-Grande

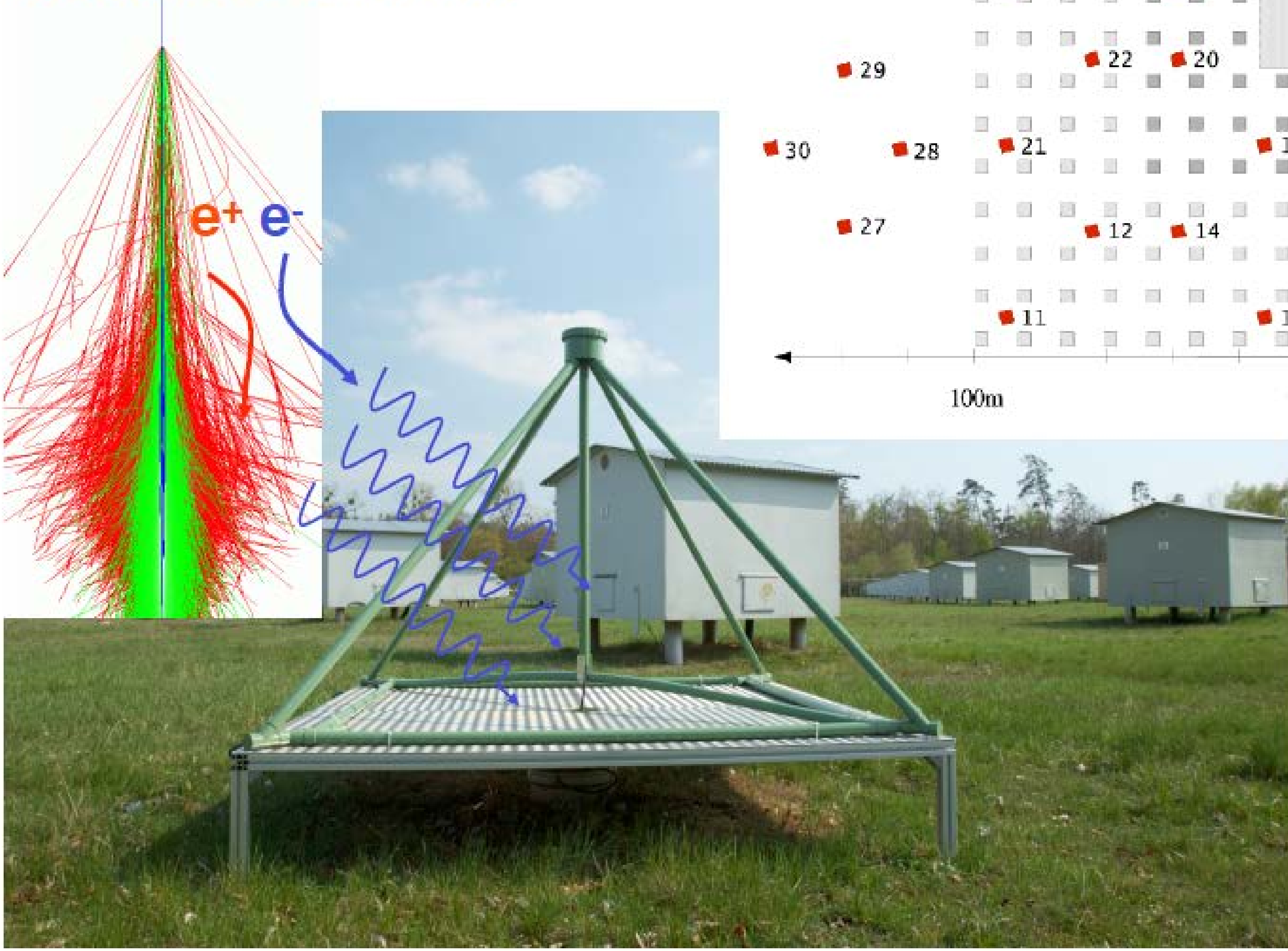

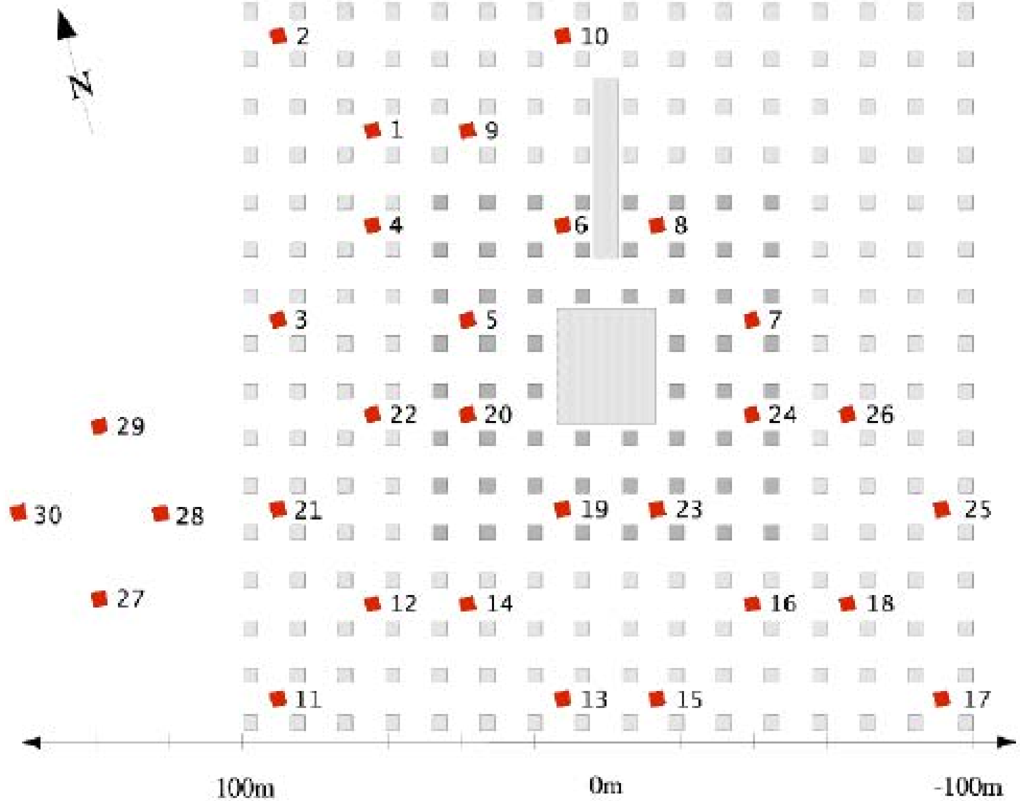

Correlation between radio signal and
air shower parameters

.. number of muons, i.e. primary energy

.. angle with respect to geomagnetic field

.. distance to shower axis

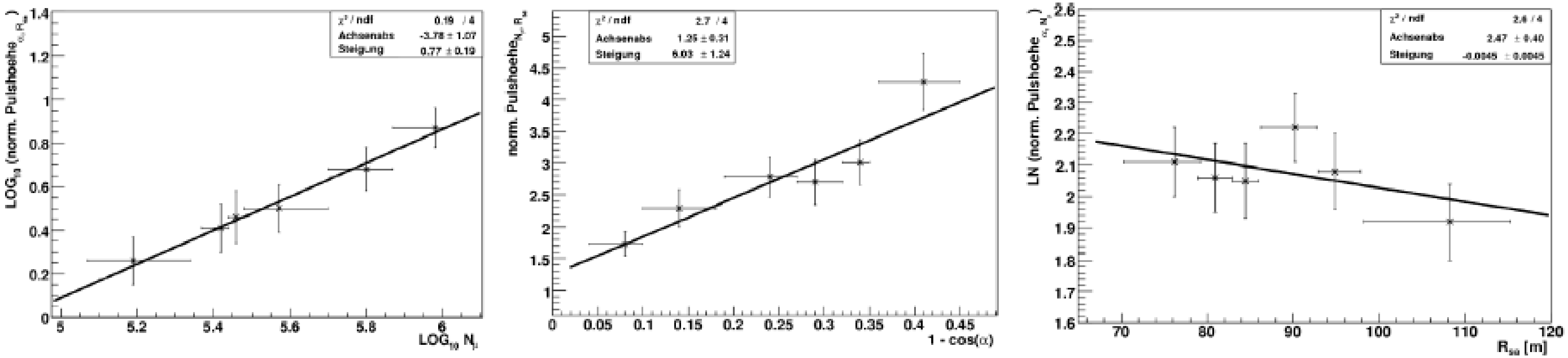

E. Bettini, diploma thesis, U Karlsruhe, 2006

$$\varepsilon_{est} = (11 \pm 1)((1.16 \pm 0.025) - \cos\alpha)\cos\theta \exp\left(\frac{-R}{236 \pm 81\ \mathrm{m}}\right)\left(\frac{E_p}{10^{17}\ \mathrm{eV}}\right)^{0.95 \pm 0.04}\left[\frac{\mu\mathrm{V}}{\mathrm{m\,MHz}}\right]$$

- α geomagnetic angle
- θ zenith angle
- r distance to shower axis
- E_0 energy of primary particle

A. Horneffer et al., 30th ICRC 4 (2008) 83

Results of air shower experiments

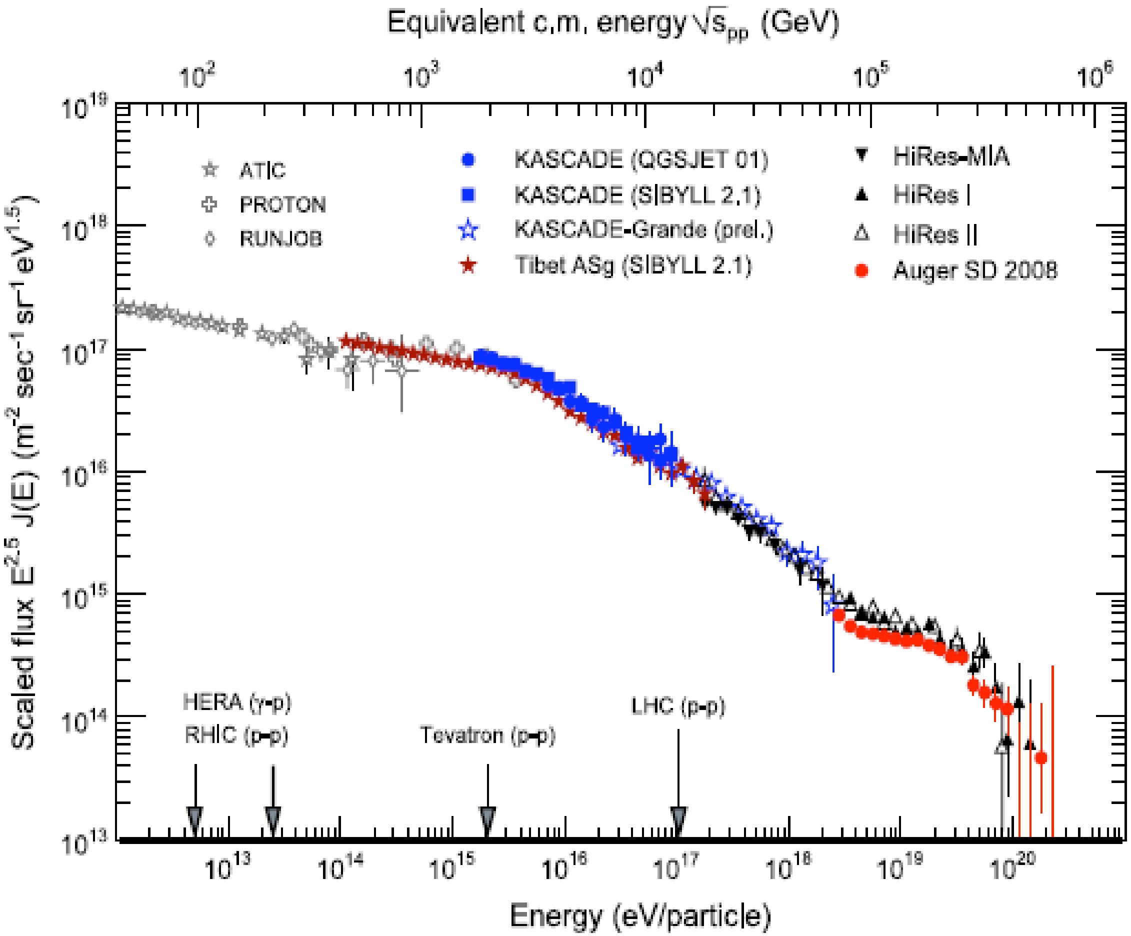

Fig. 7. All-particle cosmic-ray energy spectrum as obtained by direct measurements above the atmosphere by the ATIC [219,220], PROTON [221], and RUNJOB [222] as well as results from air shower experiments. Shown are Tibet ASγ results obtained with SIBYLL 2.1 [223], KASCADE data (interpreted with two hadronic interaction models) [224], preliminary KASCADE-Grande results [225], and Akeno data [226,33]. The measurements at high energy are represented by HiRes-MIA [227,228], HiRes I and II [229], and Auger [169].

Origin of the knee

$$\frac{dN}{dE} \sim E^{-\gamma},\ \gamma_1 \sim 2.7 \text{ at } E_0 < E_{knee}$$

$$\gamma_2 \sim 3.1 \text{ at } E_0 > E_{knee},\ E_{knee} = 4 \cdot 10^{15}\ \text{eV}$$

Possible reasons for the knee:

1) **maximum energy attained during acceleration process in galactic sources**

$$E_{max}^{SN} \sim Z \cdot R \cdot B \sim Z \cdot 10^{15}\ \text{eV}$$

2) **Leakage from Galaxi – propagation effect**

$$E_{knee} \sim Z$$

+ anisotropy of arrival directions of CR (more particles from the direction of Galactic plane)

3) **Interaction with background particles**

$$E_{knee} \sim A$$

4) **New physics in the atmosphere (change of hadronic interactions)**

Table 2
Synopsis of all models discussed

Model	Author(s)
Source/Acceleration	
Acceleration in SNR	Berezhko and Ksenofontov [18]
Acceleration in SNR + radio galaxies	Stanev et al. [19]
Acceleration by oblique shocks	Kobayakawa et al. [20]
Acceleration in variety of SNR	Sveshnikova [21]
Single source model	Erlykin and Wolfendale [22]
Reacceleration in the galactic wind	Völk and Zirakashvili [23]
Cannonball model	Plaga [24]
Propagation/Leakage from Galaxy:	
Minimum pathlength model	Swordy [25]
Anomalous diffusion model	Lagutin et al. [26]
Hall diffusion model	Ptuskin et al. [27], Kalmykov and Pavlov [42]
Diffusion in turbulent magnetic fields	Ogio and Kakimoto [28]
Diffusion and drift	Roulet et al [29]
Interactions with background particles	
Diffusion model + photo-disintegration	Tkaczyk [30]
Interaction with neutrinos in galactic halo	Dova et al. [31]
Photo-disintegration (optical and UV photons)	Candia et al. [32]
New interactions in the atmosphere	
Gravitons, SUSY, technicolor	Kazanas and Nicolaidis [33,34]

Correlated shower size distribution

frequency of showers dependent on 2 observables

zenith angle < 18° , eff. measurement time: 900 days

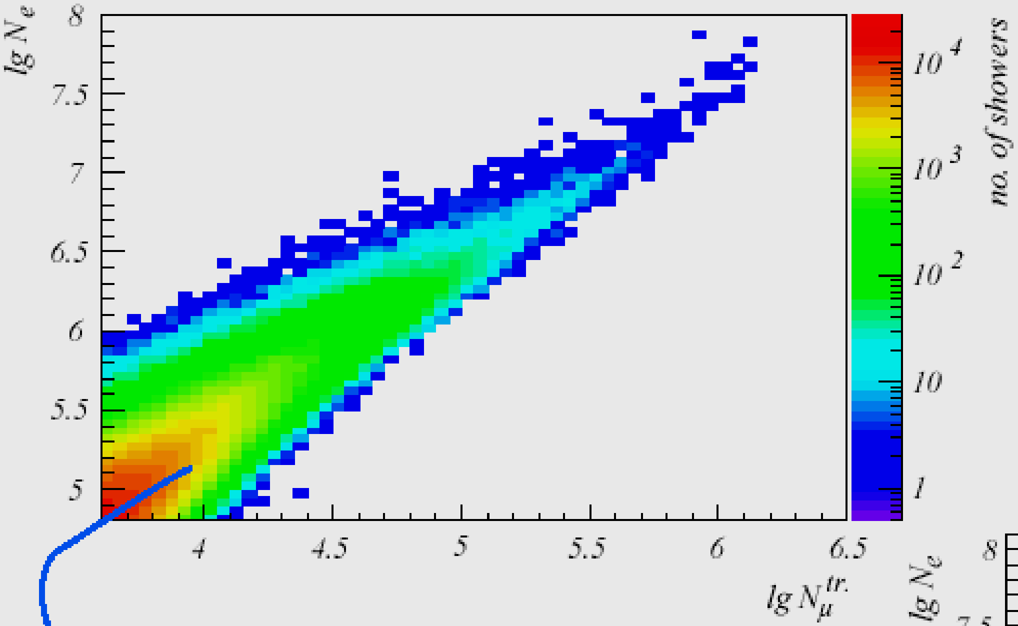

$$\frac{dJ}{d\lg N_e \, d\lg N_\mu^{tr}} =$$

$$\sum_A \int_{-\infty}^{+\infty} \frac{dJ_A}{d\lg E} \, p_A(\lg N_e, \lg N_\mu^{tr} \,|\, \lg E) \, d\lg E$$

→ *system of coupled Fredholm integral equations*

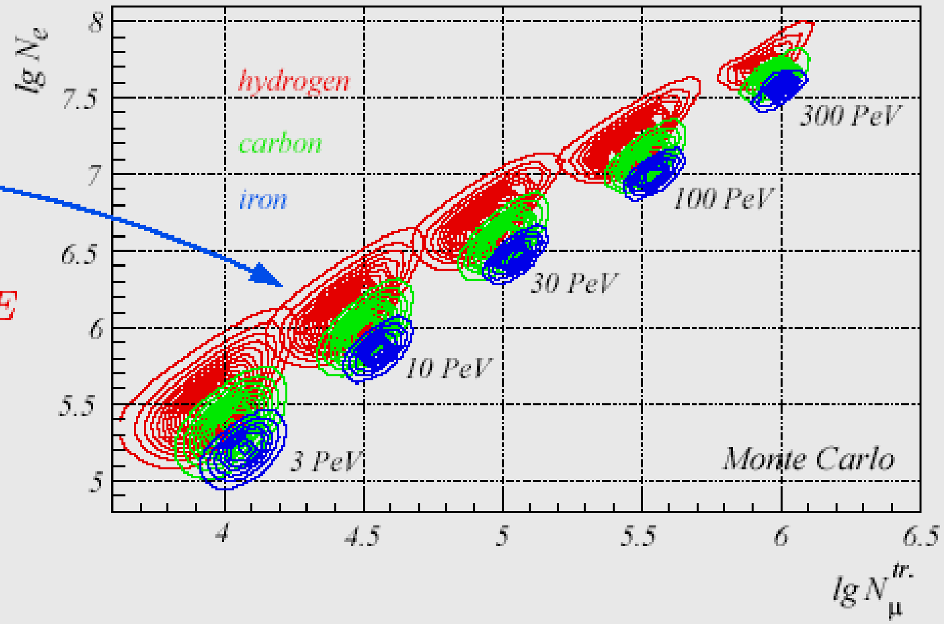

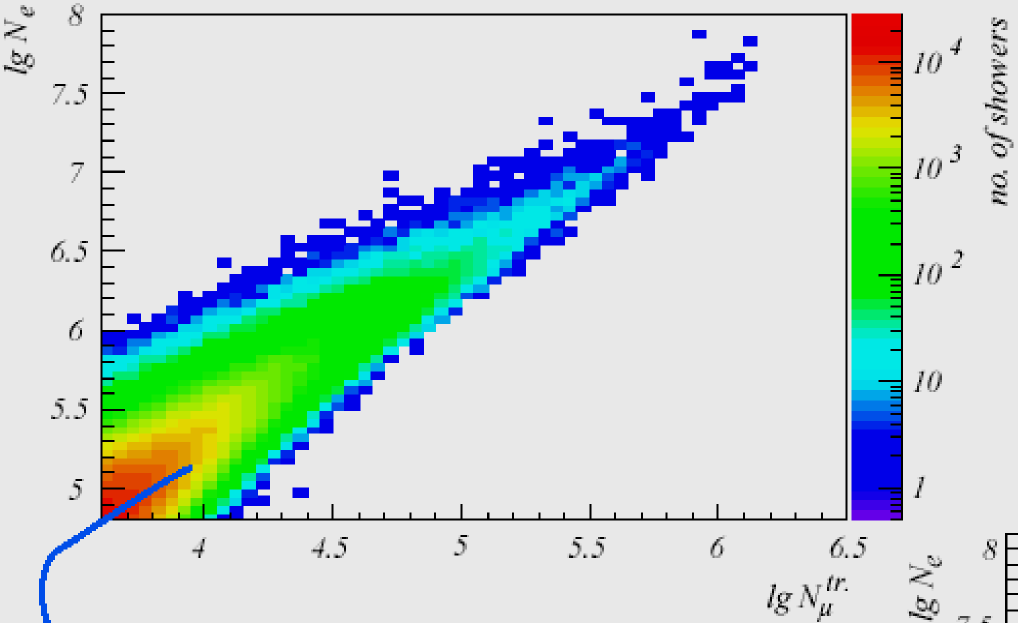

Correlated shower size distribution

frequency of showers dependent on 2 observables

zenith angle < 18°, eff. measurement time: 900 days

$$\frac{dJ}{d\lg N_e \, d\lg N_\mu^{tr}} = \sum_A \int_{-\infty}^{+\infty} \frac{dJ_A}{d\lg E} \, p_A(\lg N_e, \lg N_\mu^{tr} \mid \lg E) \, d\lg E$$

→ *system of coupled Fredholm integral equations*

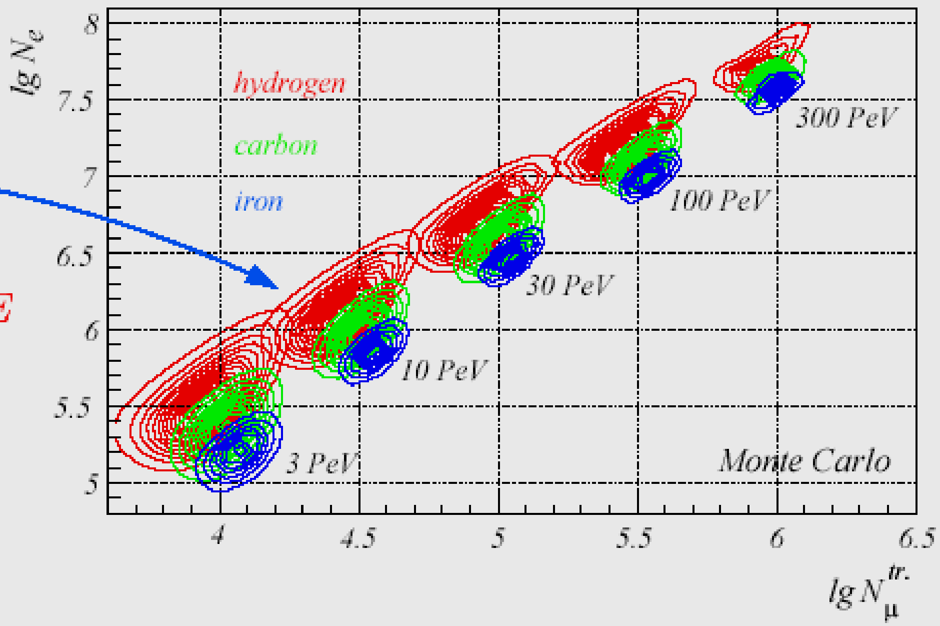

Energy spectra for groups of elements, according to KASCADE.

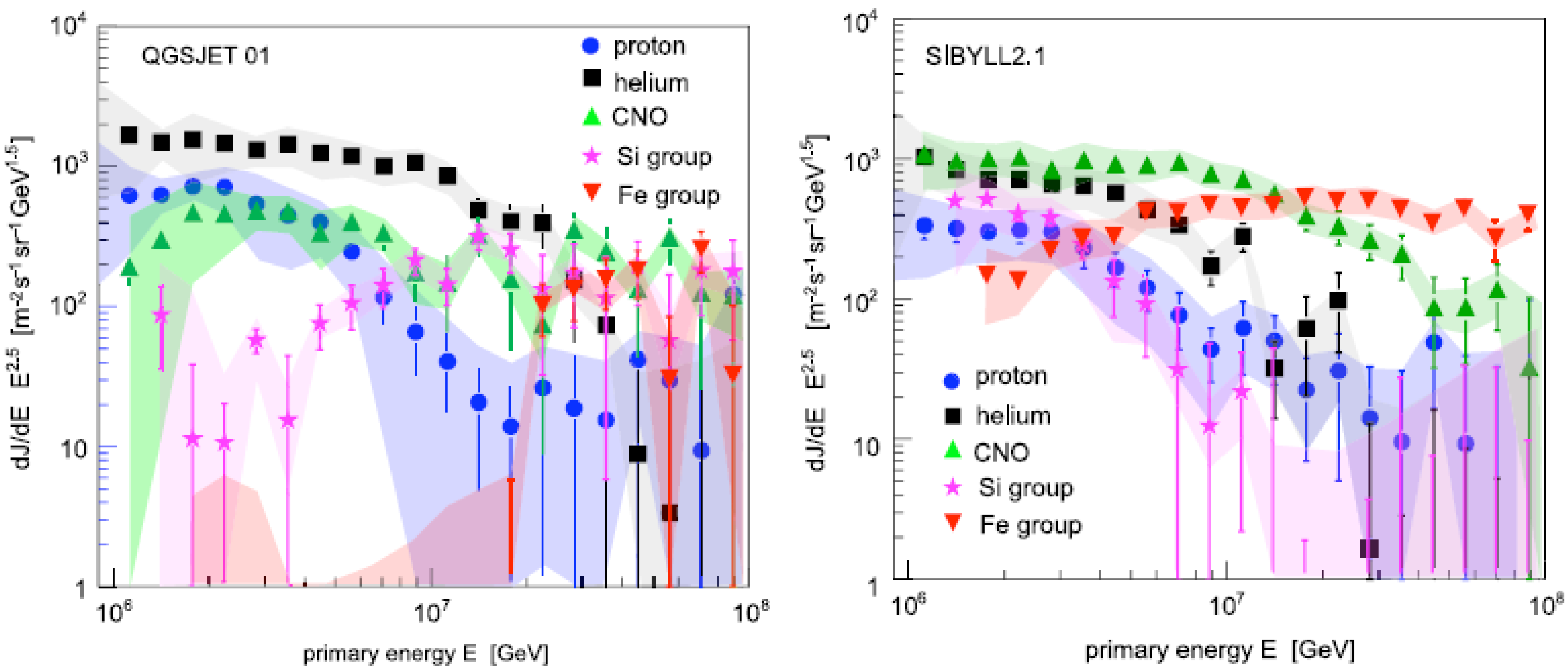

Fig. 15. Cosmic-ray energy spectrum for five groups of elements as reconstructed by the KASCADE experiment using the hadronic interaction models QGSJET 01 (*left*) and SIBYLL 2.1 (*right*) to interpret the measured data [224].

To solve the inverse problem the Kascade group applied unfolding procedure: strong Influence of hadronic interaction model

A knee-like structure in the spectrum of the heavy component of cosmic rays

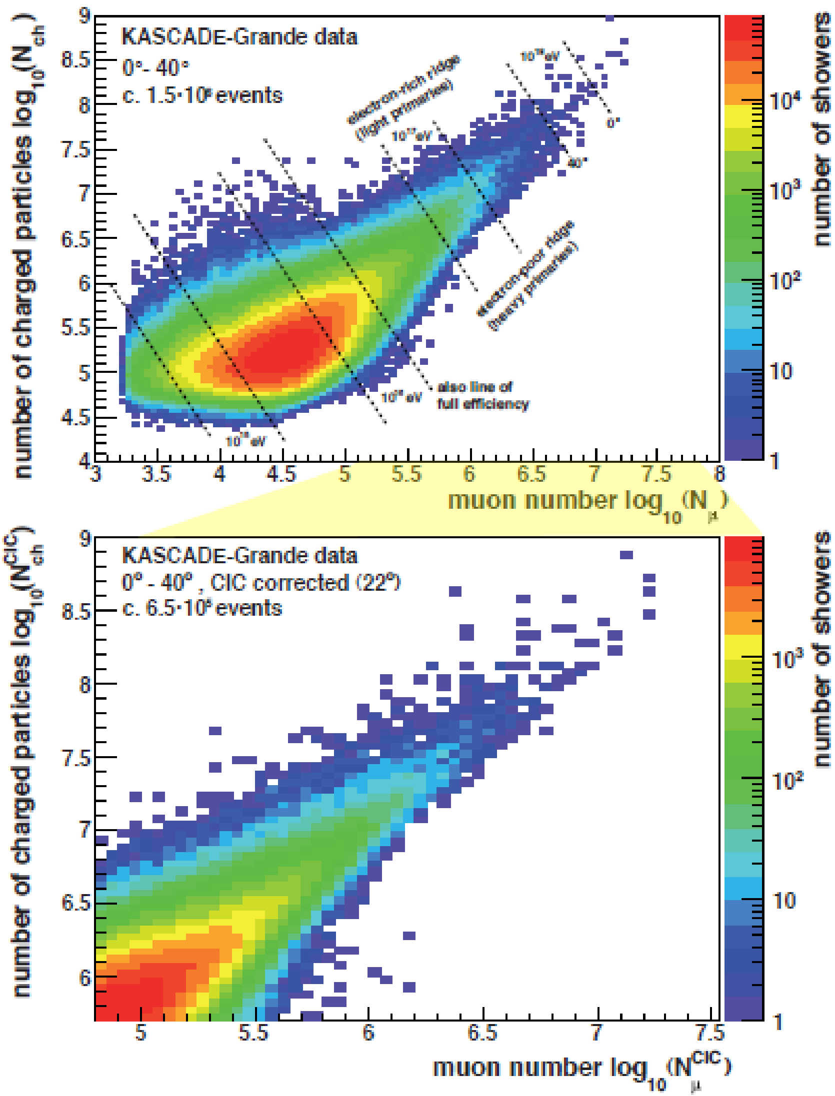

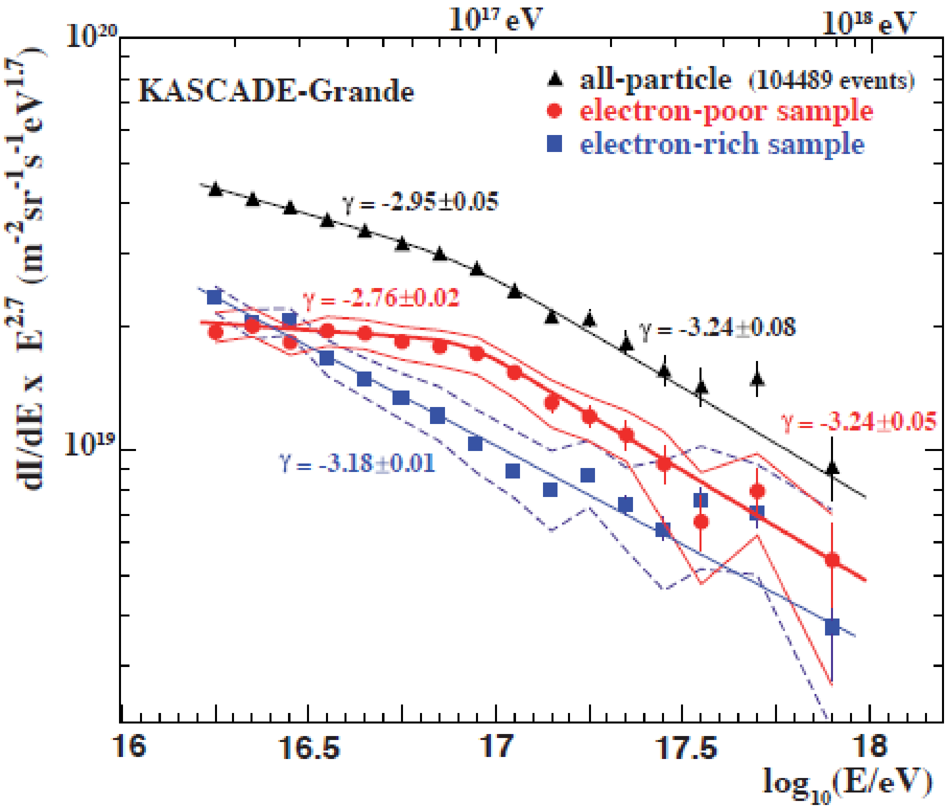

W.D. Apel et al, PRL 107 (2011) 171104

energy spectra for individual elements/ groups of elements

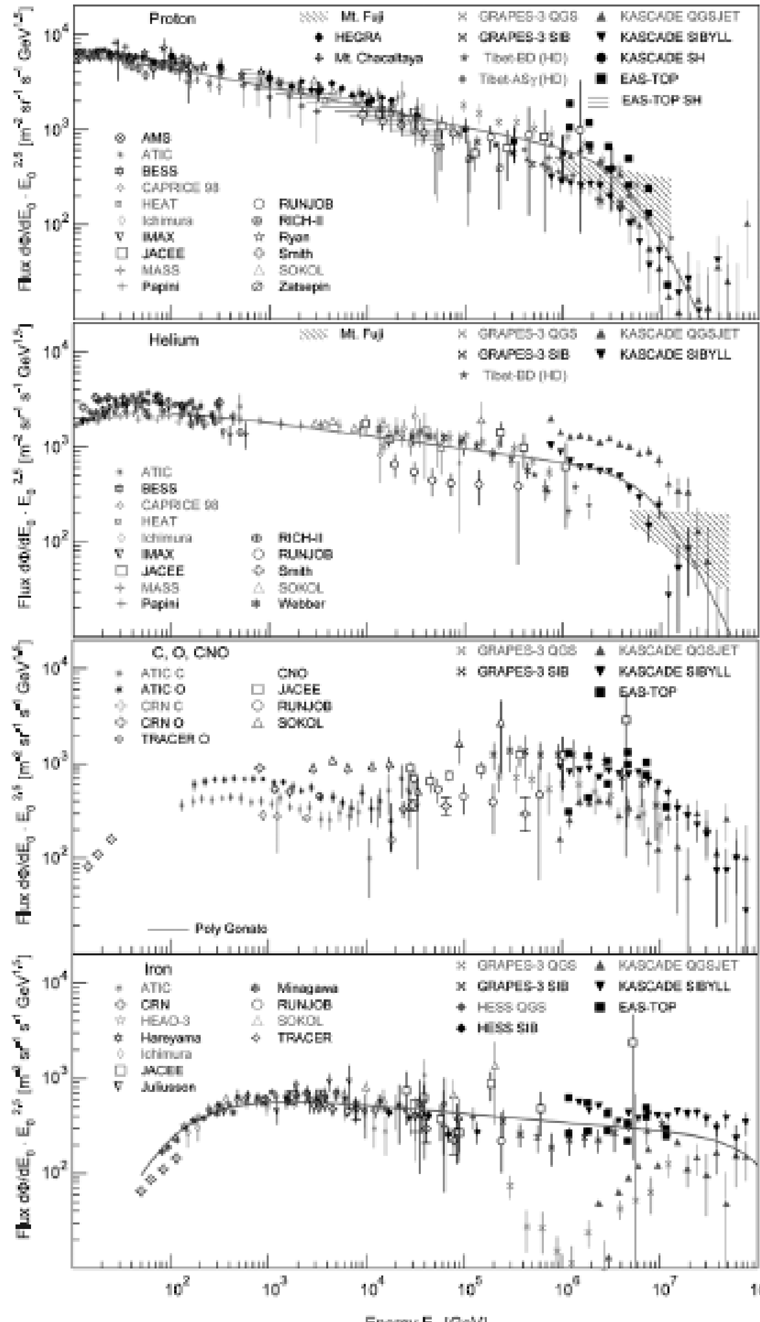

Fig. 9. Cosmic-ray energy spectra for four groups of elements, from top to bottom: protons, helium, CNO group, and iron group. **Protons:** Results from direct measurements above the atmosphere by AMS [242], ATIC [243], BESS [244], CAPRICE [245], HEAT [246,247], IMAX [248], JACEE [249], MASS [250, 251], RUNJOB [222], RICH-II [252–254], SOKOL [231,255], and fluxes obtained from indirect measurements by KASCADE electrons and muons for two hadronic interaction models [224] and single hadrons [256], EAS-TOP (electrons and muons) [257] and single hadrons [258], GRAPES-3 interpreted with two hadronic interaction models [259], HEGRA [260], Mt. Chacaltaya [261], Mts. Fuji and Kanbala [262], Tibet burst detector (HD) [263] and ASγ (HD) [264]. **Helium:** Results from direct measurements above the atmosphere by ATIC [243], BESS [244], CAPRICE [245], HEAT [246,247], IMAX [248], JACEE [249], MASS [250,251], RICH-II [252], RUNJOB [222,254], SOKOL [231,265], and fluxes obtained from indirect measurements by KASCADE electrons and muons for two hadronic interaction models [224], GRAPES-3 interpreted with two hadronic interaction models [259], Mts. Fuji and Kanbala [262], and Tibet burst detector (HD) [263]. **CNO group:** Results from direct measurements above the atmosphere by ATIC (C+O) [266], CRN (C+O) [267], TRACER (O) [268], JACEE (CNO) [269], RUNJOB (CNO) [222], SOKOL (CNO) [231], and fluxes obtained from indirect measurements by KASCADE electrons and muons [224], GRAPES-3 [259], the latter two give results for two hadronic interaction models, and EAS-TOP [257]. **Iron:** Results from direct measurements above the atmosphere by ATIC [266], CRN [267], HEAO-3 [270–272], TRACER [268] (single element resolution) and [273,247], JACEE [230], RUNJOB [222], SOKOL [231] (iron group), as well as fluxes from indirect measurements (iron group) by EAS-TOP [257], KASCADE electrons and muons [224], GRAPES-3 [259], and H.E.S.S. direct Cherenkov light [274]. The latter three experiments give results according to interpretations of the measured air-shower data with two hadronic interaction models, namely QGSJET and SIBYLL. The gray solid lines indicate spectra according to the poly-gonato model [2].

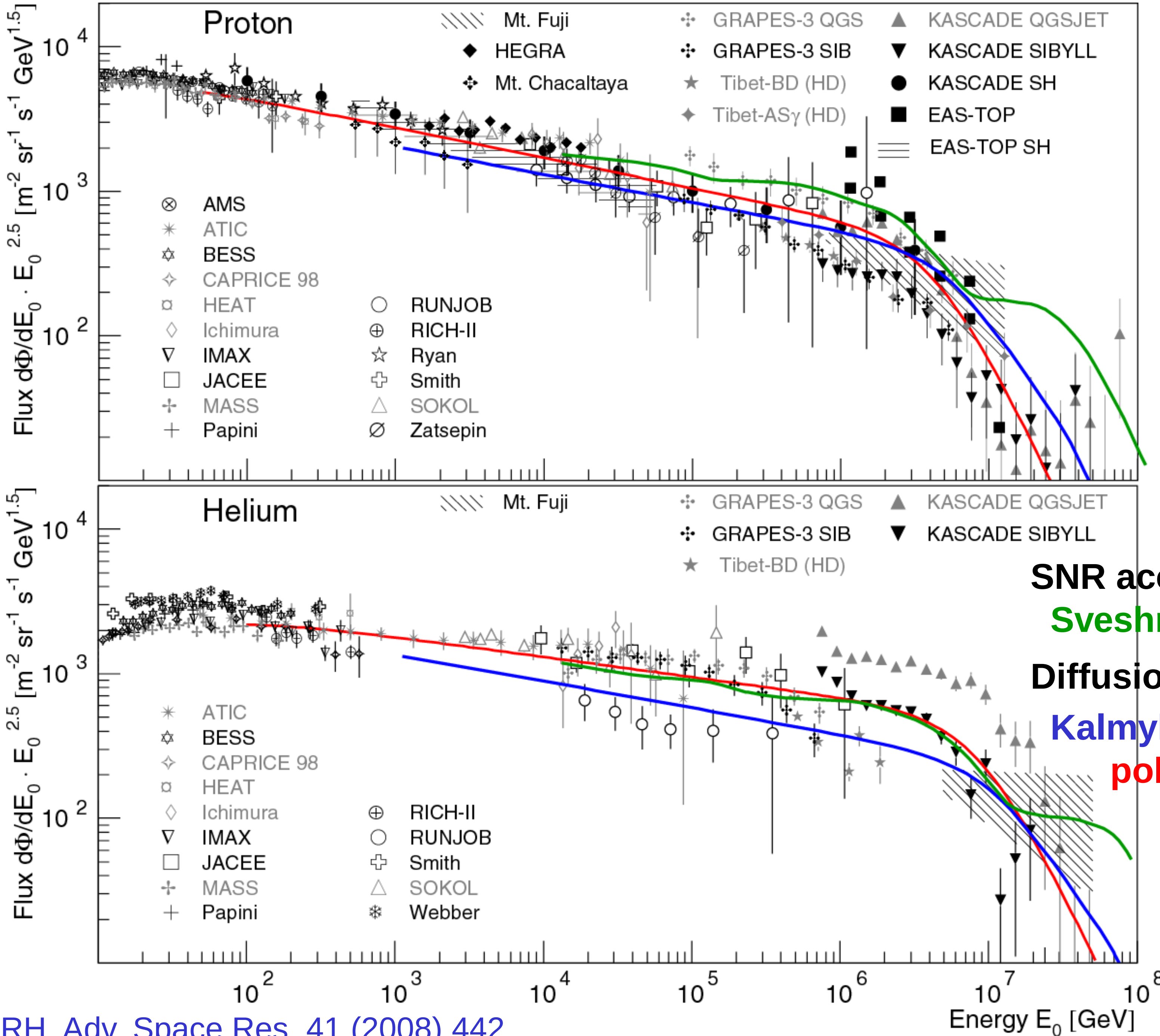

SNR acceleration:
Sveshnikova++ 2003

Diffusion:
Kalmykov+JRH 2007

poly gonato ~Z

JRH, Adv. Space Res. 41 (2008) 442

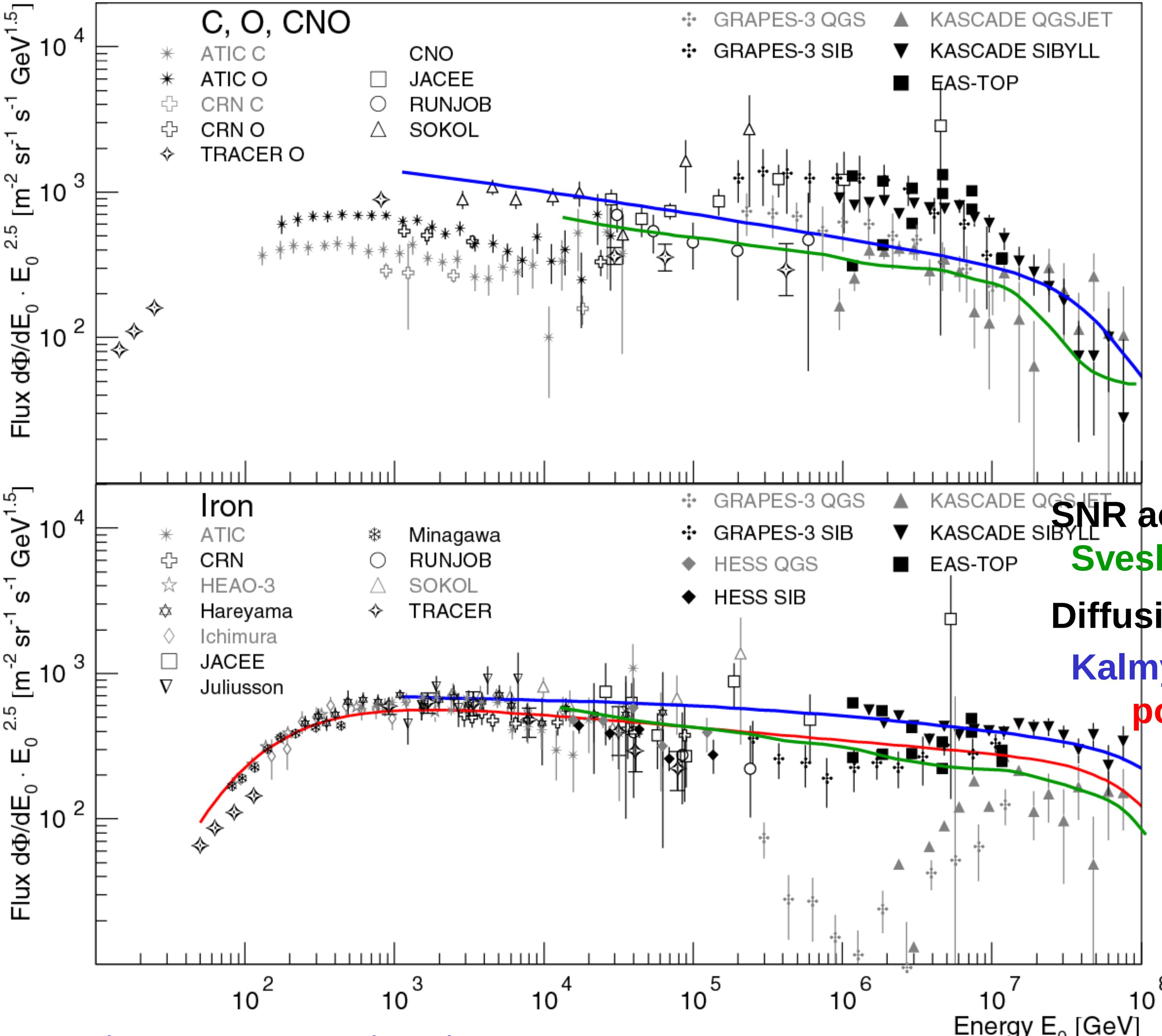

SNR acceleration:

Sveshnikova++ 2003

Diffusion:

Kalmykov+JRH 2007

poly gonato ~Z

JRH, Adv. Space Res. 41 (2008) 442

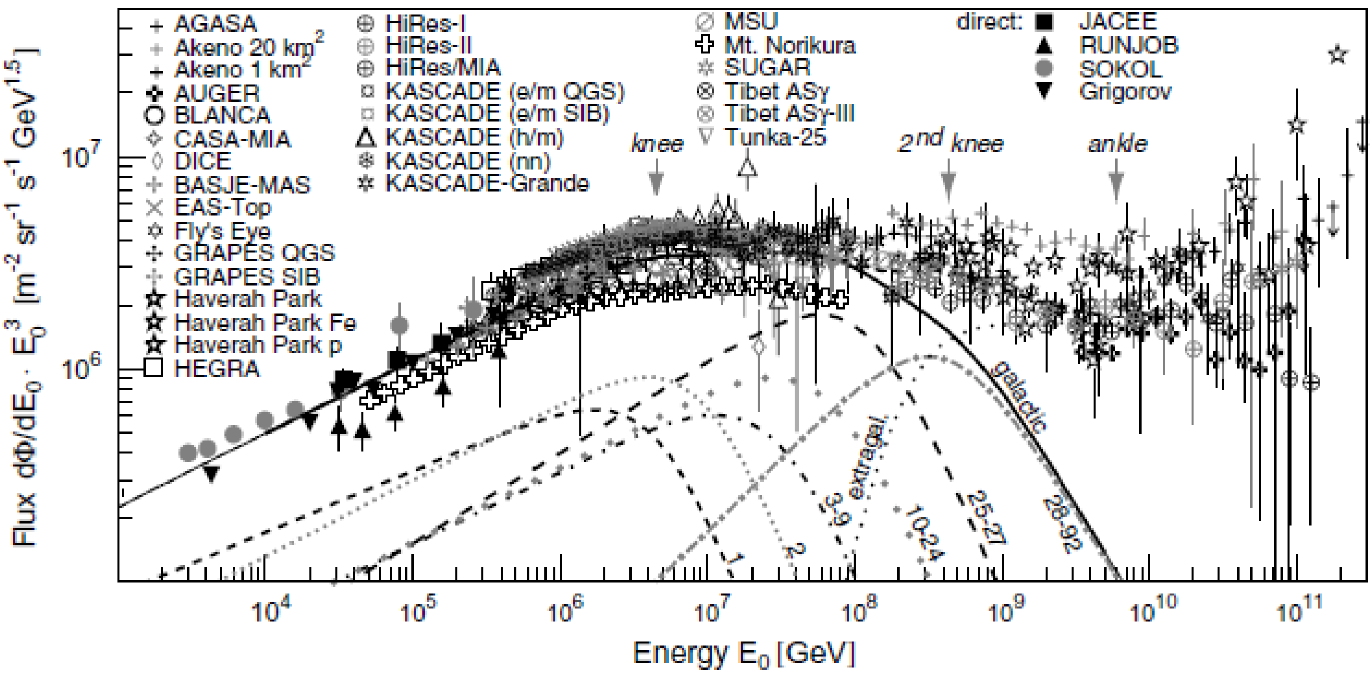

Fig. 8. All-particle energy spectrum of cosmic rays, the flux is multiplied by E^3. Results from direct measurements by Grigorov et al. (1999), JACEE (Asakimori et al., 1995), RUNJOB (Derbina et al., 2005), and SOKOL (Ivanenko et al., 1993) as well as from the air shower experiments AGASA (Takeda et al., 2003), Akeno 1 km^2 (Nagano et al., 1984a), and 20 km^2 (Nagano et al., 1984b), AUGER (Sommers et al., 2005), BASJE-MAS (Ogio et al., 2004), BLANCA (Fowler et al., 2001), CASA-MIA (Glasmacher et al., 1999b), DICE (Swordy and Kieda, 2000), EAS-TOP (Aglietta et al., 1999), Fly's Eye (Corbato et al., 1994), GRAPES-3 interpreted with two hadronic interaction models (Hayashi et al., 2005), Haverah Park (Lawrence et al., 1991) and (Ave et al., 2003), HEGRA (Arqueros et al., 2000), HiRes–MIA (Abu-Zayyad et al., 2001a), HiRes-I (Abbasi et al., 2004), HiRes-II (Abbasi et al., 2005), KASCADE electrons and muons interpreted with two hadronic interaction models (Antoni et al., 2005), hadrons (Hörandel et al., 1999), and a neural network analysis combining different shower components (Antoni et al., 2002), KASCADE-Grande (preliminary) (Haungs et al., in press), MSU (Fomin et al., 1991), Mt. Norikura (Ito et al., 1997), SUGAR (Anchordoqui and Goldberg, 2004), Tibet ASγ (Amenomori et al., 2000a) and ASγ-III (Amenomori et al., 2003), Tunka-25 (Chernov et al., 2006), and Yakutsk (Glushkov et al., 2003). The lines represent spectra for elemental groups (with nuclear charge numbers Z as indicated) according to the poly-gonato model (Hörandel, 2003a). The sum of all elements (galactic) and a presumably extragalactic component are shown as well. The dashed line indicates the average all-particle flux at high energies.

The all-particle flux can be described as the sum of the spectra of individual elements.

average depth of the shower maximum X_{max}

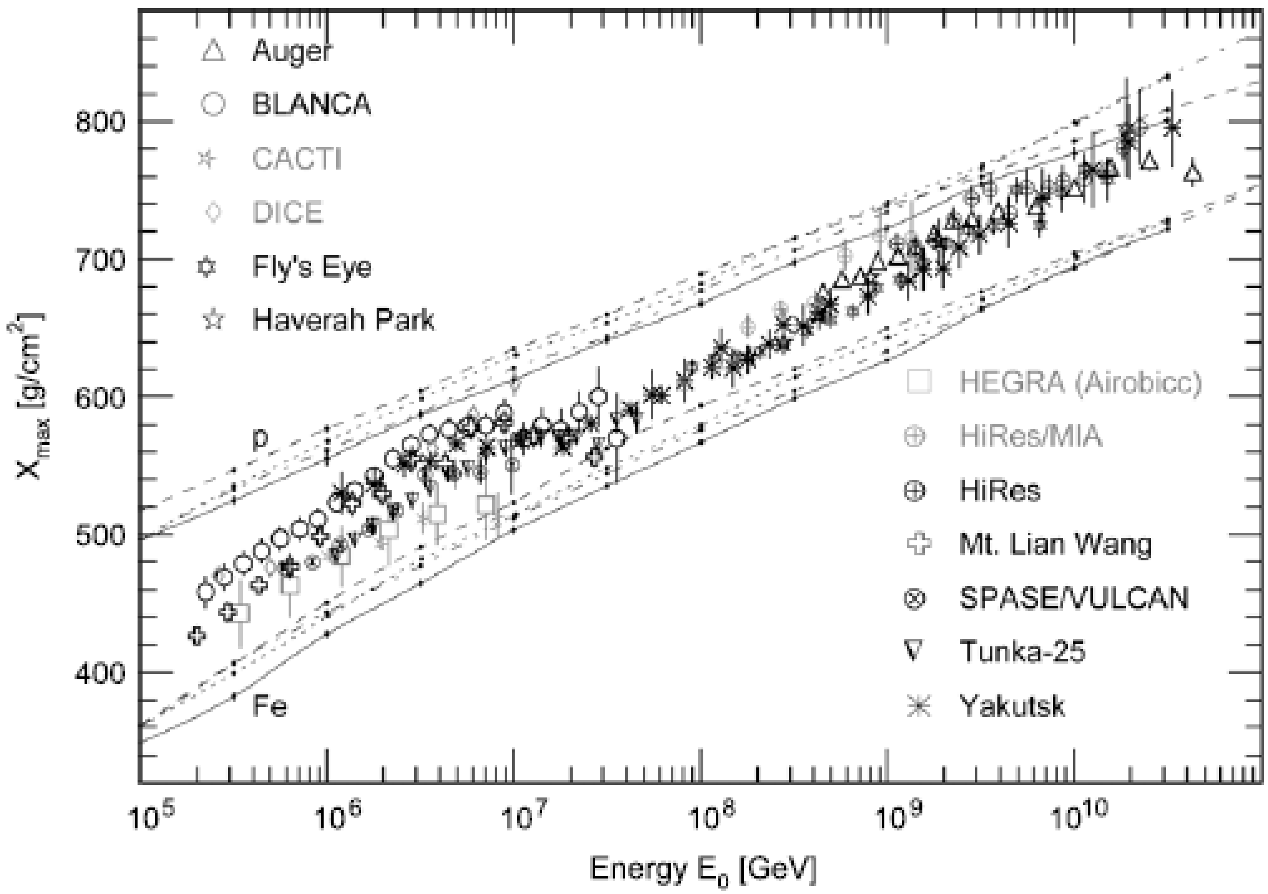

Fig. 13. Average depth of the shower maximum X_{max} as function of primary energy as obtained by Auger [305], BLANCA [173], CACTI [306], DICE [182], Fly's Eye [307], Haverah Park [308], HEGRA [174], HiRes/MIA [228], HiRes [309], Mt. Lian Wang [310], SPASE/VULCAN [311], Tunka-25 [176], Yakutsk [312]. The lines indicate simulations for proton and iron induced showers using the CORSIKA code with the hadronic interaction model QGSJET 01 (—), QGSJET II-3 (- - -), SIBYLL 2.1 (. . .), and EPOS 1.6 (-·-·-).

Mean logarithmic mass derived from Xmax measurements

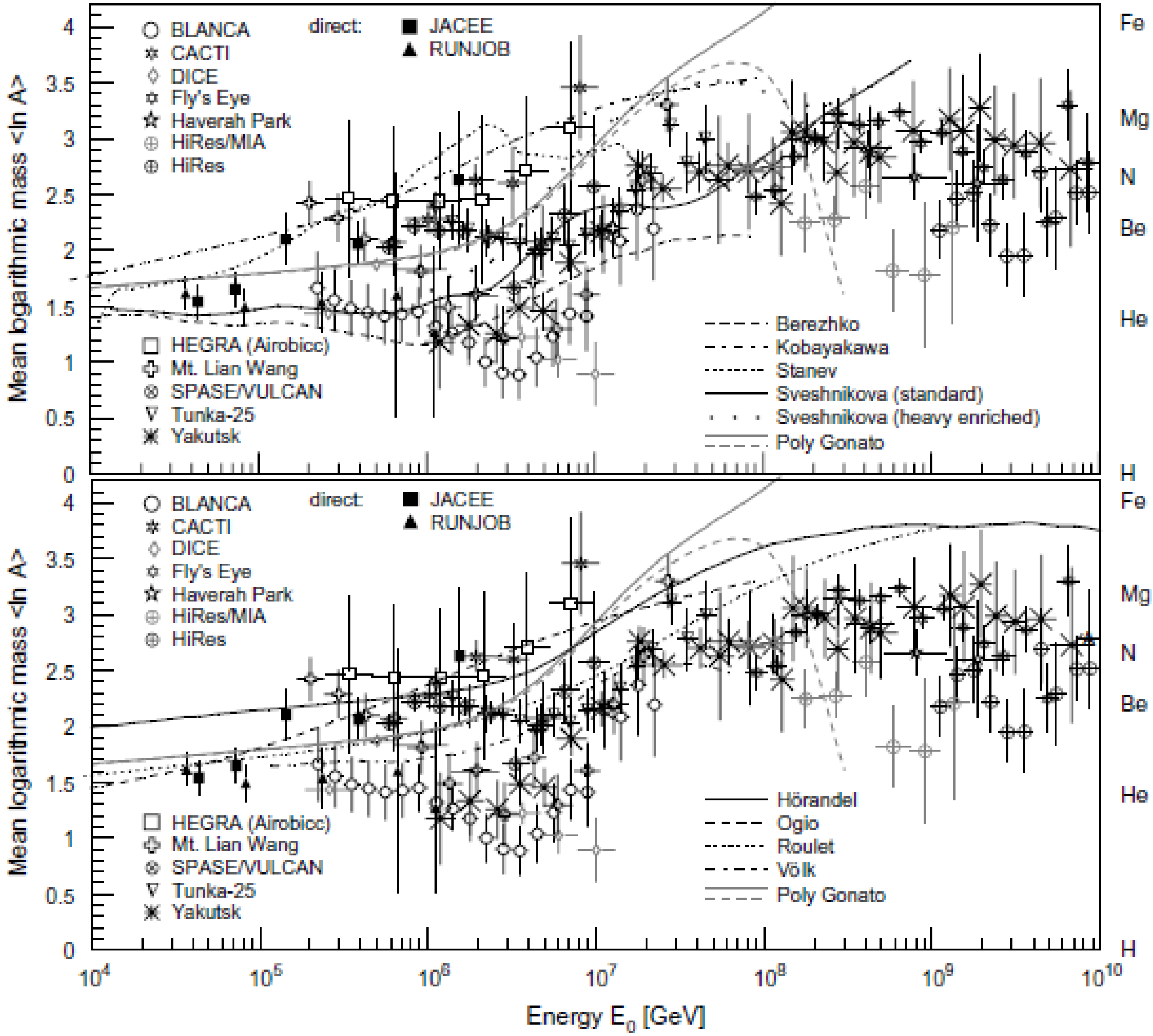

Fig. 12. Mean logarithmic mass of cosmic-rays derived from the average depth of the shower maximum, see Fig. 10. As hadronic interaction model used to interpret the measurements serves a modified version of QGSJET 01 with lower cross sections and a slightly increased elasticity (model 3a Hörandel, 2003b). For experimental references, see caption in Fig. 10. For comparison, results from direct measurements are shown as well from the JACEE (JACEE collaboration, 1999) and RUNJOB (Derbina et al., 2005) experiments. *Models:* The grey solid and dashed lines indicate spectra according to the poly-gonato model (Hörandel, 2003a). Top: The lines indicate spectra for models explaining the knee due to the maximum energy attained during the acceleration process according to Sveshnikova (2003) (—, · · ·), Berezhko and Ksenofontov (1999) (- - -), Stanev et al. (1993) (· · ·), Kobayakawa et al. (2002) (-·-·-). Bottom: The lines indicate spectra for models explaining the knee as effect of leakage from the Galaxy during the propagation process according to Hörandel et al. (2007) (—), Ogio and Kakimoto (2003) (- - -), Roulet (2004) (· · ·), as well as Völk and Zirakashvili (2003) (-·-·-).

Mean logarithmic mass derived from the measurement of electrons, muons, and hadrons at ground level

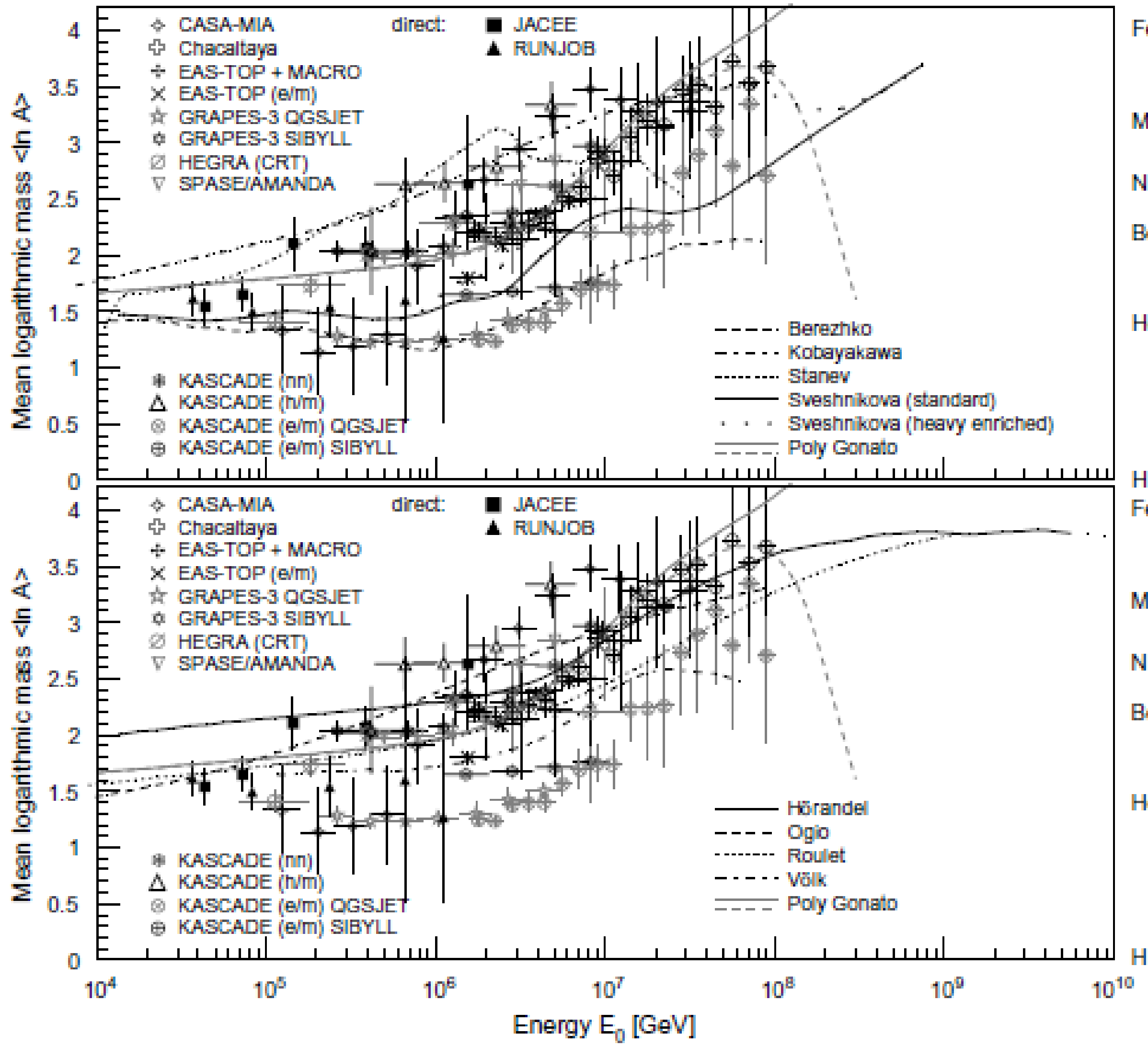

Fig. 9. Mean logarithmic mass of cosmic-rays derived from the measurements of electrons, muons, and hadrons at ground level. Results are shown from CASA-MIA (Glasmacher et al., 1999a), Chacaltaya (Aguirre et al., 2000), EAS-TOP electrons and GeV muons (Aglietta et al., 2004a), EAS-TOP/MACRO (TeV muons) (Aglietta et al., 2004b), GRAPES-3 data interpreted with two hadronic interaction models (Hayashi et al., 2005), HEGRA CRT (Bernlöhr et al., 1998), KASCADE electrons and muons interpreted with two hadronic interaction models (Antoni et al., 2005), hadrons and muons (Hörandel, 1998), as well as an analysis combining different observables with a neural network (Antoni et al., 2002), and SPASE/AMANDA (Rawlins et al., 2003). For comparison, results from direct measurements are shown as well from the JACEE (JACEE collaboration, 1999) and RUNJOB (Derbina et al., 2005) experiments. For orientation, ln *A* for selected elements is indicated on the right-hand side. *Models:* The grey solid and dashed lines indicate spectra according to the poly-gonato model (Hörandel, 2003a). Top: The lines indicate spectra for models explaining the knee due to the maximum energy attained during the acceleration process according to Sveshnikova (2003) (—, · · ·), Berezhko and Ksenofontov (1999) (- - -), Stanev et al. (1993) (· · ·), Kobayakawa et al. (2002) (-·-·-). Bottom: The lines indicate spectra for models explaining the knee as effect of leakage from the Galaxy during the propagation process according to Hörandel et al. (2007) (—), Ogio and Kakimoto (2003) (- - -), Roulet (2004) (· · ·), as well as Völk and Zirakashvili (2003) (-·-·-).

Accelerator dimensions and magnetic field

B[μG] L[pc] > 2 E[PeV]/(Zβ)

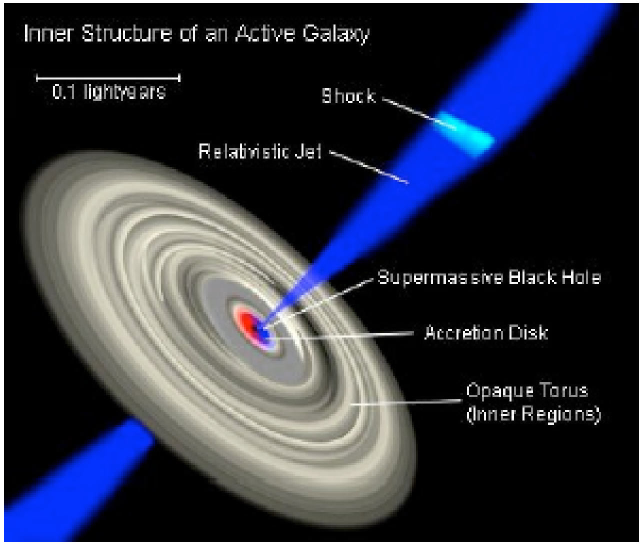

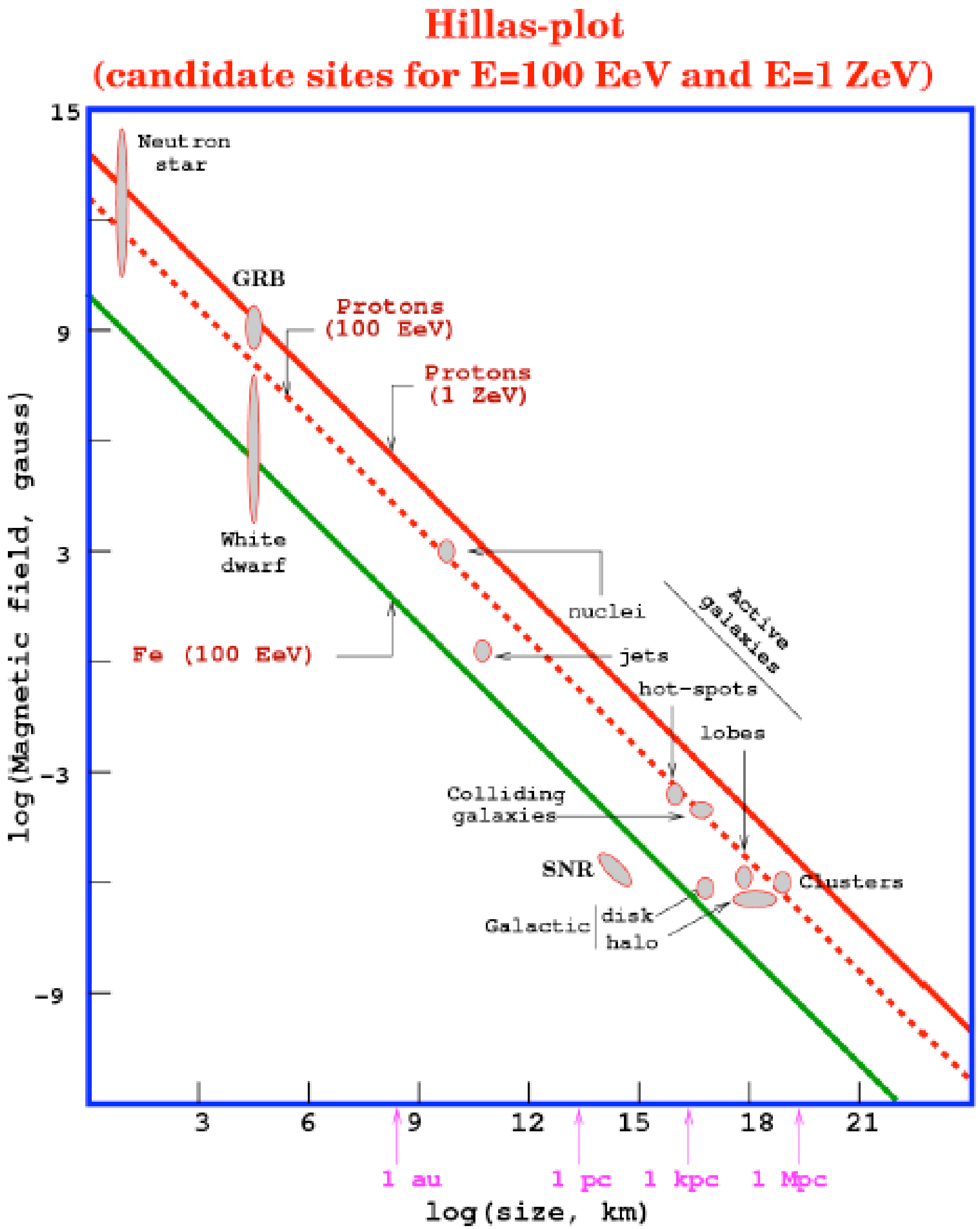

$E_{max} \sim ZBL$ (Fermi)

$E_{max} \sim ZBL\Gamma$ (Ultra-relativistic shocks-GRB)

Possible sources of extragalactic cosmic rays

Bottom up models

- Active galactic nuclei (AGN)
- Coalescence of neutron stars, black holes
- Gamma ray bursts

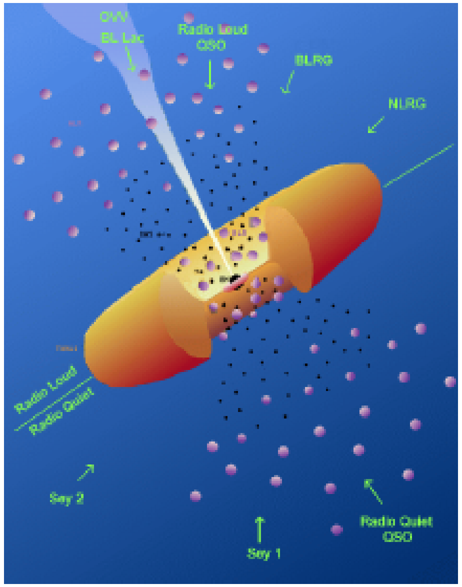

$$p+p \text{ or } p+\gamma \rightarrow \pi^{+/-} \rightarrow \nu_\mu + \nu_e + \ldots$$
$$\rightarrow \pi^0 \rightarrow \gamma + \gamma$$

Top down models

Super heavy relicts of Big-Ba… …ol. defects)

↳ X-particle (m … eV)

↳ …ons

↳ γ, ν, p…

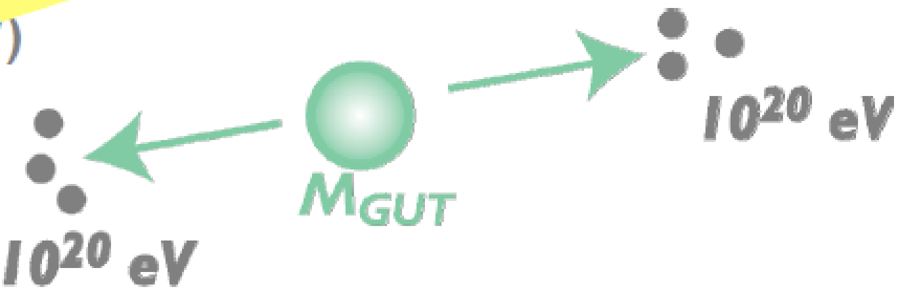

Already severe constraints by Auger

→ Multi Messenger Approach

Neutrino astronomy	Proton astronomy	TeV γ-ray astronomy
km³ net Ice Cube	Pierre Auger (full sky)	HESS, MAGIC, CTA

CR energy spectra according to talks presented at ICRC 2015

LHAASO – Hybrid

ICRC2015: *Z.Cao, 261*

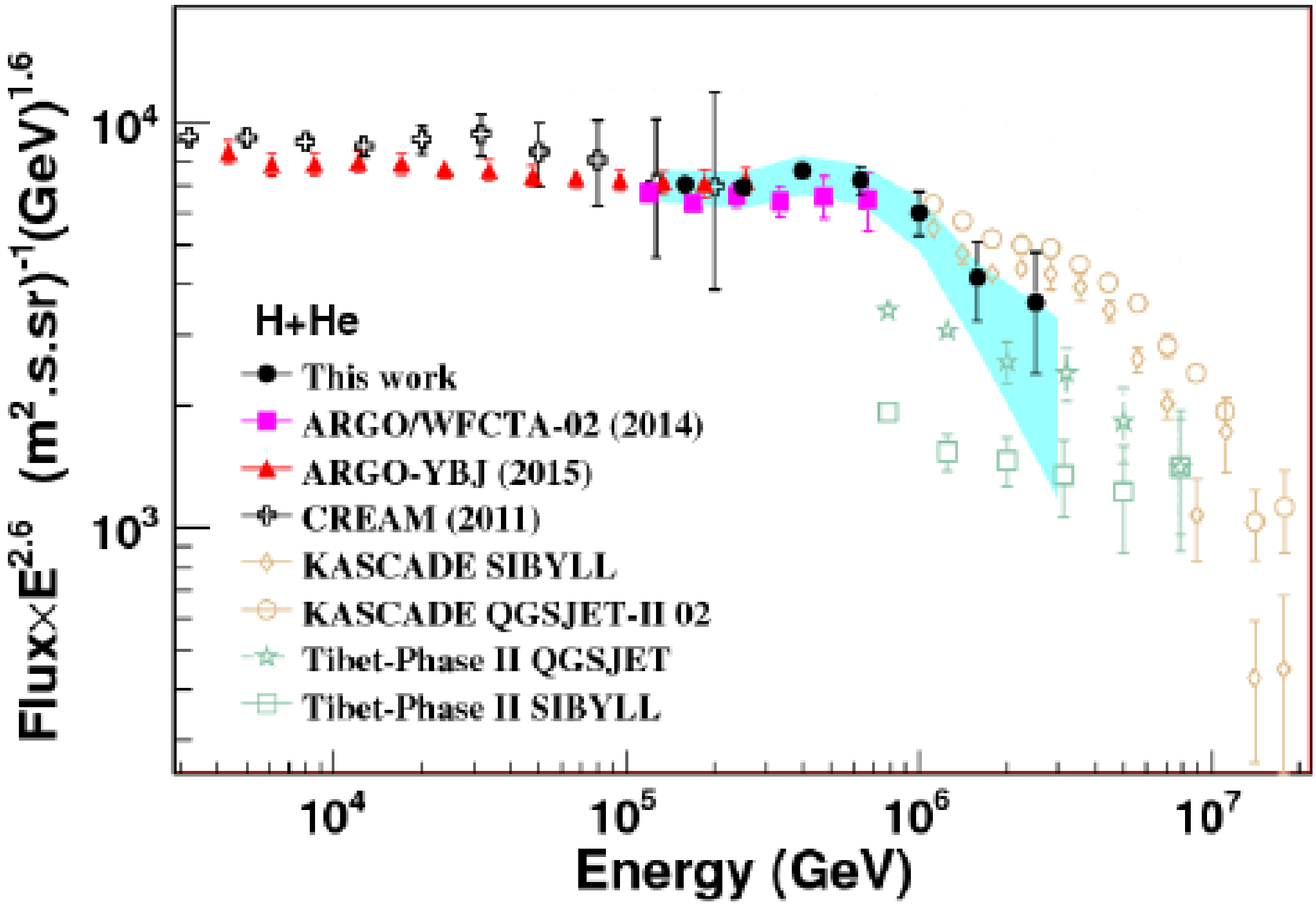

p/He spectrum bending below 1 PeV

LHAASO – Hybrid

ICRC2015*: Z.Cao, 261*

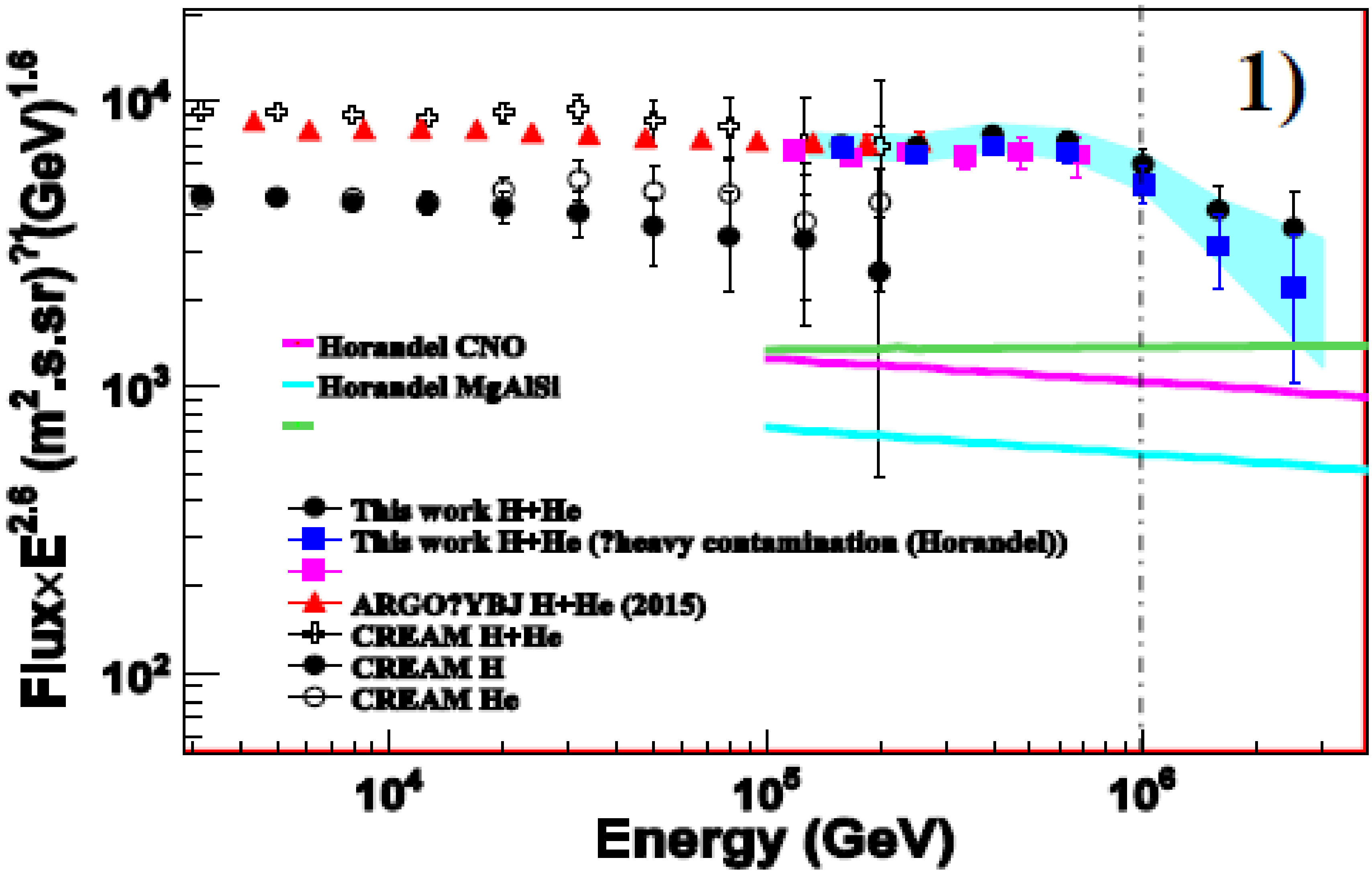

p/He spectrum bending below 1 PeV

ARGO-YBJ

- benefit of analog charge
- readout very close to the core

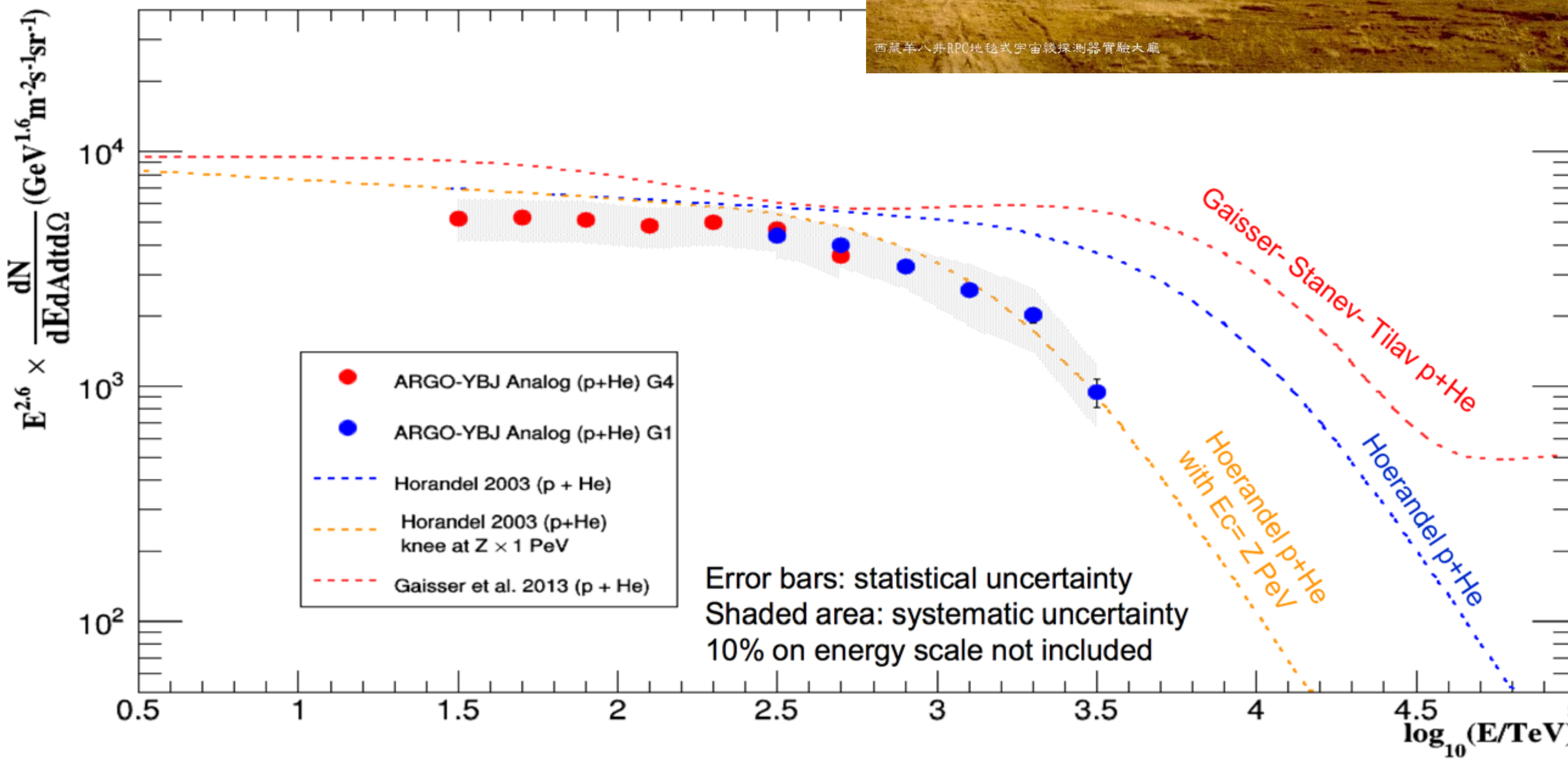

ICRC2015*: I. De Mitri, 366*

p/He spectrum bending below 1 PeV

ARGO-YBJ

- benefit of analog - bayesan
- readout very close to the core

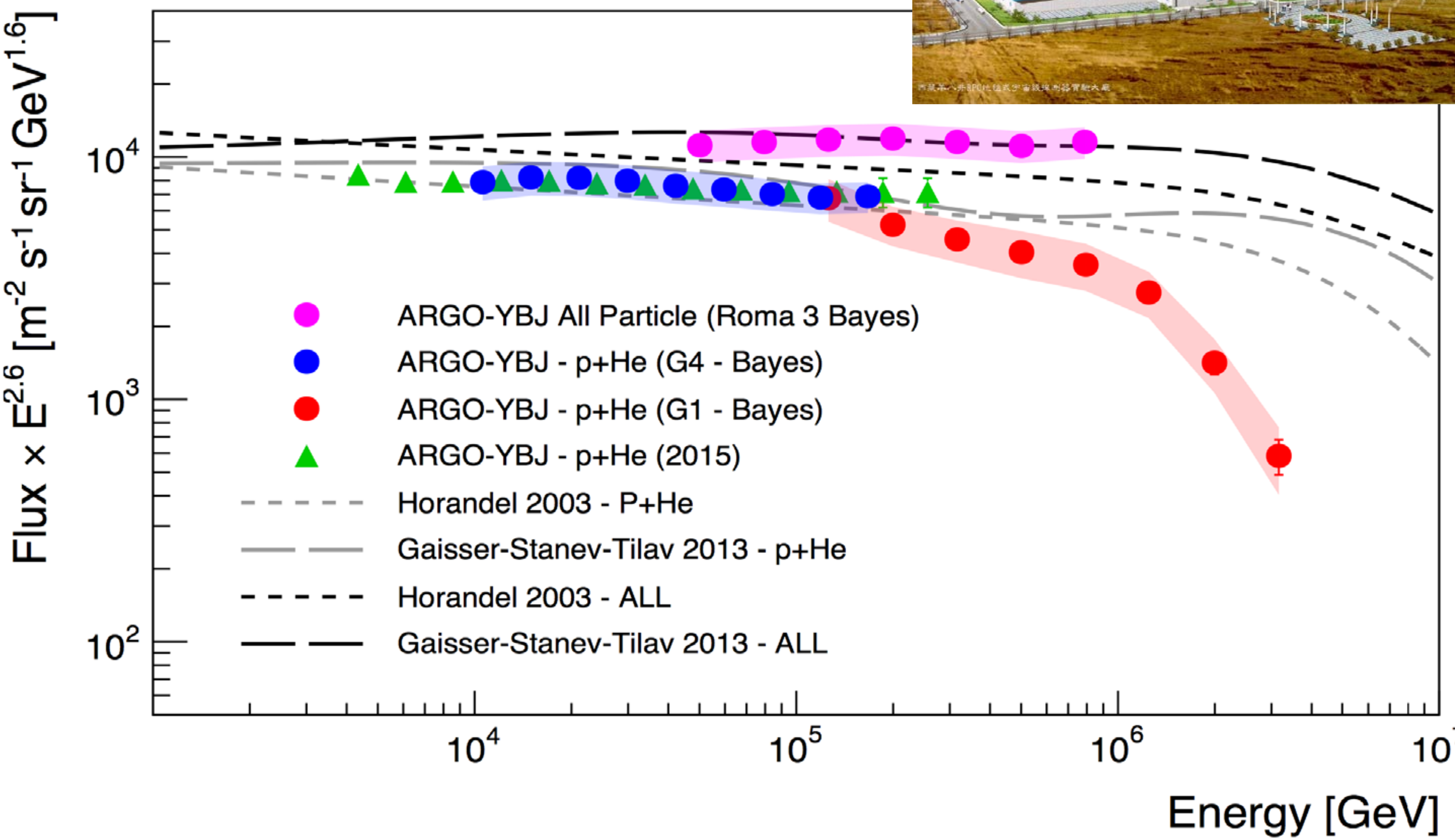

p/He spectrum bending below 1 PeV

ARGO-YBJ

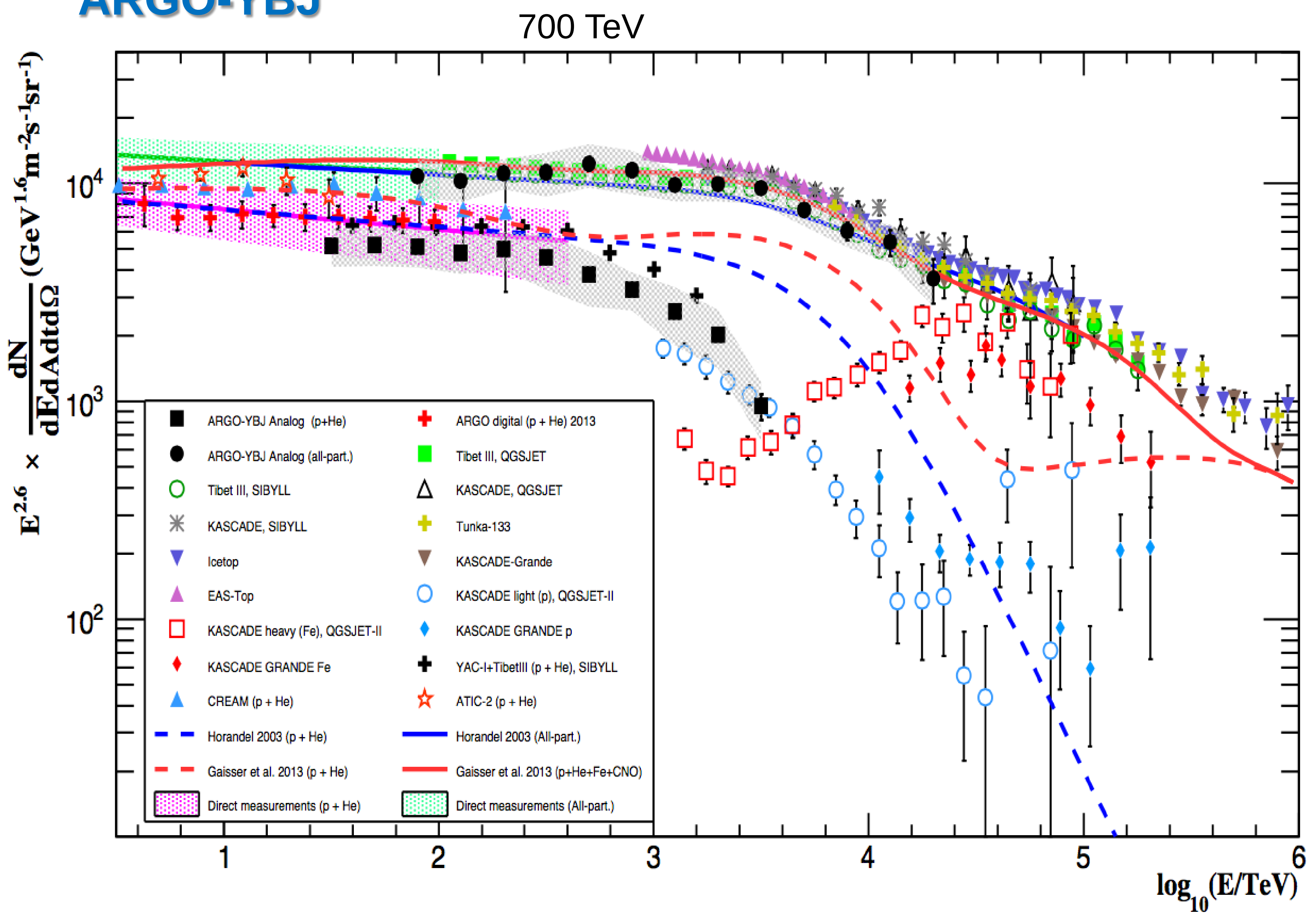

ICRC2015: *I. De Mitri, 366*

Above the knee

KASCADE/KASCADE-Grande

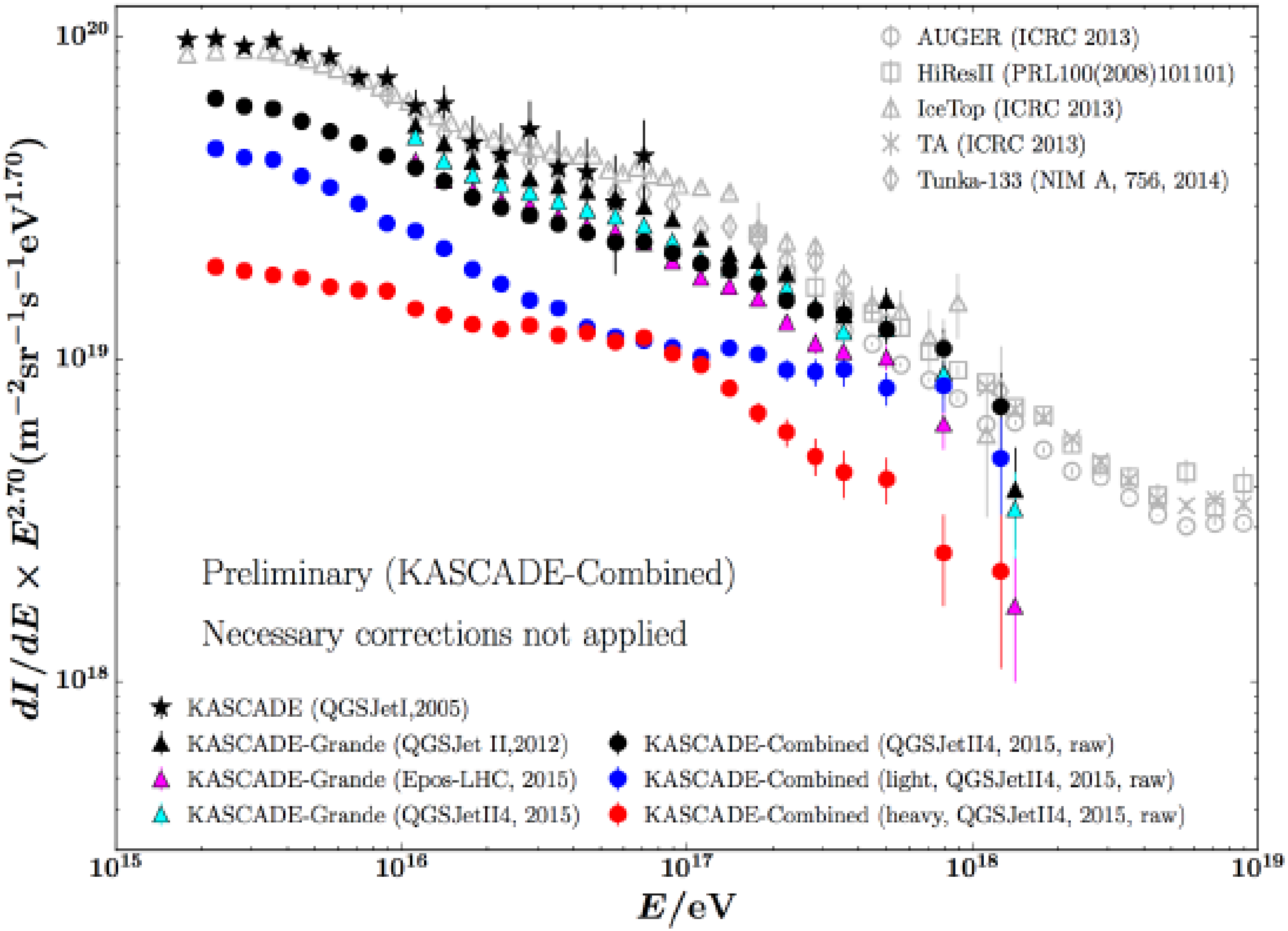

ARGO-YBJ

- benefit of analog charge
- readout very close to the core

ICRC2015*: P. Montini, 371*

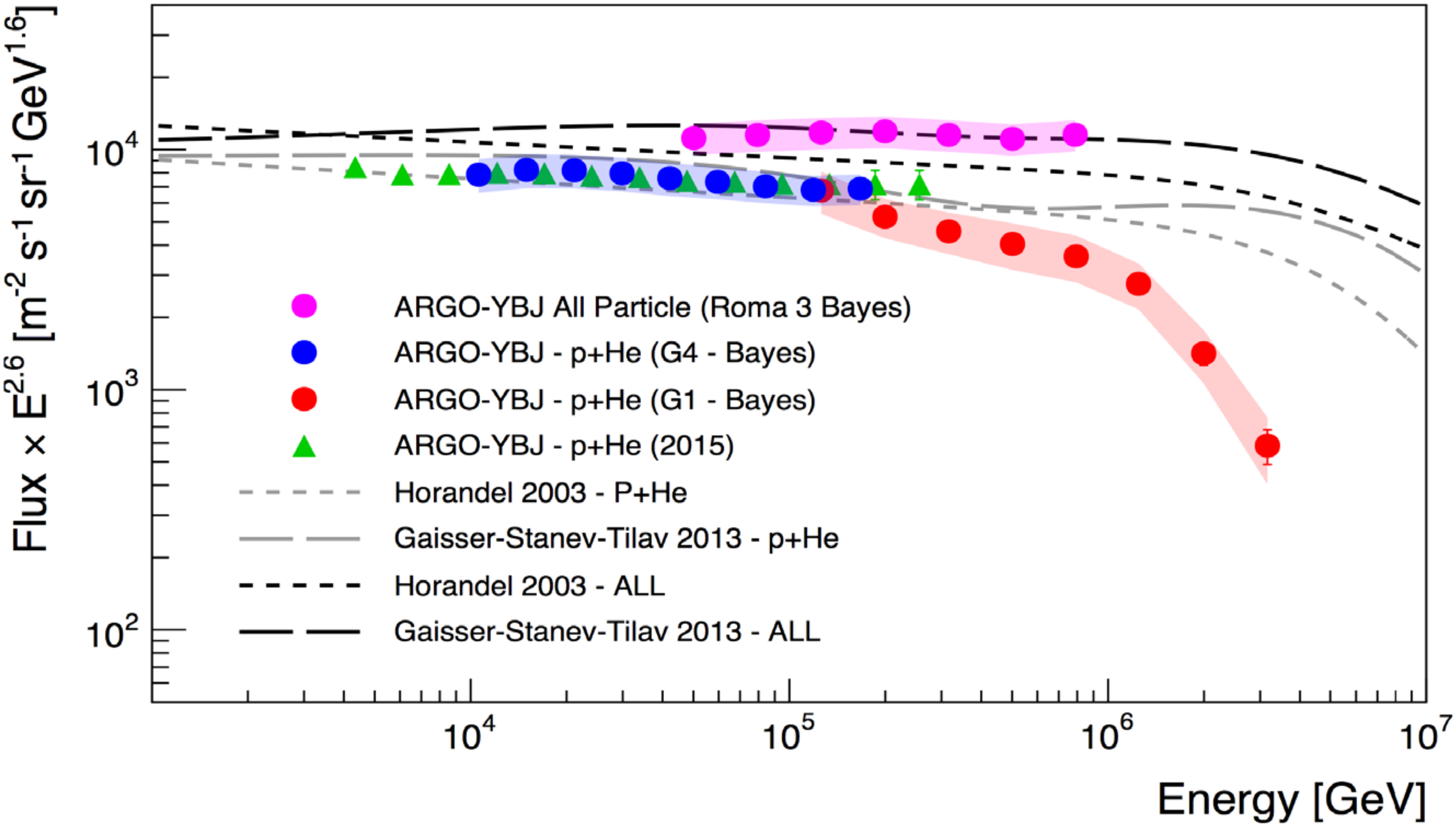

p/He spectrum bending below 1 PeV

MY KIND WISHES FOR SUCCESSES IN EDUCATION AND RESEARCH !!!